Light-Fired Thyristor Development

EL-776
Research Project 567-1

Interim Report, April 1978

Prepared by

WESTINGHOUSE ELECTRIC CORPORATION
Research and Development Center
1310 Beulah Road
Pittsburgh, Pennsylvania 15235

Principal Investigators
Derrick J. Page
Lewis L. Lowry
Prosenjit Rai-Choudhury

Prepared for

Electric Power Research Institute
3412 Hillview Avenue
Palo Alto, California 94304

EPRI Project Manager
Stig L. Nilsson
Electrical Systems Division

LEGAL NOTICE

ABSTRACT

A high power light-triggered thyristor has been developed and demonstrated. A series-connected string of eight such thyristors was tested to show feasibility for commercial utility applications in VAR generator applications.

The chief benefit to be derived from light-triggered thyristors is that a high voltage stack of such thyristors can be switched directly by a light signal transmitted through electrically insulating fiber optics cables. Such a system eliminates the need for costly isolation of the gate circuitry and provides immunity to noise-induced false triggering signals.

Design considerations applicable to light-triggered thyristors are described and means of optimizing the light source-fiber optic cable system are discussed. A hermetically sealed package for light-triggered thyristors is described. Test results on individual light-triggered thyristors are presented, and the operation of a module consisting of light source, fiber optics cables, and a series string of eight light-triggered thyristors is described.

It is concluded that the technology developed in this program is suitable for application in high voltage VAR generator applications. Further technology improvement can result in reduced cost and improved reliability and recommendations for further development effort are made.

EPRI PERSPECTIVE

PROJECT DESCRIPTION

Controlled VAR-generators and HVDC converter valves make extensive use of power thyristors. The thyristors are used as the key switching elements, connected in series and parallel, so that each element takes its share of the voltage and current stresses. Since a thyristor easily fails if it is subjected to overvoltages and overcurrents, each thyristor must be carefully protected and controlled. This requires a substantial number of auxiliary components, which leads to relatively high costs for thyristor-based, high-voltage equipment.

A thyristor-triggering system utilizing light pulses applied directly onto the silicon wafer of the thyristor opens the way for many possible design simplifications. A light-triggering system generates the required triggering pulses for multiple thyristors with nanosecond time differences between the pulses to the individual thyristor devices. Elimination of the inefficient power supply system used today for the electrical firing systems will improve the efficiency of the valve. The serviceability of the valves and switches would also be improved since all of the critical pulse generation circuits are at ground potential; they need not be within the energized portions of the power equipment. Hence, with proper redundancy in the firing circuits, a failed component in the triggering system may be replaced without de-energizing the equipment.

This project, RP567,under contract with the Westinghouse Electric Corporation, is directed toward the development of a prototype light-triggered thyristor system, including the thyristor wafer itself, the packaging of the wafer, an optical wave-guide and the light source for the triggering of the thyristor. This report is an interim report documenting the first phase of the project that will end with a field demonstration of a light-triggered thyristor switch in a controlled VAR-generator.

PROJECT OBJECTIVES

The objectives of the first phase of this project are:

- To design and build a thyristor that can be triggered from a suitable light source via an optical wave guide.
- To design and build a new thyristor package for the light-triggered thyristor.
- To evaluate, select and demonstrate, using commercially available components, the optimum light source for reliable, low-cost triggering of the thyristor.
- To evaluate, select and demonstrate, using commercially available materials, the optimum optical light guide for the selected light source and thyristor wafer.
- To assemble thyristors, light sources and optical light guides into a 15-kV thyristor switch module of the type used for a controlled VAR-generator, and demonstrate the operation of the module in the laboratory.

Thus, the technical and economical feasibility of the technology would be established in this first phase of the project. This phase is now successfully completed. The project has been extended to include a field demonstration of the technology. This will be accomplished through a replacement of one phase of a 15-kV electrically-triggered, 3-phase thyristor switch in an existing controlled VAR-generator.

CONCLUSIONS AND RECOMMENDATIONS

Light-triggered thyristors offer a good approach to HVDC thyristor valves and VAR-control switches of simpler design. This is the main conclusion of this project. It has been demonstrated that light-triggered thyristors can be built with performance equivalent to electrically-triggered thyristors. They will offer the equipment designers simpler solutions to many applications problems.

Light-triggered thyristors equivalent to Westinghouse's electrically-triggered T920 device (2000V, 800A, 53 mm diameter thyristor) have been built and tested. A sufficient number of thyristors have been built to establish confidence in the technology. The thyristor has been packaged in a modified package of the same type normally used for electrically-triggered devices. Some packaging problems have been encountered that still need to be resolved, but the problems do not seem to be insurmountable at this time.

Laser diodes and multi-fiber optical fiber-cables (using glass fibers) have been identified as the best components for the light-triggering system. A switch module, consisting of eight series-connected, light-triggered, water-cooled thyristors, has been built and successfully tested in the laboratory. The results from the first phase of the project indicated that future research is needed in the following areas:

(a) Thyristor device packaging to insure their reliability in production quantities. Even though advanced cooling systems do not appear to be a problem associated directly with light-triggering systems, these approaches would have to be considered in the design of packages.

(b) Light sources optimized for light-triggering systems. The industry trend seems to divert from the optimum light source and fibers for thyristor-triggering systems.

S. L. Nilsson
Project Manager

ACKNOWLEDGMENTS

The research project described in this report was sponsored by the HVDC Converter Station and Equipment Program of the Electrical Systems Division of EPRI. The members of the research team wish to thank Dr. Narian Hingorani, Program Manager, and Stig Nilsson and Ivars Vancers, Project Managers, for their suggestions, guidance, and encouragement. They also would like to acknowledge the guidance provided by the Industry Advisors, Vernon L. Pruett, Los Angeles Department of Water and Power, Superintendent, Sylmar Converter Station and Paul R. Shockley, Assistant Superintendent, Sylmar Converter Station.

The assistance and cooperation of Joe Johnson, Engineering Manager, of the Westinghouse Semiconductor Division, and of his staff were invaluable throughout the program.

MEMBERS OF THE RESEARCH TEAM AT
THE WESTINGHOUSE RESEARCH AND DEVELOPMENT CENTER

The following people contributed to this research project:

Professional Staff	Technicians
Jerry B. Brewster	Herman F. Abt
Frank Cibulka	Richard W. Barr
Lazlo Gyugyi	Richard J. Fiedor
Maurice H. Hanes	L. Earl Hohn
J. Richard Hansen	John E. Marinchak
Lewis R. Lowry, Principal Investigator	Joanne C. Neidigh
Derrick J. Page, Principal Investigator	Leonard V. Rohall
Prosenjit Rai-Choudhury, Prin. Investigator	Robert F. Yut
Jack S. Roberts	Anthony J. Zigarovich
Eugene L. Rodgers	
John Rosa	
Earl S. Schlegel	
Eugene C. Strycula	

CONTENTS

FIGURES

FIGURES (Continued)

FIGURES (Continued)

FIGURES (Continued)

FIGURES (Continued)

TABLES

Section 1

INTRODUCTION AND SUMMARY

1.1 BACKGROUND

There are fundamental limitations that prevent the very high voltages commonly encountered in the electric utility industry from being achieved in individual power semiconductor devices. In high voltage switching applications, it is therefore necessary to build the devices into series strings. However, when this is done, difficulties are encountered in supplying the triggering signal to the devices that are at high voltage relative to ground. Techniques commonly adopted include the use of high-voltage current transformers or light pipes fed to local pulse forming circuits. These techniques are complex and lead to reliability and cost problems.

A preferred method of triggering the thyristors is to use optical techniques directly. That is, to design the device to be triggered by light applied to the gate area of the thyristor rather than by the conventional electrical impulse.

The object of the program reported herein has been to develop solid state thyristors which can be triggered directly by a light signal. The development of such devices would provide several advantages in handling large amounts of power:

- Series stacks of devices could be operated in conjunction with relatively simple gating circuits.
- Elimination of expensive gate isolation circuitry and components.
- Reduction or elimination of auxiliary balancing circuitry.
- Superior immunity to accidental triggering by induced noise.
- Simpler design of larger systems.

The successful conclusion of this program should lead to a commercial product that is suitable for use in Electric Utility systems.

Light triggering of thyristors is technically feasible since when light of certain wavelengths is absorbed in silicon, electron-hole pairs are instantaneously created. The movement of these charged carriers under the influence of electric fields creates an electrical current. In a properly designed thyristor, this electrical current serves the same purpose as does a gate current directly applied, and the thyristor is turned on.

The choice of the wavelength of the light used to trigger the device is important. If the wavelength is too short, the absorption will be strong and most of the electron-hole pairs will be created near the silicon surface and not in the depletion region. If the wavelength is too long there will be little absorption in the silicon and few, if any, electron-hole pairs generated, and turn-on will not occur. The most useful wavelength is in the near infrared region at about 1 μm. Two types of suitable solid state light sources exist: GaAs light-emitting diodes (LED) and laser diodes (LD).

Prior to this contract, the only work conducted on high power light fired thyristors had been carried out at the Westinghouse Research and Development Center. By using LED light sources, turn-on performance comparable to that achieved by electrical triggering had been obtained. Unfortunately, the LED had to be mounted directly in the thyristor package to achieve this performance. Preliminary attempts to couple the light into the package via a light pipe had not been very successful since the received light power was inadequate. The light emitted from a standard commercial LED is radiated over a wide angle and only a fraction of this radiation can be captured and fed to the thyristor by a light pipe.

Each time the radiation from a light source is transferred from one medium to another, a fraction of the light is lost. Any optical system should therefore contain as few optical interfaces as possible.

The light radiated from a solid state laser diode is much more directional than that from an LED. A much larger fraction can be coupled into a light pipe and good thyristor turn-on has been demonstrated. Under a previous contract with the Department of the Navy, Naval Electronics Systems Command, Westinghouse successfully switched thyristors using a laser diode. Values of dI/dt of 100 A/μsec, rising to 500A from an 800V blocking state were demonstrated. (These results were obtained in high gain devices, without emitter shunts, that could not be operated in excess of 100°C.) By using light pipes in conjunction with three laser diodes, three thyristors had been operated in series at 50 Hz to switch 1500V.

Although previous developments on the light-triggered thyristor were significant, much development work remained to be done before the device could become a commercial reality. In particular, three areas were in need of further improvement:

- Sensitivity of the thyristor so that it will turn on with less optical power, or will turn on faster for a given optical drive.
- Optical coupling between the light-emitting crystal (LED or laser diode) and the sensitive area of the silicon device so that long lengths of light pipe could be used to provide good electrical isolation.
- A hermetic package design with an optical window so that the device could exhibit the same reliability as that of hermetically sealed conventional thyristors.

The scope of this contract has been to solve these problems by developing a suitable thyristor, light-source, light coupling, and hermetic package combination. That the developed thyristor and its triggering subsystem have solved the problems was demonstrated by fabricating and evaluating a switch comprising a series string of 8 thyristors and the necessary ancillary components.

The light-triggered thyristor described herein is designed to be very similar to a commercially-available electrically-triggered power thyristor. Thus there is no significant difference between the two in the following capabilities:

- Blocking voltages and leakage currents
- Forward voltage drop or current carrying capability
- Turn off time
- Critical dV/dt
- Reverse recovery characteristics
- Latching and holding currents
- Operating and storage temperatures
- Thermal resistance
- Effects of temperature on these parameters

The differences lie in the method by which turn-on is achieved and, for this application, in the energy which is available to initiate the turn-on process. In an electrically-triggered thyristor, this energy is supplied by the gate current pulse and is typically on the order of 100 μJ. The triggering energy available to a light-triggered thyristor is presently limited by available practical light sources and associated optics; it is typically less than 1.0 μJ.

In the electrically-triggered thyristor, the initial electrical charge which initiates turn-on is provided by the applied gate current. In the light-triggered thyristor, the initial electrical charge is provided by the absorption of light in silicon, instantaneously generating electron-hole pairs. The phenomena by which this electrical charge is converted to anode current during the turn-on process are common to both types of thyristors.

Both electrically-triggered thyristors and light-triggered thyristors can be designed for fast turn-on, with high dI/dt capability, through the use of digitated cathode structures and gate amplification, and/or through the use of higher triggering energy. In the present application, VAR generators, fast turn-on is not required, the additional cost associated with higher energy light pulses is not warranted, and a simple gate structure provides a desirable trade-off between device sensitivity and turn-on speed. In other applications, where faster turn-on is required, it can be attained by an optimized combination of cathode geometry design and increased light energy.

1.2 SUMMARY OF RESULTS

Thyristor design began with that of a proven commercially available, 2000V, 800A, gate triggered thyristor. Only the gate structure was changed to provide for the light triggering.

In order to determine the best structure for the gating region, special test pattern devices were made for studying a wide variety of gate designs. These all shared the same blocking junctions so that variations in trigger sensitivity could be directly attributed to the gate design and not be confused by variations elsewhere in the device. Various sizes of amplifying gate and non-amplifying gate configurations were located both in the interior and at the edge of the thyristor. This structure provided the means by which light cables could easily be moved from one pattern to the next to study the effects of the design variables on the triggering characteristics. Besides the dimensional and geometrical variations, the effects of variations in circuit limited dI/dt, light cable diameter, or the presence of a diffused cathode in the light sensitive region were studied.

The investigation resulted in a decision to use a centrally-located, non-amplifying gate structure, without a cathode region in the light sensitive area, with an optical window and light cable 1.1 mm in diameter. The light sensitive area was polished and thermally oxidized.

The result of this design was a light-triggered thyristor which met or exceeded the same electrical specifications as are applicable to the analogous electrically gated thyristor.

Design of the optical system for the light-triggered thyristor was governed by considerations of the optimum light wavelength and maximum deliverable optical power together with cost and reliability. Investigations of light emitting diodes and laser diodes of various output power capabilities and package configurations resulted in the choice of a 12 watt laser diode as that source which most nearly satisfied all requirements.

One of these requirements was that the light source be capable of efficiently delivering light into a fiber optic cable. It was experimentally shown that coupling efficiency could be improved through modification of the laser diode package, but that the additional cost and complexity involved did not justify further development of the technique at this time.

The fiber optics cable which transmits the optical signal from the light source to the light-triggered thyristor must also meet several requirements. For efficient coupling to the light source, the cable must be of large diameter and possess a high numerical aperture.

Transmission loss (loss due to light absorption and scattering within the cable fibers) must be low, but the highest quality fibers designed for data transmission applications are not required in this application. The maximum practical diameter of the fiber optics cable is limited by cost and by considerations of efficient coupling to the light-sensitive region of the thyristor. A "medium" loss, high numerical aperture glass cable of 1.1 mm diameter was found to be suitable.

Demountable connectors where the fiber optics cable interfaces with the light source at one end and with the thyristor at the other end must meet rigid dimensional specifications for efficient coupling. Commercially available connectors meeting these specifications were found to be suitable and were used in the system.

Light source redundancy for increased reliability is incorporated into the system by means of a multifurcated fiber optics cable. In this arrangement, the optical energy required to trigger simultaneously a string of eight thyristors is obtained from a bank of eight individual laser diodes. By means of separating and regrouping the individual fibers from each laser diode, the light from each diode is distributed to all thyristors in the string. Because the total amount of light from the laser diode bank is more than sufficient to trigger all eight thyristors, the complete failure of one or two laser diodes will not interrupt the operation of the thyristor switch.

The package used for the light-triggered thyristor is designed to resemble as closely as possible the package used for an electrically-gated thyristor of the same power capability. In this way, the important electrical, thermal, and mechanical characteristics of a proven package design have been retained.

Inside the package, the triggering signal is guided to the light-sensitive region of the thyristor by a solid glass light pipe -- one end affixed to the thyristor, the other end extending through the package wall to a demountable connector which couples to one end of the fiber optics cable. The light pipe is sealed to the ceramic package wall so that the entire package is hermetic.

At present, it is expected that the manufacturing costs for the light-triggered thyristor will be higher than the costs for a conventional thyristor. A cost estimate study was made, assuming an annual production of 2000 thyristors manufactured in lots of 100 per batch. According to this study, the cost of the light-triggered thyristor itself is estimated to be only slightly higher than the cost of an equivalent electrically gated thyristor. Increased manufacturing cost of the thyristor package is more significant; the total manufactured cost of the packaged light-triggered thyristor is estimated to be 3% higher than the cost of an equivalent electrically gated thyristor. It must be pointed out that comparative selling prices of the two types of thyristors will depend upon and be determined by the market, and not solely by the manufacturing cost. The anticipated higher cost of light-triggered thyristors must be balanced against anticipated cost savings in circuitry and components made possible by improved high voltage isolation and noise immunity provided by the light-triggered system.

Individual packaged thyristors were electrically tested to ensure that they meet the specifications which are applicable to electrically-gated thyristors of the same power capability. Other tests relevant to the unique light-triggered nature of these devices were devised and carried out as needed.

Finally, a high power switch consisting of a series string of eight light-triggered thyristors was designed and constructed. The mechanical and electrical design of this switch was similar to designs applicable to electrically-gated thyristor switches, except, of course, that gate isolation circuitry and components were not required. The switch was first operated at nominal voltage and current and then with overvoltage and overcurrent surges to demonstrate its successful operation.

It has been agreed that further development of light-triggered thyristor switches will be carried out. The goal of this future effort is to construct a switch consisting of three series banks of thyristors connected for AC operation. This switch will be field tested at a host utility site to demonstrate its economic and reliability benefits.

1.3 ANTICIPATED TECHNOLOGY IMPROVEMENTS

High power, light-triggered thyristors, like any new device should be expected to improve in performance as experience is gained and new technologies are incorporated. Some design improvements are already in the planning stage; others will become apparent with time.

The extension of V_{DRM} and V_{RRM} to higher blocking voltages can be attained with recently developed materials and processes. This design improvement will result in substantially reduced installation costs and improved efficiency.

Attainment of improved dI/dt can be achieved through gate geometry changes for applications where this is a consideration. An optimum gate design, probably incorporating an auxiliary (amplifying) gate would require additional development.

Thyristor self-protection against transient voltage surges and overvoltage can be incorporated directly into the thyristor silicon through some of several proposed designs. These design changes can be expected to reduce systems costs due to elimination of at least some auxiliary protection circuits.

Improvements in optical components for light-triggered systems are occurring rapidly. Laser diodes of improved power, efficiency, and reliability are becoming available. Fiber optics cables with reduced transmission losses can be expected to be available at lower cost than that of present cables.

Packages for light-triggered thyristors can be redesigned for lower cost and greater reliability. At present, the package cost is a major part of the cost of a high power thyristor. Recent tests at the Westinghouse Semiconductor Division have shown that packages can be simplified to reduce cost while retaining the important characteristics of the present package.

Finally, the commercial use of high voltage, high power solid state switches is still in its infancy. It is anticipated that, as energy savings become increasingly important and as experience leads to improved circuit designs and wider applications, the cost of installed systems will decrease while efficiency improves. The attainment of higher efficiency systems will make the use of light-triggering increasingly valuable and effective.

Section 2

THYRISTOR DESIGN AND FABRICATION

2.1 SPECIFICATIONS

The performance goals of the light-triggered thyristor are analogous to the specifications of the Westinghouse T920 20 08 electrically gated thyristor. The light-triggered thyristor target specifications are summarized in Table 2.1.

2.2 THEORETICAL ANALYSIS

2.2.1 Conversion of Light into Current

First, the variables involved in converting light energy into triggering current will be examined. Fundamentally, this current is created by the absorption of light photons with sufficient energy to create electron-hole carrier pairs. Thus, in silicon, the photon energy must be at least 1.12 eV, corresponding to a vacuum wavelength of 1.10 μm. Because the density of states in the allowed energy bands near the edges of the energy gap is low, the photon energy must be slightly greater than 1.12 eV to ensure a sufficient probability of carrier pair generation for useful operation. On the other hand, photons of energy much greater than 1.12 eV are inefficient since each photon creates only one carrier pair and the excess energy of each photon is wasted.

The probability of carrier pair generation with light of wavelength less than 1.1 μm is proportional to the absorption coefficient, α, which is shown as a function of light wavelength (vacuum) in Fig. 2.1. The absorption coefficient is a parameter in the equation expressing Lambert's Law:

$$I = I_o e^{-\alpha x} \qquad (2.1)$$

which describes the decrease in light intensity (I) as a function of absorption coefficient (α) and distance (x) in the absorbing medium. The value of α is

Table 2.1

LIGHT TRIGGERED THYRISTOR
TARGET SPECIFICATIONS

Forward Current 1100 to 1255 Amps RMS
700 to 800 Amperes Half-Wave Average
Forward Blocking Voltages to 2200 Volts

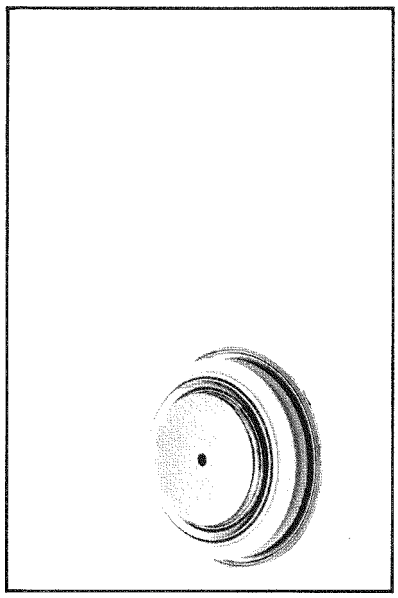

- Low V_{TM}
- Low Thermal Impedance
- High surge current capability
- Compression Bonded Encapsulation
- I^2t package rating

Pow-R-Disc thyristor package offers:

- Single or double-sided cooling
- Reversible mounting polarity
- Compact size and weight
- Long creepage & strike paths
- Hermetic seal

Dimensions in Inches (and Millimeters)

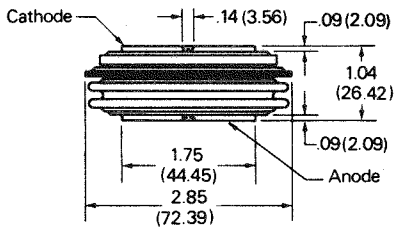

Approximate Weight 16 oz. (454 gms.)

Outline T92

Air-cooled and water-cooled heat exchangers are available.

Ordering Information

Type	Voltage		Current		Turn-off	
Code	V_{DRM} and V_{RRM} (V)	Code	$I_{T(av)}$ (A)	Code	tq μsec	Code
T920	2000	20	800	08	250 (typical)	0

Table 2.1 (Cont'd.)

Forward Current 1100 to 1255 Amps RMS
700 to 800 Amperes Half-Wave Average

Voltage

Blocking State Maximums (T_J = 125°C)	Symbol	
Repetitive peak forward blocking voltage, V	V_{DRM}	2000
Repetitive peak reverse voltage②, V	V_{RRM}	2000
Non-repetitive transient peak reverse voltage, V ≤ 5.0 msec	V_{RSM}	2100
Forward leakage current, mA peak	I_{DRM}	50
Reverse leakage current, mA peak	I_{RRM}	50

Current

Conducting State Maximums (T_J = 125°C)	Symbol	T920—08
RMS forward current, A	$I_{T(rms)}$	1255
Ave. forward current, A	$I_{T(av)}$	800
One-half cycle surge current③, A	I_{TSM}	17,000
3 cycle surge current③, A	I_{TSM}	12,200
10 cycle surge current③, A	I_{TSM}	10,200
I^2t for fusing (t=8.3 ms) A^2sec	I^2t	1,203,000
Max I^2t of package (t=8.3 ms), A^2sec	I^2t	90 x 10^6
Forward voltage drop at I_{TM} = 1500A and T_J = 25°C, V	V_{TM}	1.8

Switching

(T_J=25°C)	Symbol	Min	Typ	Max
Turn-off time, I_T=250A				
T_J=125°C, di_R/dt=50 A/μsec reapplied dv/dt= 20V/μsec linear to 0.8 V_{DRM}, μsec	tq		250	
Turn-On and Delay Time				
I_{TM}=1000A④, tp=450 μsec	ton		3.5	
V_D=1100V, μsec	td		1.5	
Critical dv/dt exponential to V_{DRM} T_J=125°C, V/μsec⑤	dv/dt	300		
Latching Current⑥ V_D=75V, mA	I_L		400	1000
Holding Current⑥ V_D=75V, mA	I_H		150	500

Thermal and Mechanical

	Symbol	Min	Typ	Max
Oper. junction temp., °C	T_J	—40		125
Storage temp., °C	T_{stg}	—40		150
Mounting force, lb.⑦		5000		5500
Thermal resistance with double sided cooling⑦				
Junction to case, °C/Watt	$R\theta JC$		.028	.03
Case to sink, lubricated, °C/Watt	$R\theta CS$		.008	.01

Table 2.1 (Cont'd.)

Forward Current 1255 Amps RMS
800 Amperes Half-Wave Average

Case Temperature vs. Forward Current—Double Sided Cooling

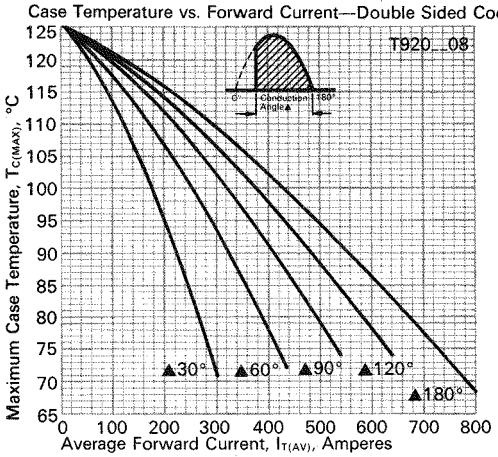

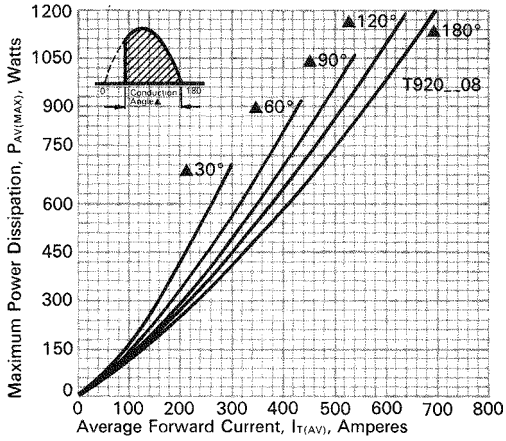

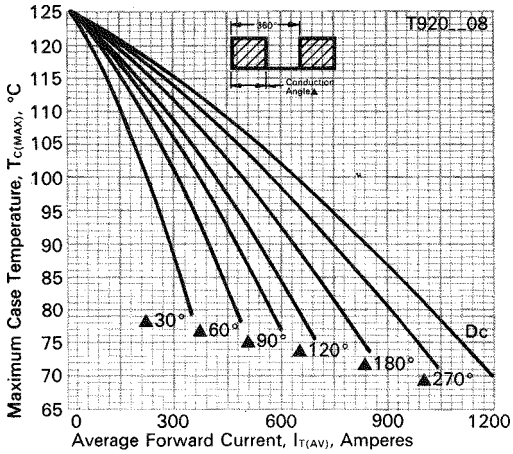

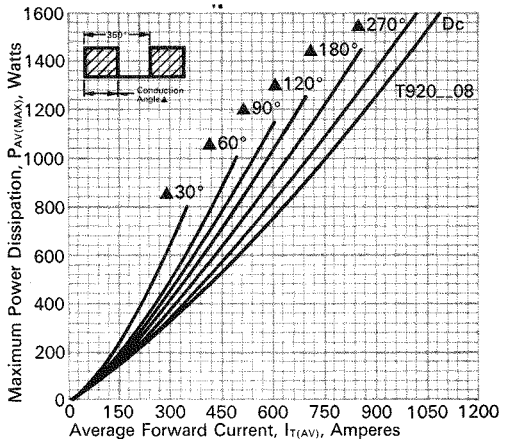

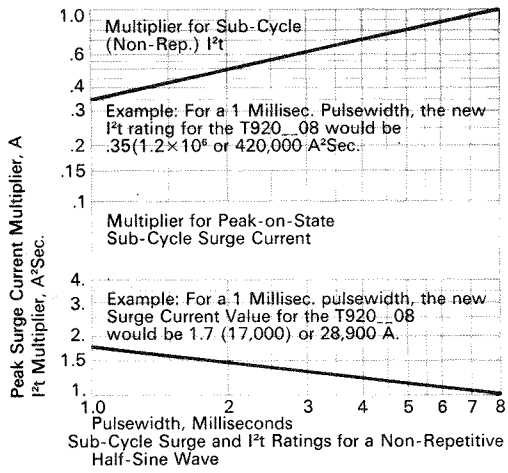

Sub-Cycle Surge and I²t Ratings for a Non-Repetitive Half-Sine Wave

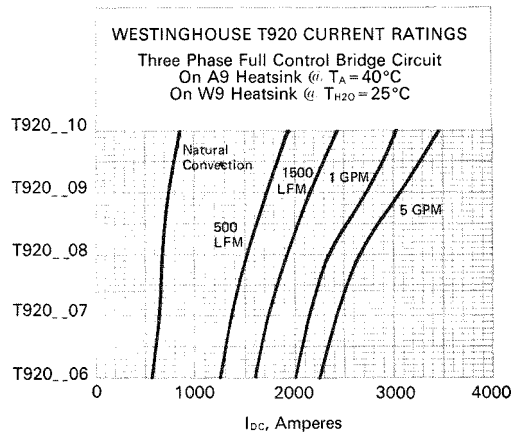

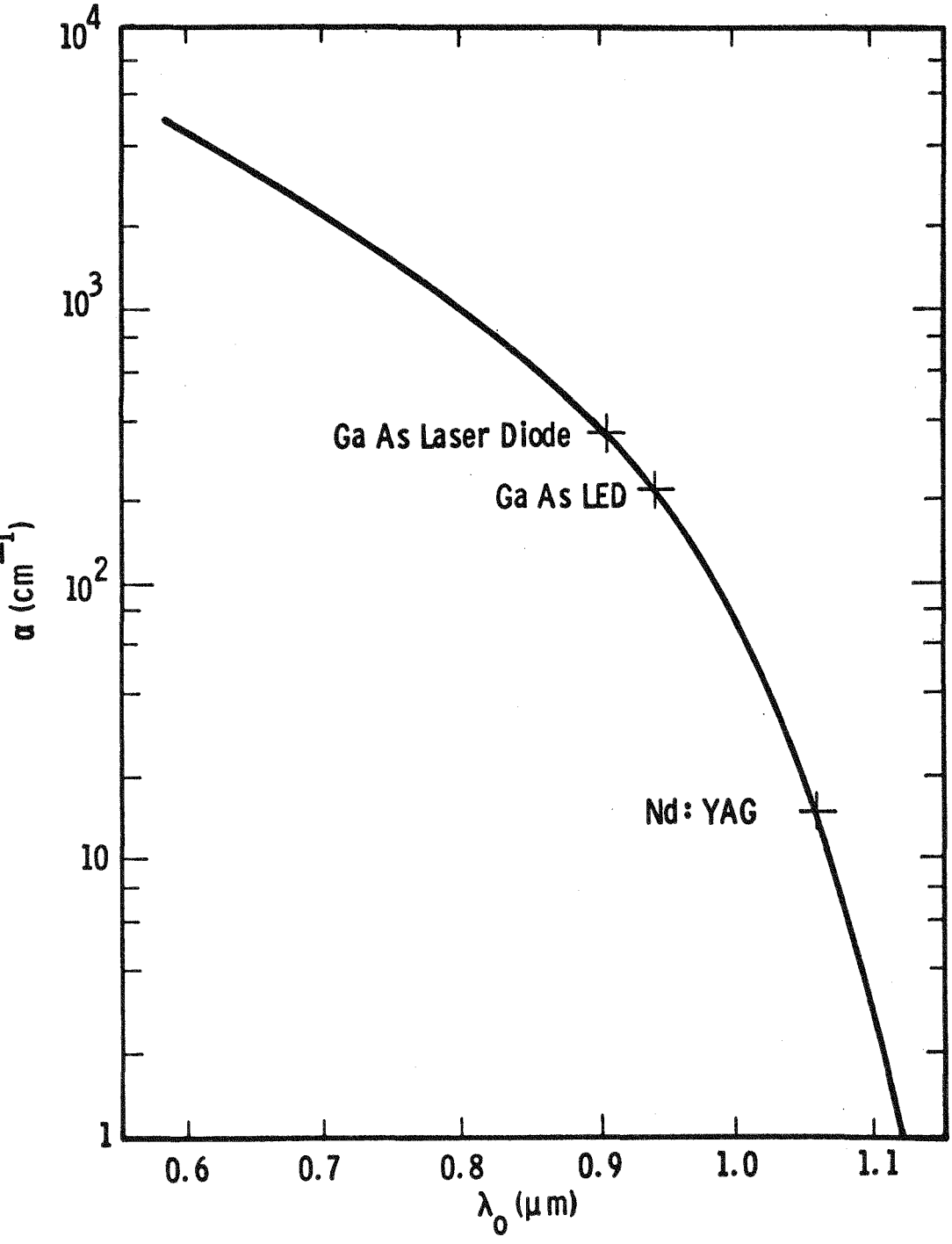

Fig. 2.1—Absorption coefficient, α, of silicon as a function of wavelength of light

independent of silicon resistivity for the wavelengths represented in Fig. 2.1.*

From the data of Fig. 2.1 the relative light intensity in silicon, as a function of depth, can be plotted for selected wavelengths of light, as shown in Fig. 2.2.

In order for light-generated carrier pairs to contribute to triggering current, they must be generated either

a) within the forward voltage blocking depletion layer or

b) sufficiently nearby that they can diffuse to that depletion layer before they disappear through recombination.

Practical high voltage thyristors are typically designed to have their forward voltage blocking junctions at a depth of 60-90 μm. In order to ensure that a considerable portion of the incident light is absorbed at that depth, it is apparent from Fig. 2.2 that the desirable light wavelengths are those from 0.90-0.95 μm. Fortunately, the available, practical, relatively intense light emitting diodes and laser diodes emit light at wavelengths of 0.940 and 0.904 μm, respectively. Subsequent calculations will be limited to these wavelengths.

It is, in fact, the almost simultaneous appearance of intense, solid state light sources emitting light of the proper wavelength and of the need for high voltage, high power solid state switches that has made this development work practical.

2.2.2.1 Carriers Generated in the Depletion Region. In the following discussion, the well-founded assumption is made that all carriers generated within the depletion layer (see Fig. 2.3) will contribute useful triggering current. The effects of other carriers generated outside the depletion layer will be discussed later.

Calculation of the number of carriers generated within the depletion layer requires a determination of the location of the boundaries of that layer for a range of applied voltages. This can be done by numerically integrating Poisson's equation,

$$\frac{dE}{dx} = -\frac{q}{\varepsilon}(N_D - N_A) \qquad (2.2)$$

*H. Y. Fan and M. Becker, "Infra-red Optical Properties of Silicon and Germanium," pp. 132-47 in Semiconducting Materials, Butterworth Scientific Publications, London, edited by H. K. Heinisch, (1950).

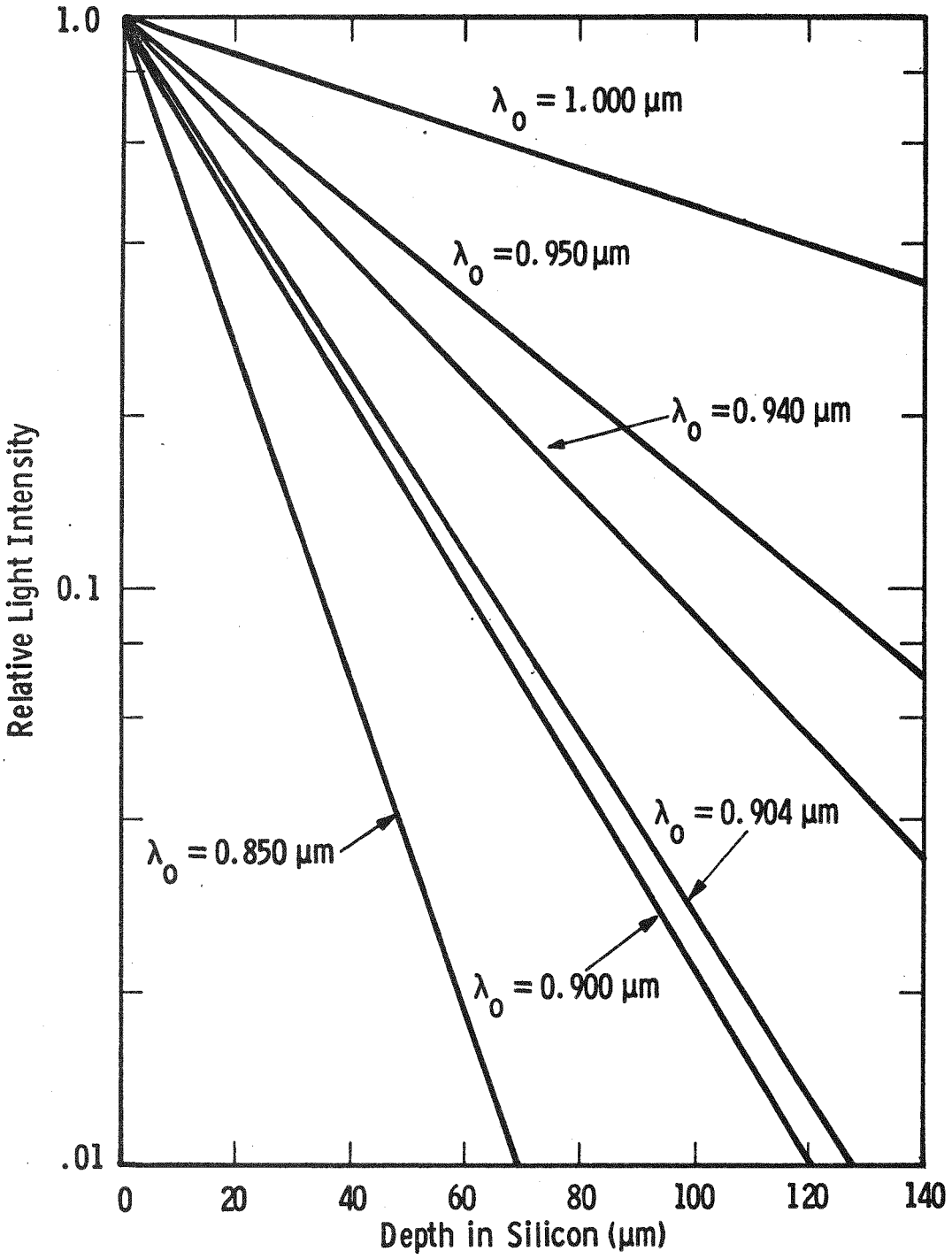

Fig. 2.2 — Relative light intensity as a function of depth in silicon

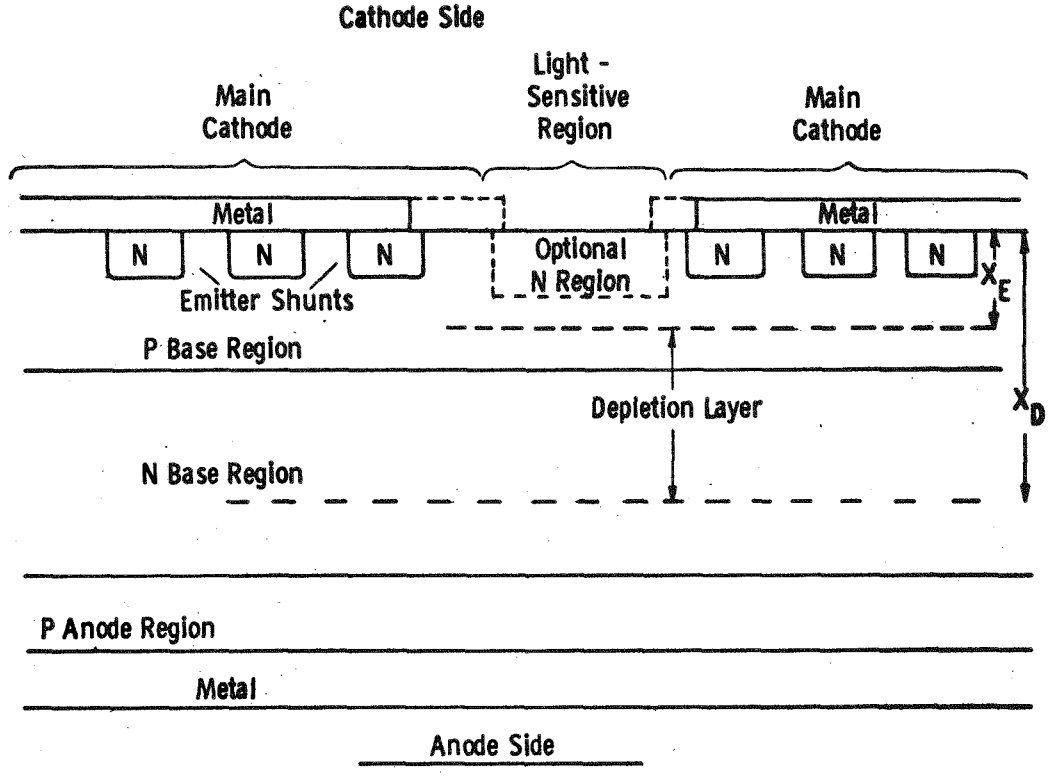

Fig. 2.3—Anatomy of a Thyristor

where $N_D - N_A$ is obtained from the known dopant concentration profile of the T92N thyristor. The results of such a calculation are shown in Fig. 2.4.

The amount of light absorbed within the depletion layer is given by

$$I_A = I_o \, (e^{-\alpha X_E} - e^{-\alpha X_D}) \qquad (2.3)$$

where I_A is the amount of light absorbed in the depletion region, I_o is the amount of light entering the silicon, α is the absorption coefficient (Fig. 2.1), X_E and X_D are the depths of the shallow and deep edges, respectively, of the depletion layer.

The depth of the shallow depletion layer edge, X_E, can be varied, in a small area of the thyristor, by etching away some of the silicon. Such an operation will increase the amount of light absorbed within the depletion layer. Figure 2.5 shows how the fraction of light absorbed in the depletion layer can be varied by changing X_E for the two light wavelengths of interest and for two values of applied voltage. This figure illustrates the advantages that might be gained by locally etching away part of the silicon in the light sensitive region.

2.2.2.2 Carriers Generated Outside the Depletion Layer. An accurate calculation of the number of carriers, generated outside the depletion region that can diffuse to the depletion region before they are lost through recombination, is more difficult. It was originally assumed that only those carriers which diffused to the depletion region during the light pulse time period would be useful. Subsequent experimental measurements of the current pulse created by the light pulse have shown that this was an overly pessimistic assumption, and that carriers contribute to useful triggering current even after the light pulse has ended. Therefore, the calculation of the useful fraction of carriers generated outside the depletion layer should be based upon diffusion length considerations rather than upon diffusion time considerations. These calculations are described below.

The probability that carriers generated at some depth $X < X_E$ will diffuse to X_E before they disappear by recombination is approximated by the same equation that gives the transport factor of a transistor:

$$\beta = \operatorname{sech} \left(\frac{X_E - X}{L}\right) \qquad (2.4)$$

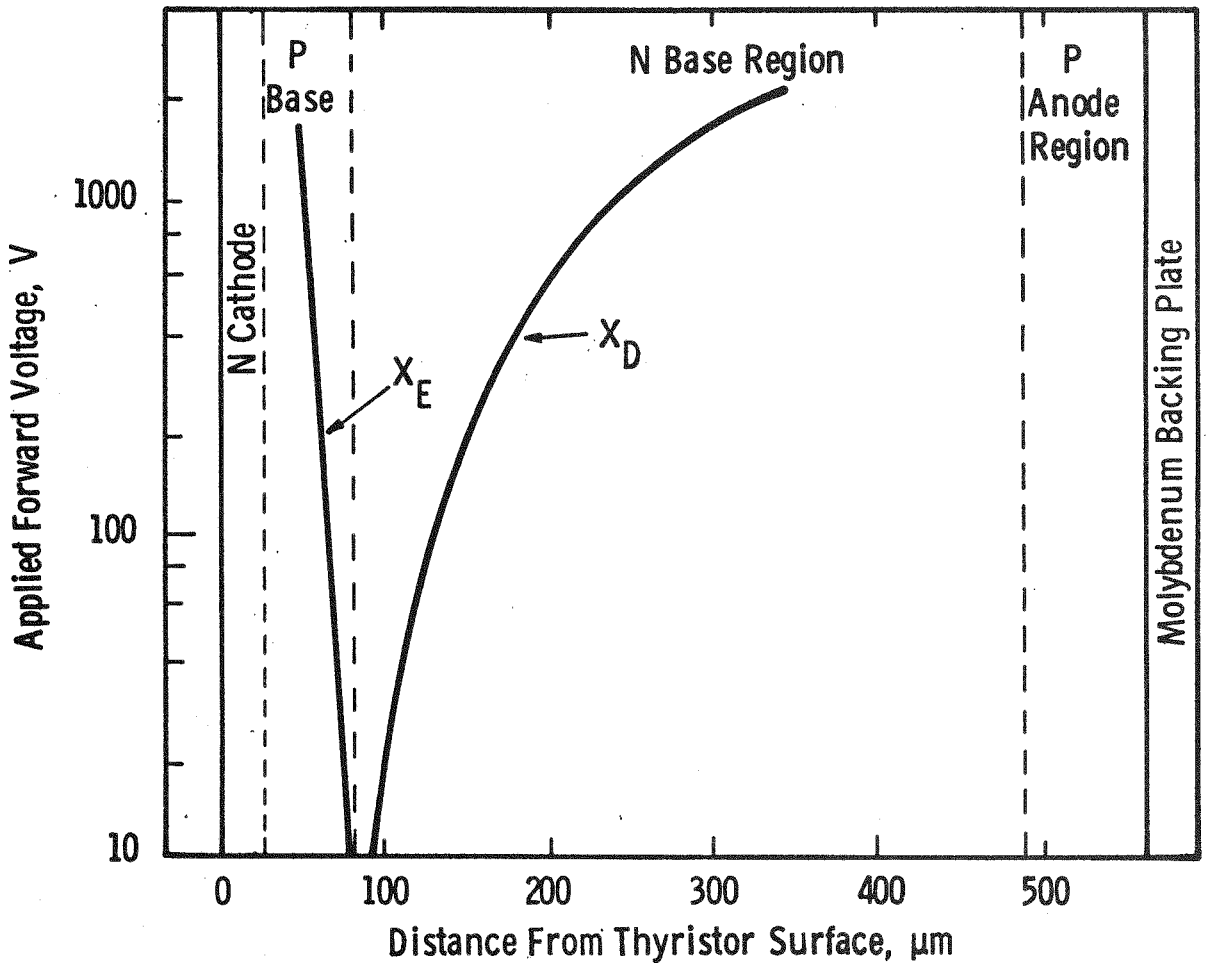

Fig.2.4— Positions of the edges of the depletion layer as a function of the applied forward voltage

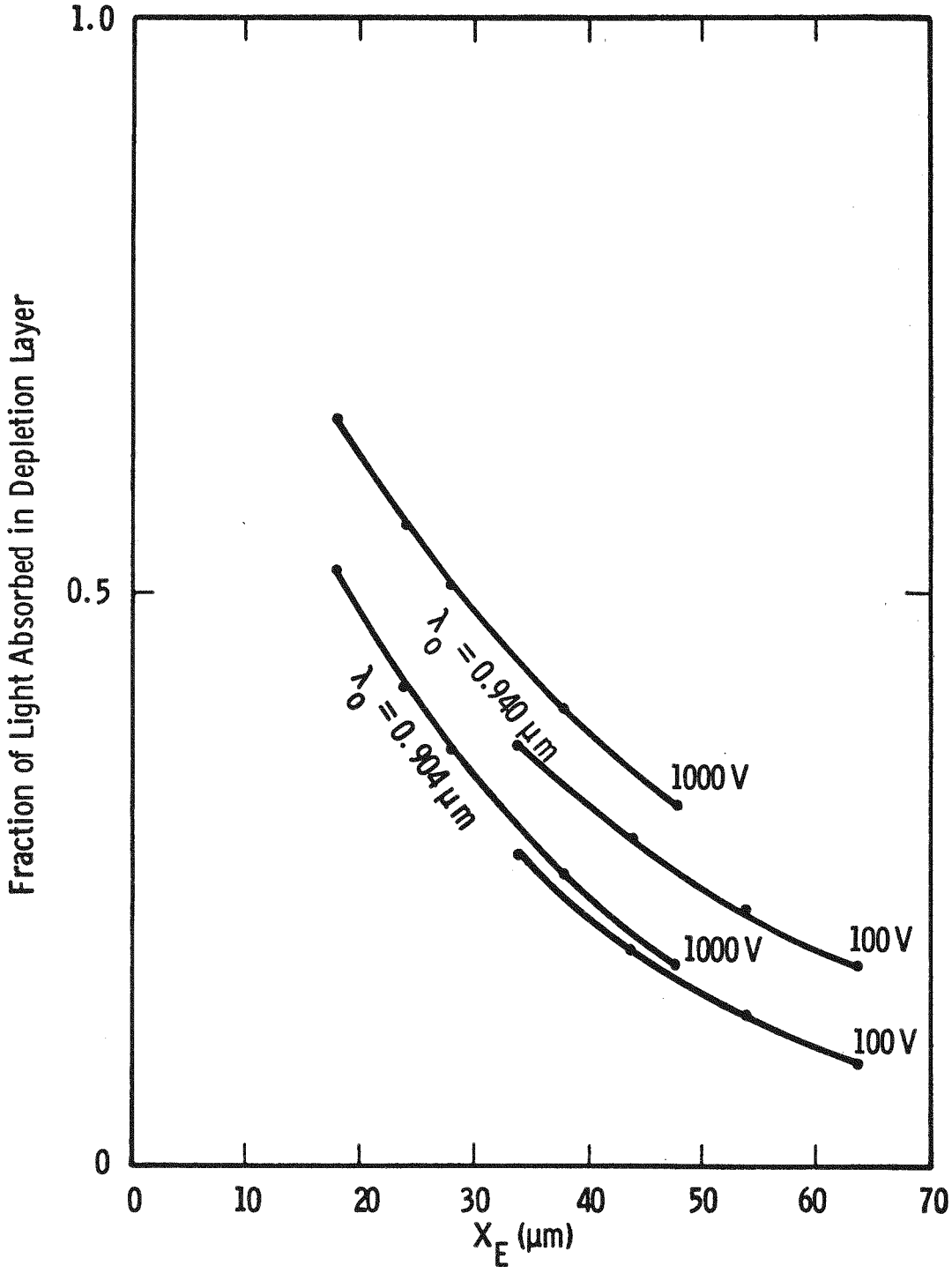

Fig. 2.5 — Fraction of light absorbed within the depletion layer

where X_E is the depth of the shallow edge of the depletion region, X is the depth at which the carriers are generated, and L is the diffusion length of minority carriers (electrons) in the p base. To take into account the exponential dependence of light absorption with changing X, a weighting factor is combined with Eq. 2.4 to give

$$\bar{\beta} = \frac{\int_0^{X_E} \alpha e^{-\alpha x} \operatorname{sech}\left(\frac{X_E - x}{L}\right) dx}{\int_0^{X_E} \alpha e^{-\alpha x} dx} \qquad (2.5)$$

$$= \frac{1}{1 - e^{-\alpha X_E}} \int_0^{X_E} \alpha e^{-\alpha x} \operatorname{sech}\left(\frac{X_E - x}{L}\right) dx.$$

The diffusion length, L, is a parameter which expresses the average distance an excess minority carrier will diffuse before it disappears through recombination. The lifetime, τ, is the corresponding length of time an excess minority carrier can be expected to exist. Either parameter can be used to characterize a particular volume of silicon; both are strongly dependent upon processing variables. Lifetime and diffusion length in the lightly doped p base region of a thyristor have been measured and are fairly high; their values in the heavily doped n emitter cannot be measured accurately and are known to be low. These parameters are important in the discussion of the two types of light sensitive region design which follows.

In the following, the fraction of useful carriers is calcualted for two conditions -- one with an n emitter diffusion in the light sensitive area and one without such a diffusion. The reason for considering an n diffusion is that it helps one develop a forward voltage on the cathode junction with fewer useful carriers. This is discussed later in 2.2.2.

In design type 1, light enters the silicon in a region which has not received an n emitter diffusion. We consider light wavelengths of either .940 μm or .904 μm and diffusion lengths in the p base region of either 132 μm or 60 μm (values typical of production thyristors). Of those carriers which are generated by light absorption between the silicon surface and the shallow edge of the depletion layer, some fraction will diffuse to the depletion region and generate useful

current. The dependence of this fraction upon the distance from the silicon surface to the shallow edge of the depletion region is described by Eq. 2.5 and is illustrated in Fig. 2.6, curves 1 through 4. It can be seen that this fraction is high, especially for the short distances which exist for high applied voltage. The effective X_E can be further decreased, if desired, by removing some silicon from the light sensitive region.

In design type 2, light enters the silicon in an area where a 20 μm deep n emitter diffusion has been formed. The assumption is made that all carriers generated within this heavily diffused region are immediately lost through recombination and do not contribute to useful current. The useful fraction of carriers generated outside the depletion region then depends upon the distance from silicon surface to depletion layer as illustrated in Fig. 2.7a, curves 5 through 8.

These curves illustrate that a significant number of generated carriers is lost when an n emitter region of zero diffusion length covers the light sensitive region of the thyristor. This loss can be reduced by locally removing part of the silicon containing the n emitter. The effect of removing 14 μm of silicon is illustrated in Fig. 2.7b.

Figures 2.6 and 2.7 clearly illustrate that design type 1 provides more useful carriers than does design type 2, even if some of the heavily doped emitter in type 2 is removed.

Two opposing effects of unknown significance have not been included. They are:

1) The diffusion length in the p region is not constant, but decreases near the silicon surface.
2) A built-in field exists in the p base which aids the diffusion of electrons toward the depletion layer.

The first effect will reduce the number of useful carriers below the value predicted by Eq. 2.5 and illustrated in Fig. 2.6; the second effect will increase the number of useful carriers. Both effects are expected to be small in the lightly doped, low concentration gradient region under consideration, and because they tend toward cancelling each other, need not be rigorously analyzed.

Finally, some carriers will be generated in the region beyond the deeper edge of the depletion layer. It can be assumed that, on the average, those carriers generated within one-half diffusion length of the depletion region will be effective in creating a trigger current.

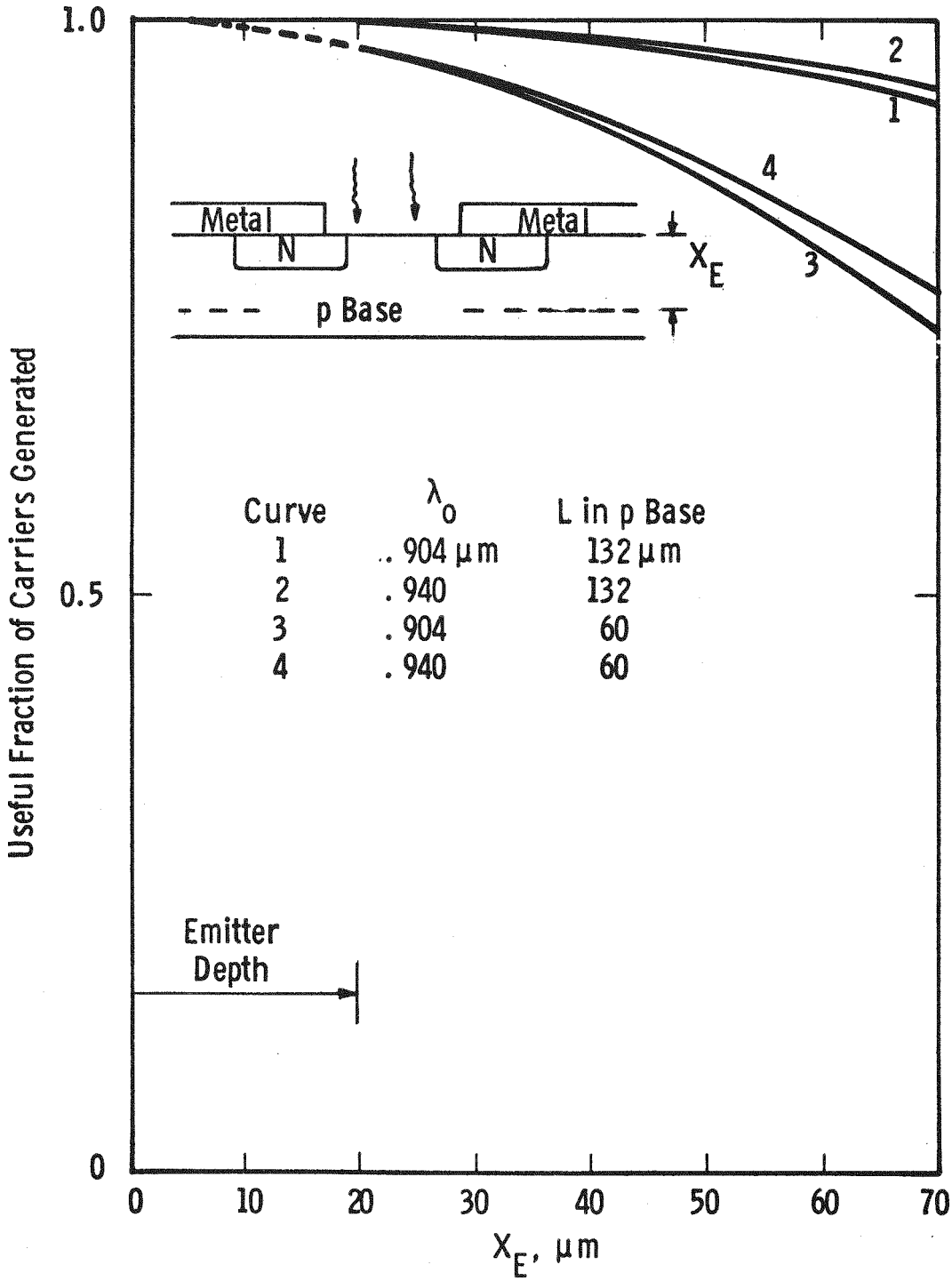

Fig.2.6—Useful fraction of carriers generated outside depletion layer, design type 1

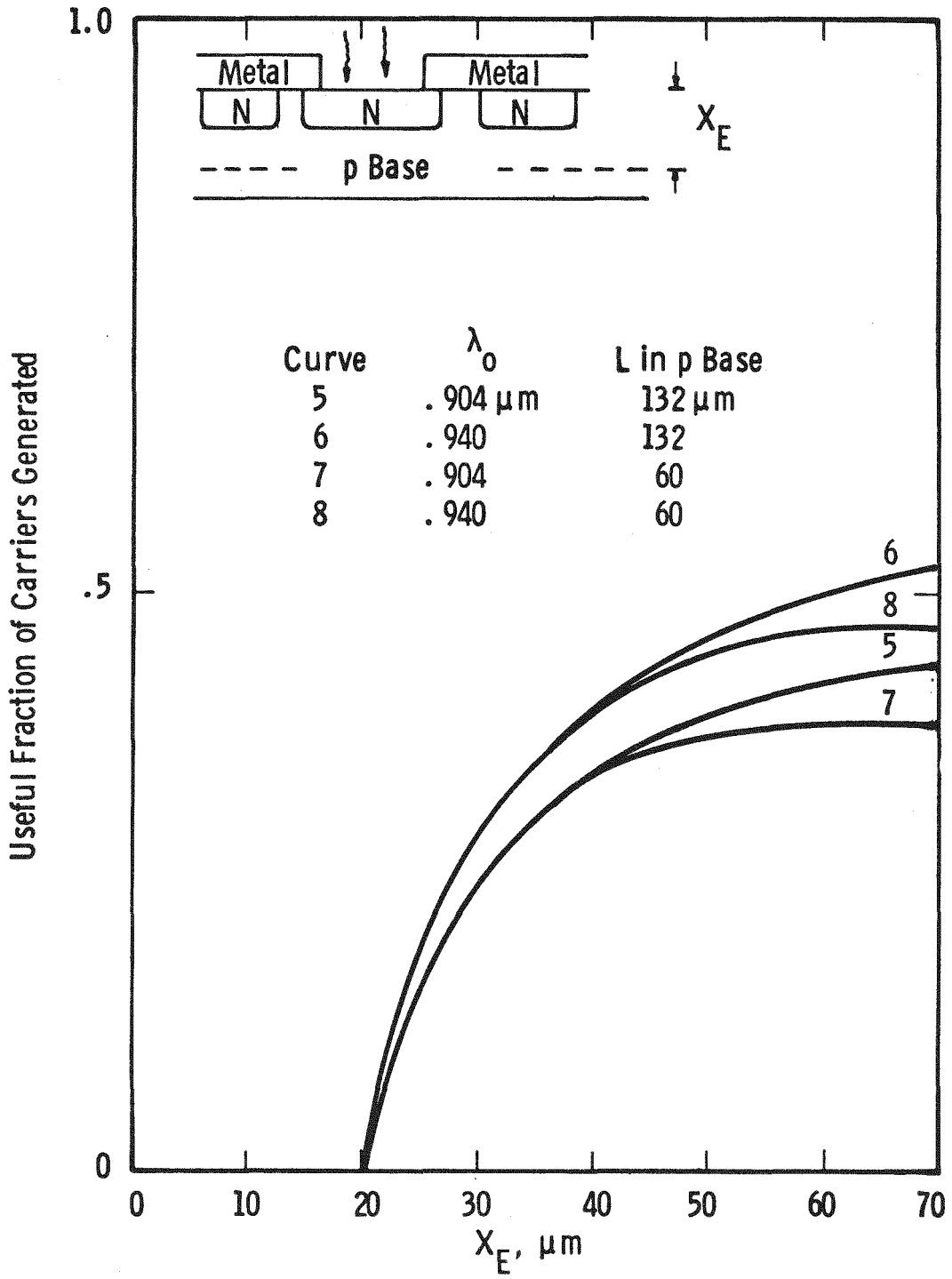

Fig. 2.7a —Useful fraction of carriers generated outside depletion layer. ·Design type 2.

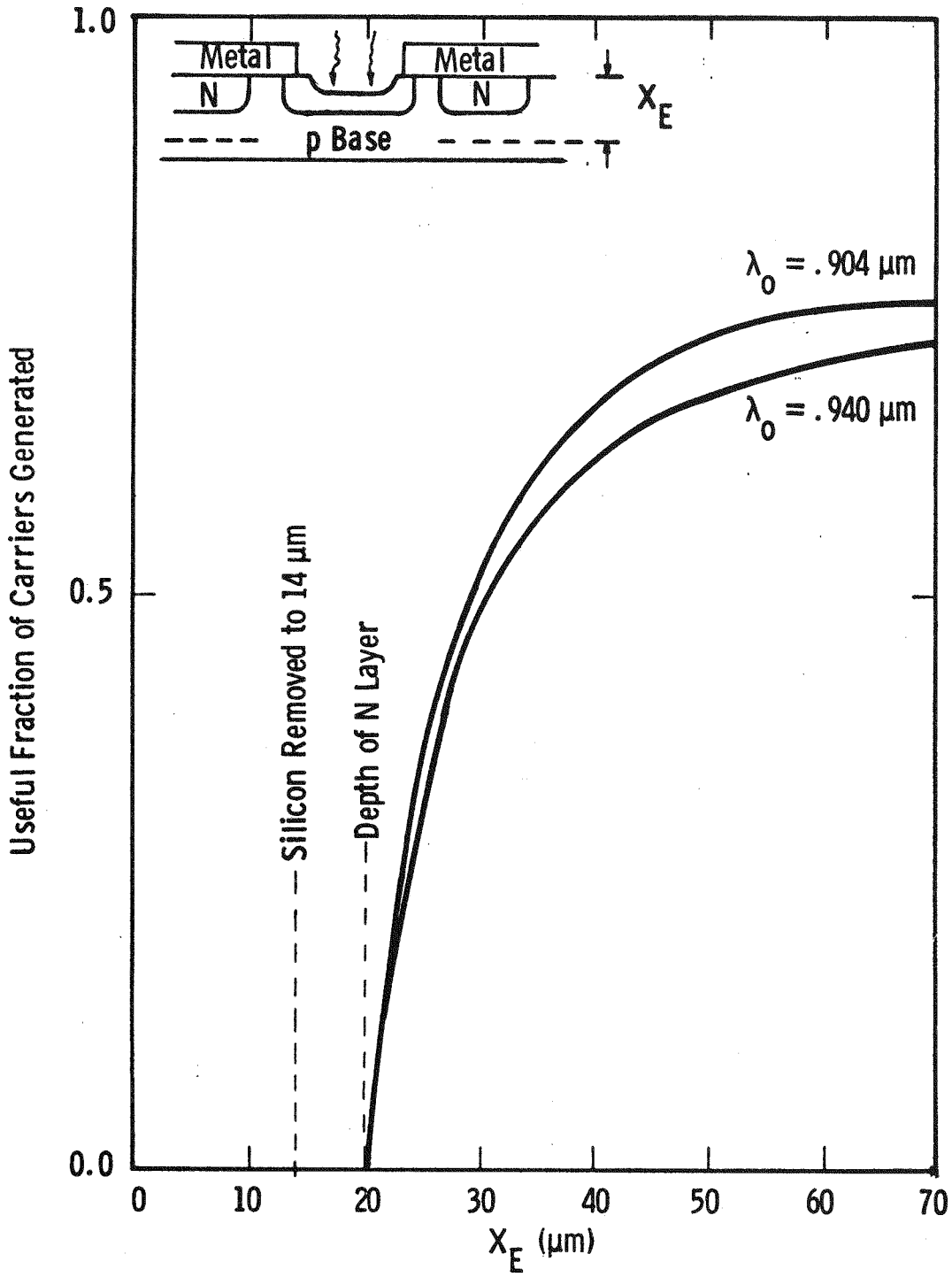

Fig.2.7b—Useful fraction of carriers generated outside depletion layer. Design type 2, 14 µm of silicon removed. L in p base = 132 µm

It is now possible to calculate the total fraction of light generated carriers which will be useful in providing trigger current to the thyristor. This fraction is the sum of:

1) those carriers, generated between the surface and X_E, which will diffuse to the depletion layer;
2) those carriers generated within the depletion layer; and
3) those carriers generated between X_D and a distance of one-half diffusion length beyond X_D.

The results of this summation for design type 1 are shown as curves in Fig. 2.8. The results for design type 2 with 14 μm of silicon removed are shown as "+" symbols.

In summary, the results in Figs. 2.6 through 2.8 show:

1) For applied voltages greater than 1000 V, the conversion of light photons to useful carriers is more than 90% efficient.
2) It is desirable to maintain diffusion length and lifetime at high values (> 132 μm, > 5 μs).
3) The conversion efficiency is not very sensitive to changes in light wavelength between 0.904 and 0.940 μm.

2.2.2 Structural Geometry of the Light Sensitive Region

The geometrical design variables relevant to the light sensitive region include:

1) all of the dimensions of the light sensitive region,
2) effects of an n region over the light sensitive area,
3) the advantages and disadvantages of gate amplification, and
4) the effects of etching away some silicon from the light sensitive region.

In order to cause the thyristor to turn on, the carriers generated by the light must cause a current to flow from the anode to the p base; this current must produce an IR voltage drop of 0.7 to 1.0 volts in the lateral resistance of the p base. Therefore, for sensitive turn-on, the lateral resistance in the p base must be made high. An upper limit on this lateral resistance is determined by the dV/dt rating required; dV/dt - induced displacement current also flows through the lateral resistance of the p base.

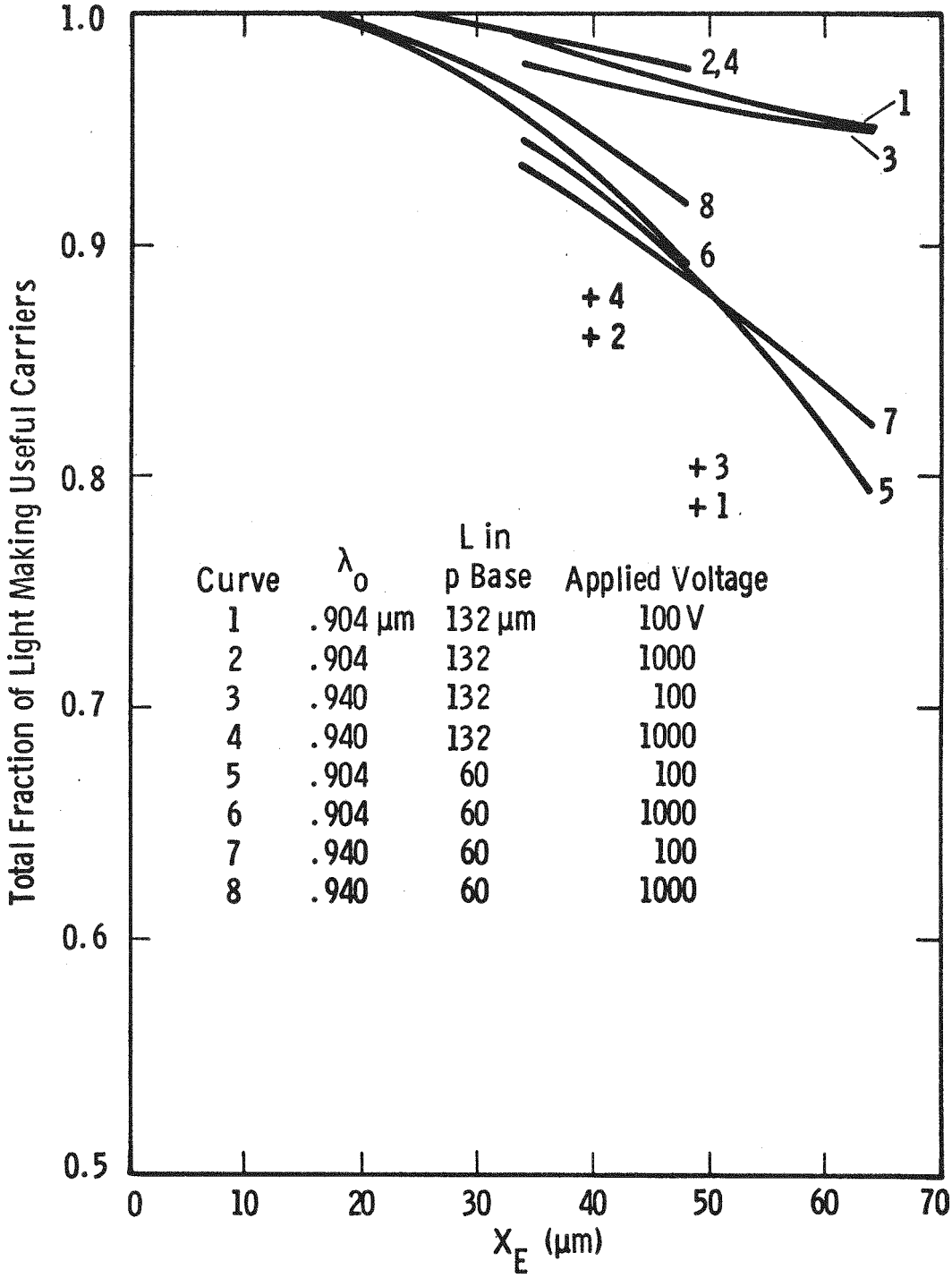

Fig. 2.8—The total fraction of light making useful carriers for various parameters

2.2.2.1 Trade-offs Between Sensitivity and dV/dt. A good design of a sensitive device with a high dV/dt rating takes advantage of the fact that, while dV/dt-induced current flows through the entire area of the thyristor, the triggering light pulse can be confined to a fairly small area, and the light-generated current can be forced to flow through p base resistances that increase as the illuminated area becomes smaller. Therefore, in general, the light-sensitive triggering region should be confined to as small an area as is practical. The following discussion provides a quantitative basis for design of the size of the light-sensitive region and the dimensions of the n region.

Consider the structure illustrated in Fig. 2.9. R_1 is the radius of a centrally located light pipe, R_2 is the radius of the inner edge of a cathode region, and R_3 is the radius of the outer edge of the cathode under which the 0.7 to 1.0 V must be developed. (This outer edge can be either the outer edge of the auxiliary cathode of an amplifying gate or the location of the first ring of emitter shunts in the main cathode.)

If current is generated uniformly in a region whose radius is R_1, and if R_2 is initially considered to be zero (i.e. the n region extends completely across the area illuminated by the light pipe), the voltage generated in the center of the illuminated area is:

$$V = \int_0^{R_1} \frac{\rho_s I_L \pi R^2}{\pi R_1^2 \pi 2R} dR + \int_{R_1}^{R_3} \frac{I_L \rho_s}{2\pi R} dR \qquad (2.6)$$

$$= \frac{I_L \rho_s}{2\pi} \left[\frac{1}{2} + \ell n \left(\frac{R_3}{R_1} \right) \right]$$

where I_L is the total light-generated current and ρ_s is the sheet resistivity of the p base.

If, instead of allowing an n region to cover the illuminated area, R_2 is designed to be 10% greater than R_1, the voltage would be:

$$V = \frac{I_1 \rho_s}{2\pi} \ell n \left(\frac{R_3}{1.1 R_1} \right) \qquad (2.7)$$

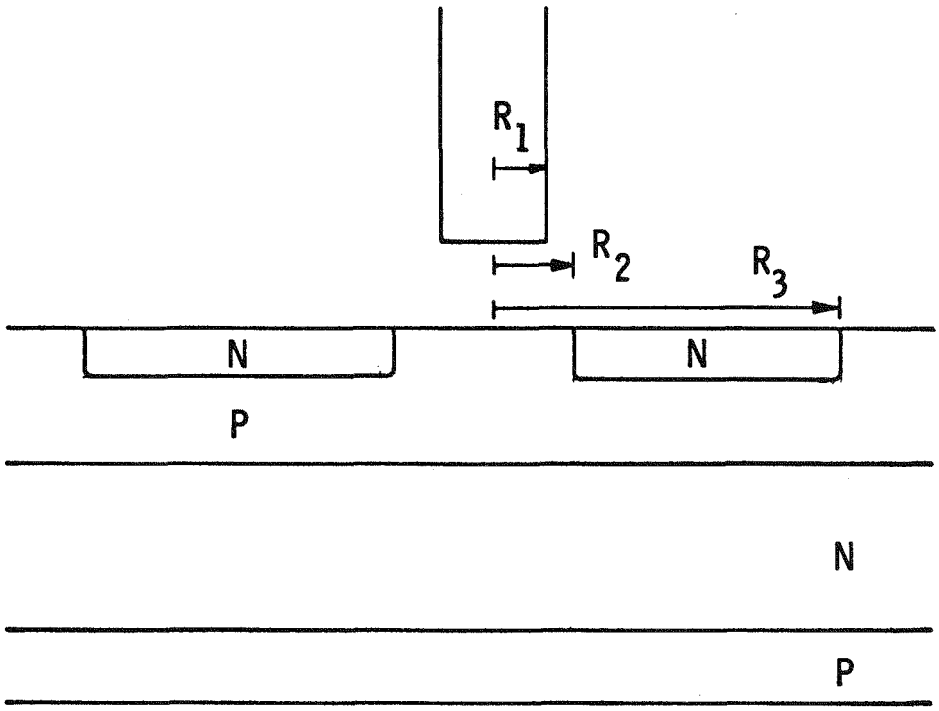

Fig. 2.9 – Diagram of the light-sensitive region

Then, assuming some reasonable values for R_1 and R_3 (say, 0.57 and 2.5 mm) it is seen that the previous design ($R_2 = 0$) would cause a voltage to be generated which is higher by the ratio:

$$\frac{1/2 + \frac{\ell n\ (\frac{2.5}{0.57})}{2.5}}{\ell n(\frac{2.5}{1.1 \times 0.57})} = 1.43 \qquad (2.8)$$

From this, it is obvious that a continuous n region over the illuminated area is desirable from the point of view of maximizing a voltage generated by a given light-induced current. On the other hand, as was shown in the preceeding section, a part of this advantage is lost because current generation is less efficient when the n layer is present.

From equations 2.6 and 2.7, it can be seen that it is desirable to keep R_1 small, i.e., to use as small a light pipe as possible without significantly decreasing the total amount of light to the thyristor.

The dV/dt rating of the thyristor is also dependent upon the design and dimensions of the light sensitive region. The T92N thyristor has a dV/dt rating of 1000 V/μs typical. This thyristor has a junction capacitance of approximately 250 pF/cm^2 at 40 V applied potential (less at higher applied potentials). A dV/dt excursion of 1000 V/μs will create a displacement current of 0.25 A/cm^2. The current flowing laterally through a circular elemental resistance of radius R will be:

$$I = 0.25\ \pi R^2 \text{ amperes.} \qquad (2.9)$$

This current will produce a voltage drop in the p base

$$dV = IdR = \frac{0.25\ \pi\ \rho_s\ R^2}{2\pi R}\ dR. \qquad (2.10)$$

Since ρ_s in the present design is approximately 600 ohms per square, integration of Eq. 2.10 from R_2 to R_3 as defined in Fig. 2.9, yields

$$V = 75\ (R_3^2 - R_2^2). \qquad (2.11)$$

To prevent accidental firing by a dV/dt excursion, V must be less than 0.7 V. Therefore, the maximum permissible value of R_3 can be calculated for various allowable values of dV/dt. (Table 2.2)

Table 2.2

MAXIMUM ALLOWABLE R_3 FOR TWO VALUES OF dV/dt RATING

MAXIMUM dV/dt RATING	R_2	MAXIMUM ALLOWABLE R_3
300 V/μs	0 cm (0 mil)	0.35 cm (138 mil)
300	0.09 cm (35 mil)	0.36 cm (142 mil)
1000	0 cm (0 mil)	0.19 cm (75 mil)
1000	0.09 cm (35 mil)	0.21 cm (83 mil)

The first generation thyristor designed for this program has R_2 = 0.09 cm and R_3=0.26 cm. These dimensions correspond to a dV/dt rating of nearly the 1000 V/μs value listed as typical for the T92N thyristor -- well above the minimum value of 300 V/μs.

2.2.2.2 Gate Amplification. Gate amplification is useful in thyristors that must operate in circuits with high dI/dt requirements. When the dI/dt is high an amplifying gate permits one to develop a fast turn-on in the relatively small auxiliary cathode and then to direct the rapidly rising anode current into a path that rapidly turns on the larger main cathode. On the other hand, when the dI/dt is small as it is in the application intended for this device, there is insufficient anode current available to rapidly turn on a large area of cathode (and therefore less need for a rapid turn-on process). In this case the presence of an amplifying gate merely degrades the dV/dt capability of the device without improving the light-triggered firing process.

2.2.3 Summary of the Theoretical Analysis

Summarizing these analyses of the structural geometry of the light sensitive region,

1) Maximizing the voltage drop in the thyristor p base maximizes the turn-on sensitivity of the thyristor for a given light-induced current. This voltage drop is maximized when the n region extends completely across the illuminated area.

2) The dV/dt capability of the thyristor is maximized when the the light sensitive region is made as small as is allowed by other considerations.

3) Gate amplification is not a desirable feature in a sensitive thyristor intended for low dI/dt operation.

2.3 EXPERIMENTAL STUDIES

There are a number of questions concerning the design of light-triggered thyristors that cannot be answered theoretically. Experimental studies were undertaken to provide the required information.

The questions that needed to be answered in this experimental effort were:

1) How does the short duration (0.08 - 0.20 μs) of the light pulse that can be obtained from high power solid state light sources affect the turn-on of a thyristor?
2) What size light pipe most effectively fires a thyristor (a large pipe will get more light to the thyristor, but a small pipe concentrates the light into a smaller volume)?
3) How do the preparation and condition of the silicon surface affect the firing sensitivity?
4) What are the relative advantages of firing near the thyristor edge as opposed to firing in the center?
5) How do anode voltage and circuit-limited dI/dt affect the firing sensitivity?
6) How does the design of the light-sensitive area affect the latching and holding current parameters?
7) Are there any unknown or unforeseen factors that affect the sensitivity, latching current, or holding current?

To study the effects of short triggering pulse widths, measurements were made on electrically gated thyristors, measuring the relationship between trigger pulse current and trigger pulse width for a pulse just sufficient to cause turn-on. The data in Fig. 2.10 show that the integrated charge required to trigger a thyristor decreases as the trigger pulse width is decreased.

To answer other questions related to the design of light-triggered thyristors, a set of test structures was designed and fabricated. Figure 2.11 is a photograph of one of these test structures, showing a variety of light-sensitive area designs.

1) With and without an n emitter region over the light-sensitive area.
2) With and without gate amplification (both single stage and two stage).
3) A range of dimensions.
4) Center-fired regions and edge-fired regions.

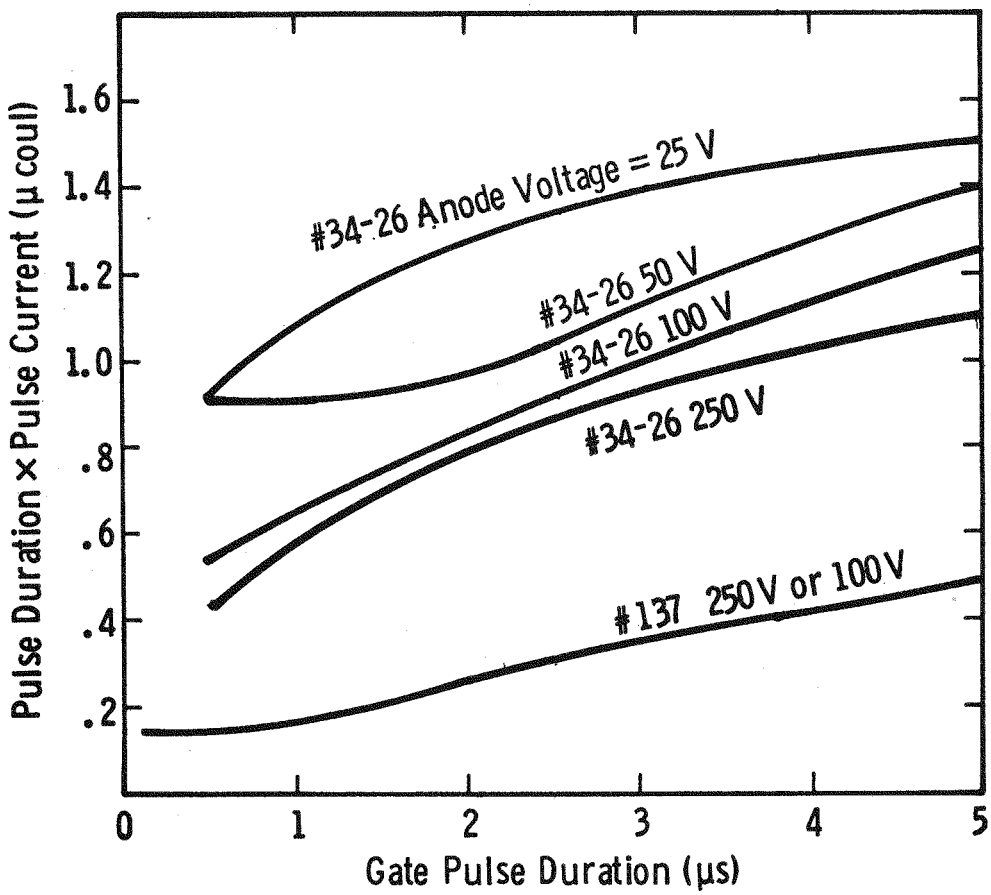

Fig. 2.10 — Minimum electrical gate signal required to fire two conventional thyristor designs (#34-26 and #137). Relationship shown between gate pulse width, gate pulse charge, and anode voltage

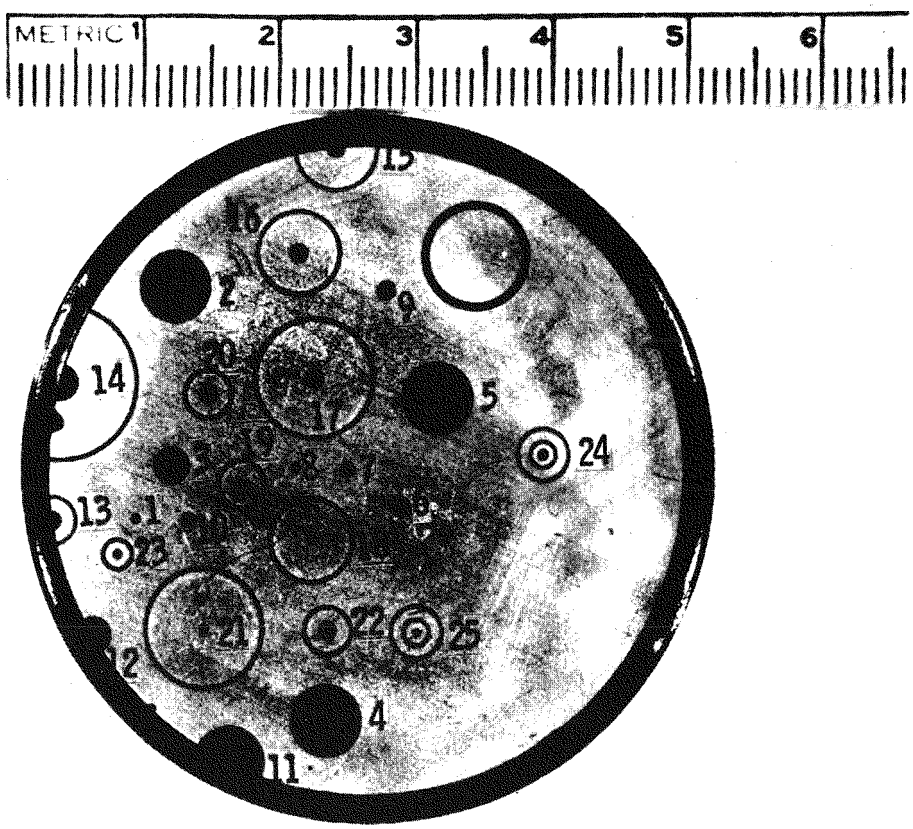

Fig. 2.11 – Test structure pattern identification

Light sources used in taking experimental data are the Spectronics 5453-4 light emitting diode and the American Laser Systems 729 A/B laser diode. These were coupled to one meter long fiber optic cables of 0.75, 1.1, and 2.2 mm diameter. The amount of light energy transmitted through these cables was measured with an EG&G model 450 radiometer. Curves of light output from each light source through each fiber optic cable with various peak drive currents are shown in Figs. 2.12 and 2.13. The current range shown in Fig. 2.13 is the entire range over which that particular model of laser diode can be used. Neutral density filters were used in some experiments to obtain lower light levels. The waveform of the drive current for the laser diode is shown in Fig. 2.14.

The output end of the light pipe under test was mounted on a three dimensional micromanipulator. Each sensitivity measurement was made with the light pipe located in an optimum x-y position for a particular light-sensitive area design.

The relative ease with which each light-sensitive area design could be fired was experimentally determined by measuring the minimum light level required for firing each pattern. The patterns are identified by numbers in Fig. 2.11; their dimensions are given in Table 2.3 The pattern identification number shown on each graph is that defined in Fig. 2.11. Figures 2.15 and 2.16 show the measured minimum light energy (at λ_o = 0.904 μm) required to fire each pattern. Applied voltage was 50 V unless otherwise noted (it was experimentally determined that light sensitivity was not a function of applied voltage above 20-30 V). The circuit-limited dI/dt was 6 A/μs.

Data are given for light sensitive regions both with (n center) and without (p center) an n region covering the illuminated area. The absence of a datum point indicates that the particular pattern did not fire with the maximum available light energy. A datum point shown as an open circle indicates that the pattern fired with less than the minimum calibrated light energy. Experimental data showed that no additional sensitivity accrued to firing thyristors near the edge, so the data in Figs. 2.15 and 2.16 do not include the edge-located patterns (patterns 11-15).

The experimental data shown in Figs. 2.15 and 2.16 show:

1) Light sensitive areas with p centers are more sensitive than those with n centers.
2) Gate amplification does not improve sensitivity.
3) The 1.1 mm diameter light pipe fired the largest number of patterns with the minimum light energy and is the best choice for system use.

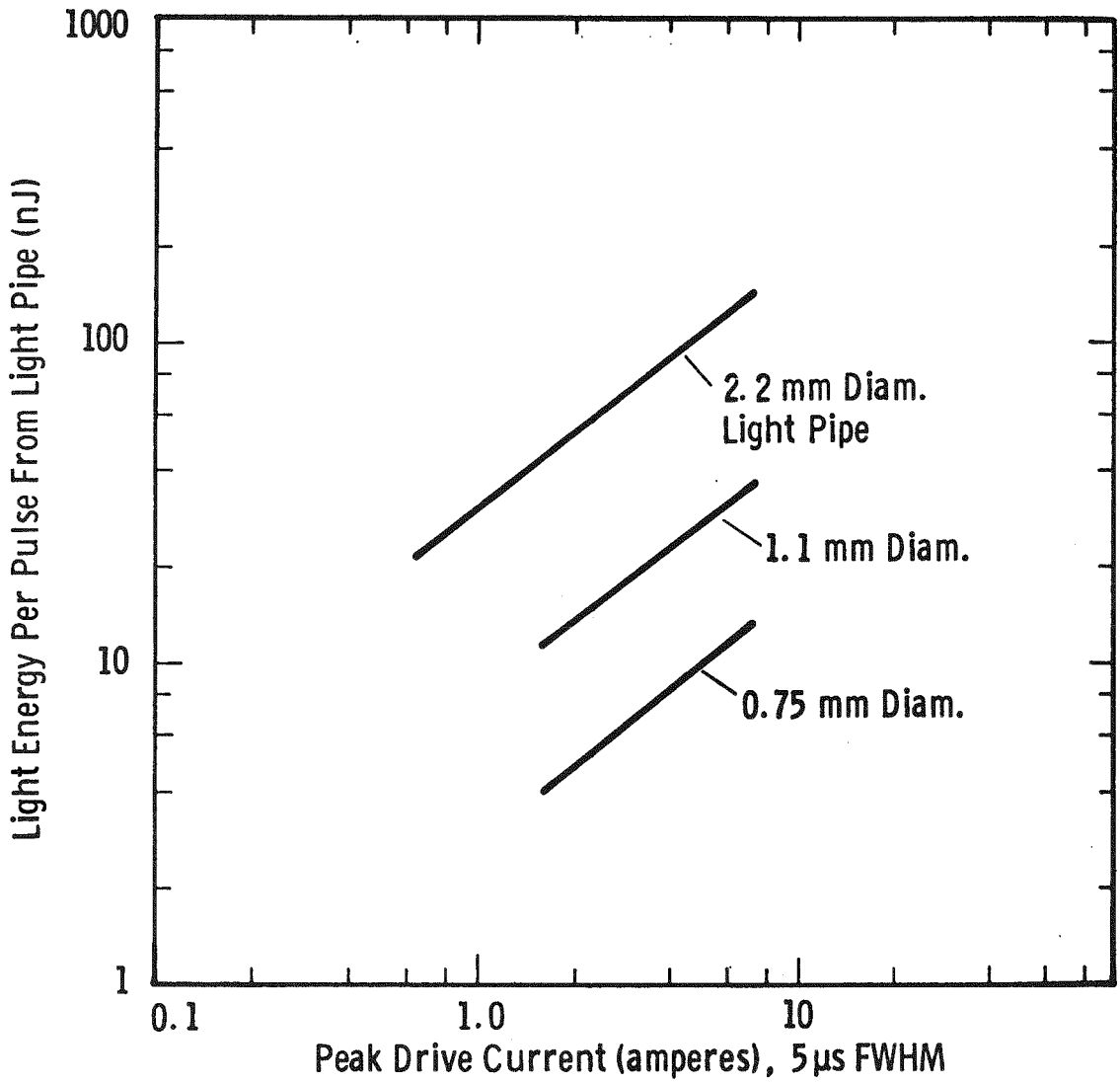

Fig. 2.12 – Spectronics 5453-4 LED. Output energy vs. drive current

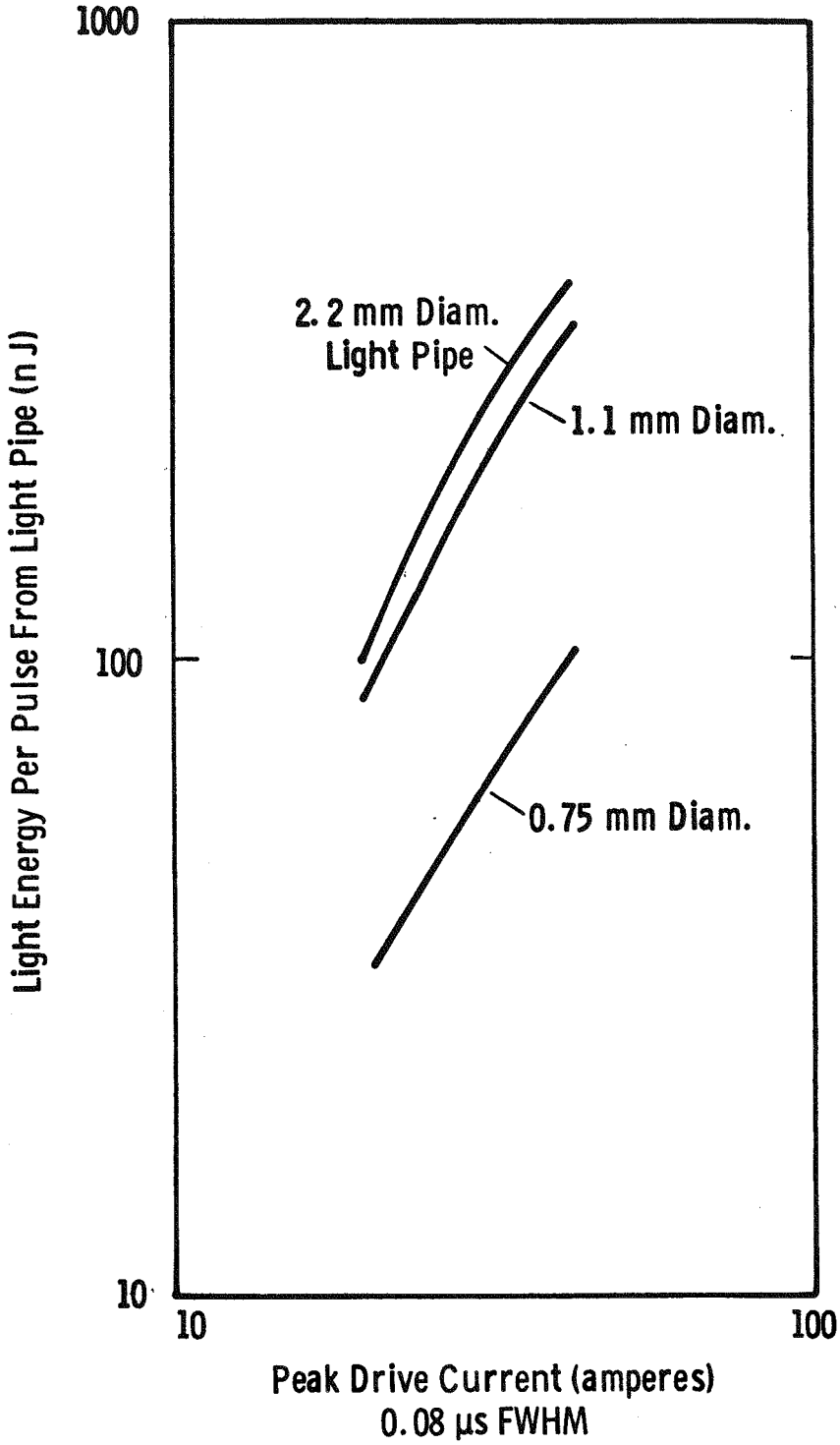

Fig. 2.13 — American laser systems 729 A/B laser diode. Output energy vs. drive current

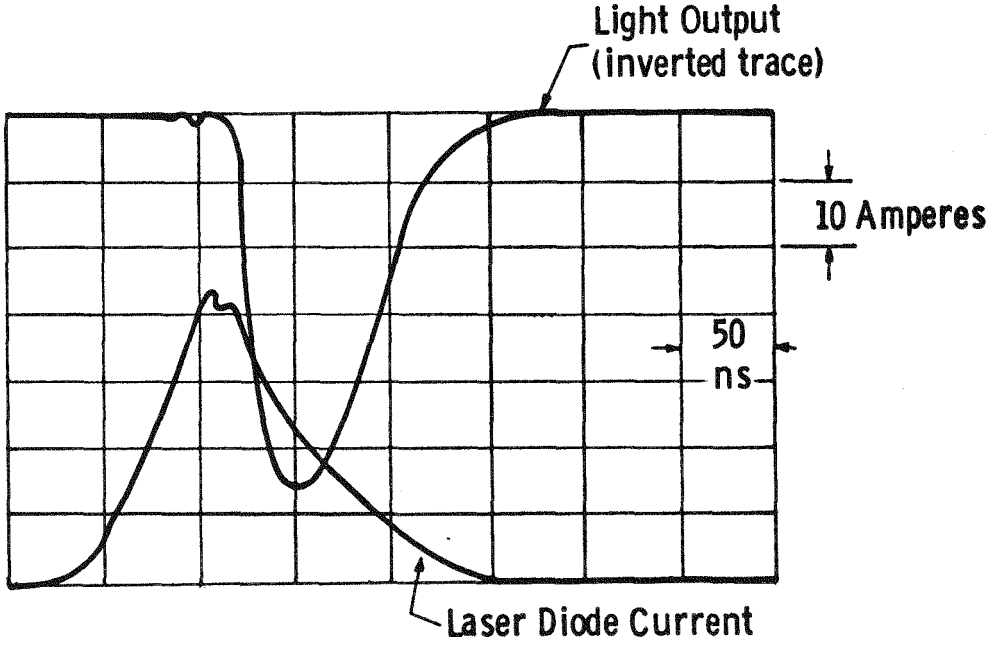

Fig. 2.14 — Waveform of drive current and light output of ALS laser diode

Table 2.3

DIMENSIONS OF TEST STRUCTURE PATTERNS

TEST PATTERN IDENTIFICATION	R_2	R_3	R_4	R_5
1				0.30 mm
2				2.50 mm
3				1.25 mm
4				2.50 mm
5				2.50 mm
6				0.63 mm
7				0.45 mm
8				0.30 mm
9				0.63 mm
10				0.45 mm
11				2.50 mm
12				1.25 mm
13		0.63 mm	1.25 mm	1.75 mm
14		1.25 mm	5.00 mm	5.50 mm
15		0.63 mm	2.50 mm	3.00 mm
16		0.63 mm	2.50 mm	3.00 mm
17		0.63 mm	3.75 mm	4.25 mm
18		0.30 mm	2.50 mm	3.00 mm
19		0.30 mm	1.25 mm	1.75 mm
20		0.63 mm	1.25 mm	1.75 mm
21		0.30 mm	3.75 mm	4.25 mm
22		0.63 mm	1.25 mm	1.75 mm
23		0.30 mm	0.63 mm	1.13 mm
24	0.50 mm	1.00 mm	1.40 mm	1.90 mm
25	0.38 mm	1.00 mm	1.40 mm	1.90 mm

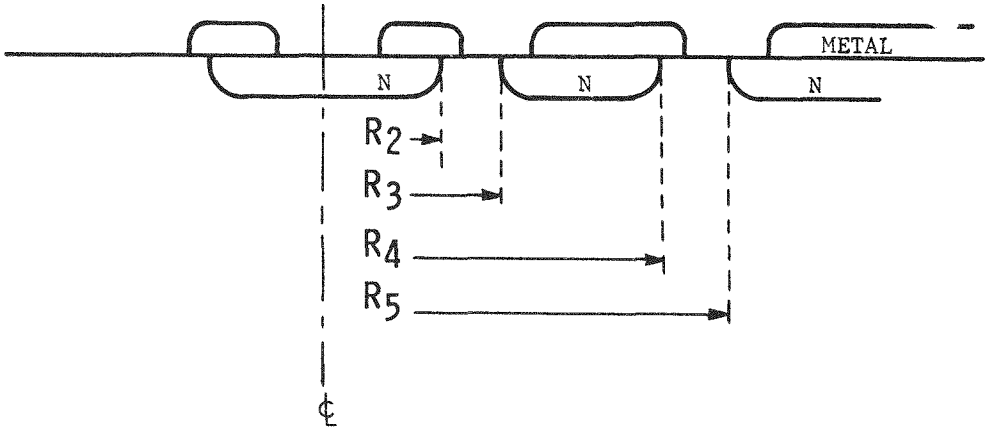

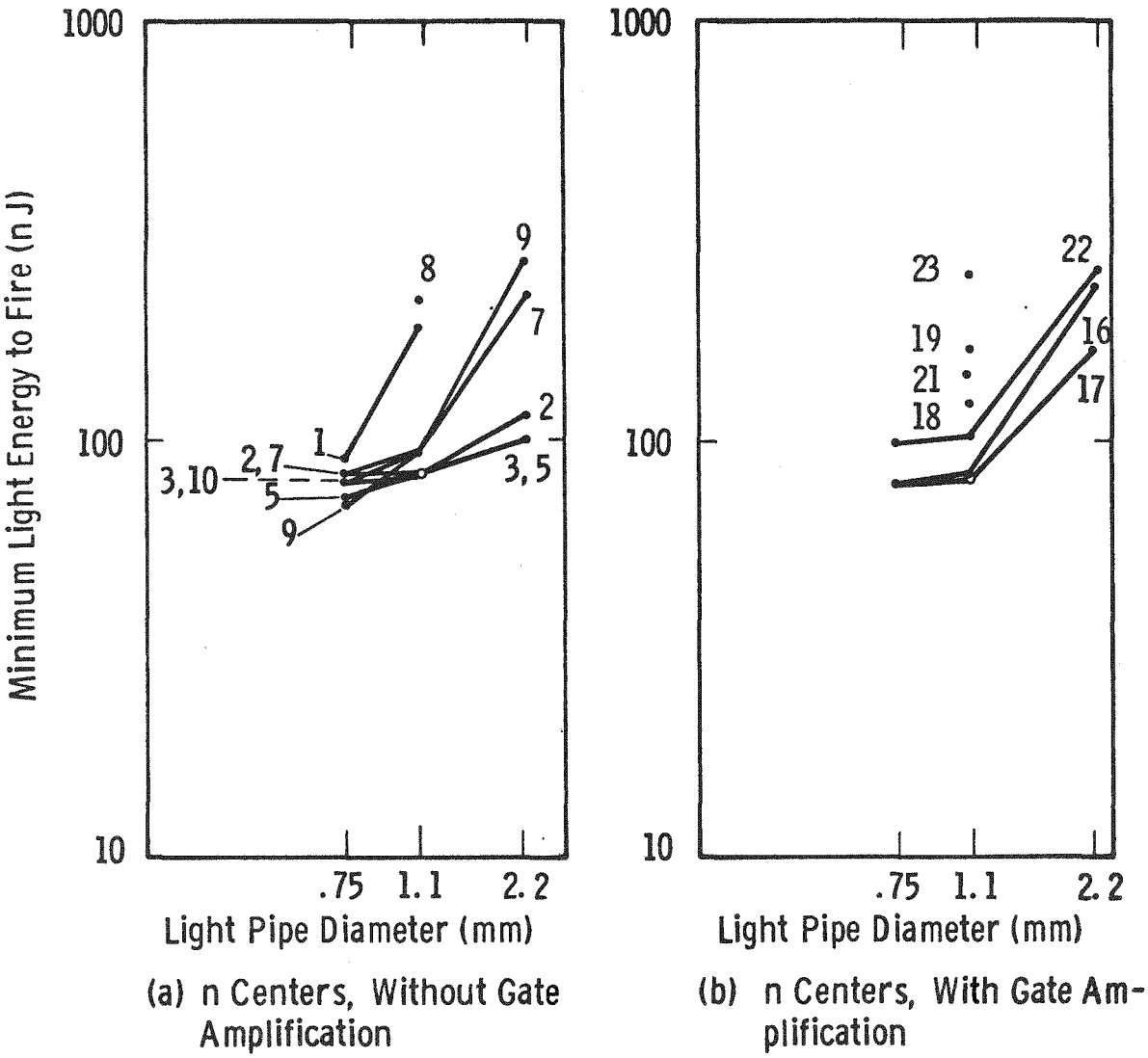

(a) n Centers, Without Gate Amplification

(b) n Centers, With Gate Amplification

Fig. 2.15 —Minimum light energy required to cause turn-on

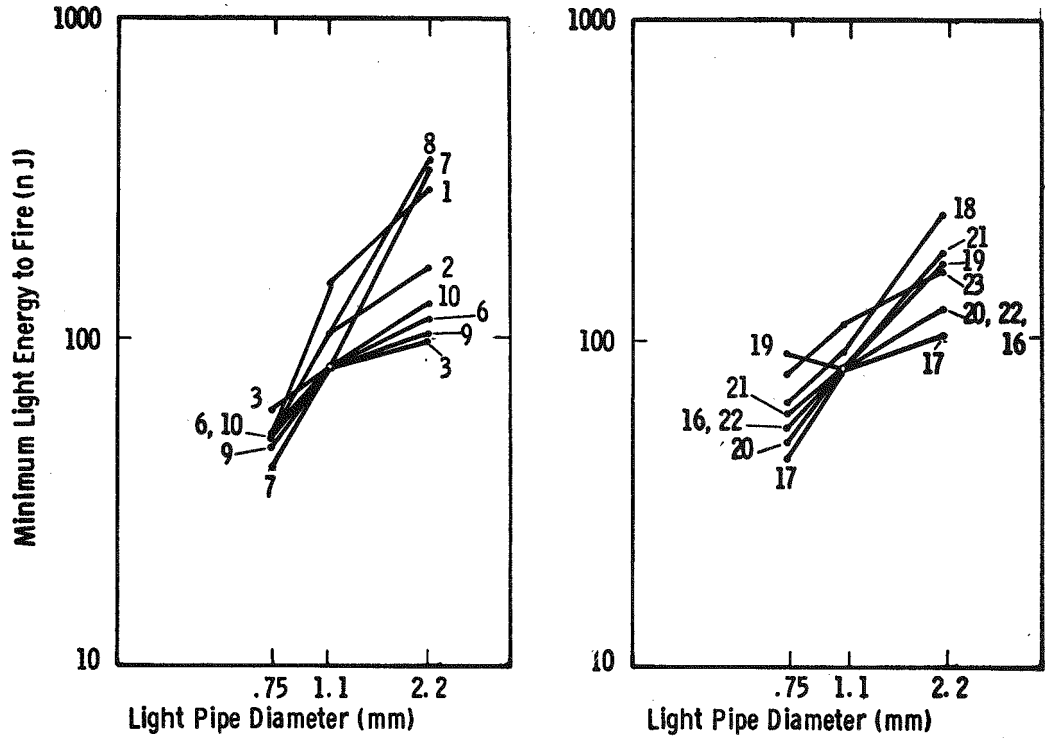

(a) p Centers Without Gate Amplification

(b) p Centers With Gate Amplification

Fig. 2.16—Minimum light energy required to cause turn-on

Figure 2.17 shows similar experimental data obtained under different conditions. The circuit-limited dI/dt was decreased from 6.0 to 0.01 A/μs (the dI/dt to be expected in the final system use is well within this range) and a set of neutral density filters was used to extend the light energy calibration to lower values. In this series of measurements, only the 1.1 mm diameter light pipe was used.

The data shown in Fig. 2.18 show:

1) Patterns with p centers are much more sensitive than those with n centers.
2) The sensitivity of all patterns is decreased somewhat at low circuit-limited dI/dt.

The latching currents for each pattern, given in Table 2.3 are well below the 400 mA typical of the T92N thyristor, so no problems are expected in this area.

The data shown in Figs. 2.15, 2.16 and 2.17 and in Table 2.4 show that for maximum sensitivity,

1) An n region should not cover the light sensitive area.
2) Gate amplification is a disadvantage.
3) The diameter of the light sensitive region should be between 0.90 and 5.0 mm.

The measurements described above were made with the light pipe in an optimum position for each pattern. Under this condition, the maximum sensitivity was not related to pattern size over a large range of sizes. However, when the light-sensitive region was much larger than the end of the light pipe, the optimum position was always near an edge of the light sensitive region, as illustrated in Fig. 2.18. An explanation of the behavior is that, when light creates carriers near an edge, the lines of current flow are concentrated near that edge. This higher current density creates locally higher electric fields and therefore higher voltage drops than if the current density were uniform around the edge. Therefore, use of a large light sensitive area will not eliminate the requirement for careful alignment of the light pipe to the thyristor. In addition, for good dV/dt performance, the optimum size of the light sensitive area should be only slightly larger than the light pipe that illuminates it. Therefore, the first generation thyristor design includes a light sensitive area of 1.78 mm diameter.

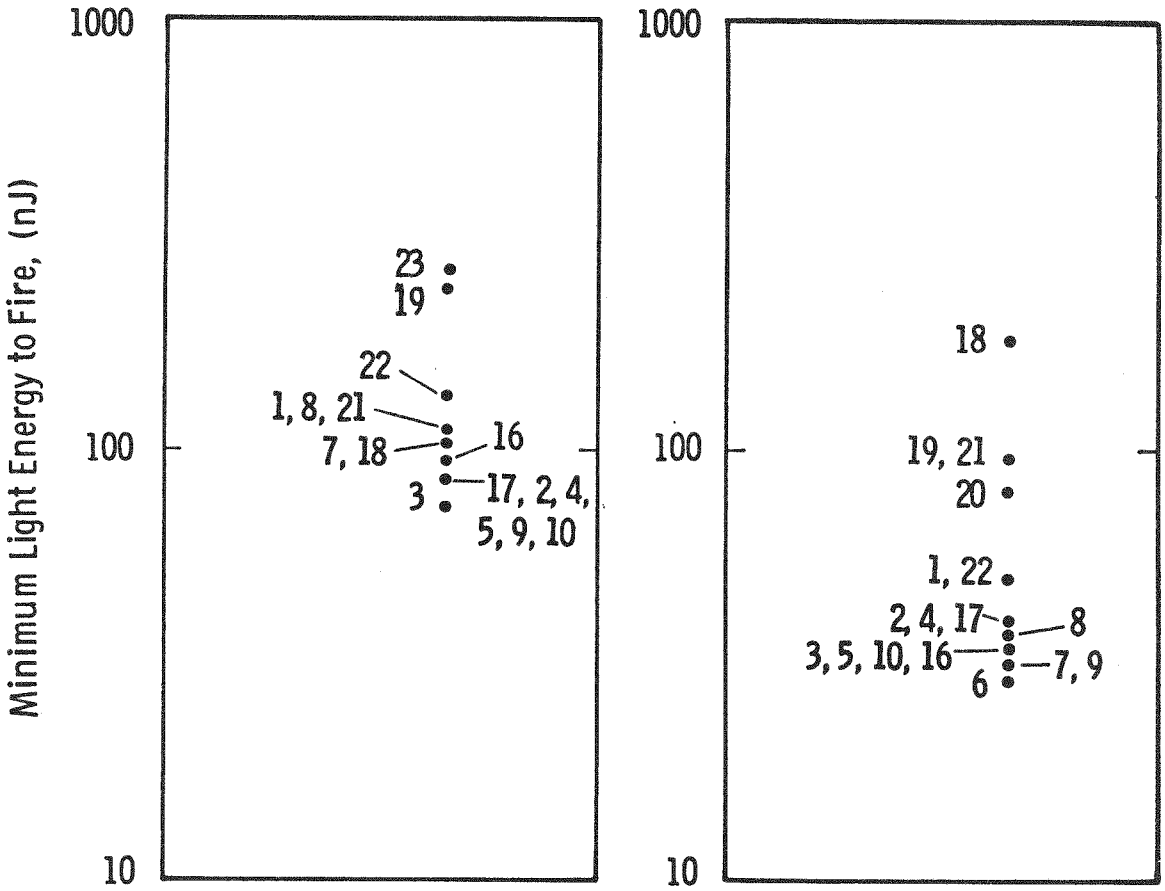

Light Pipe Diameter = 1.1 mm

(a) n Centers, 0.01 A/μs

Light Pipe Diameter = 1.1 mm

(b) p Centers, 0.01 A/μs

Fig. 2.17 — Minimum light energy required to cause turn-on at very low dI/dt

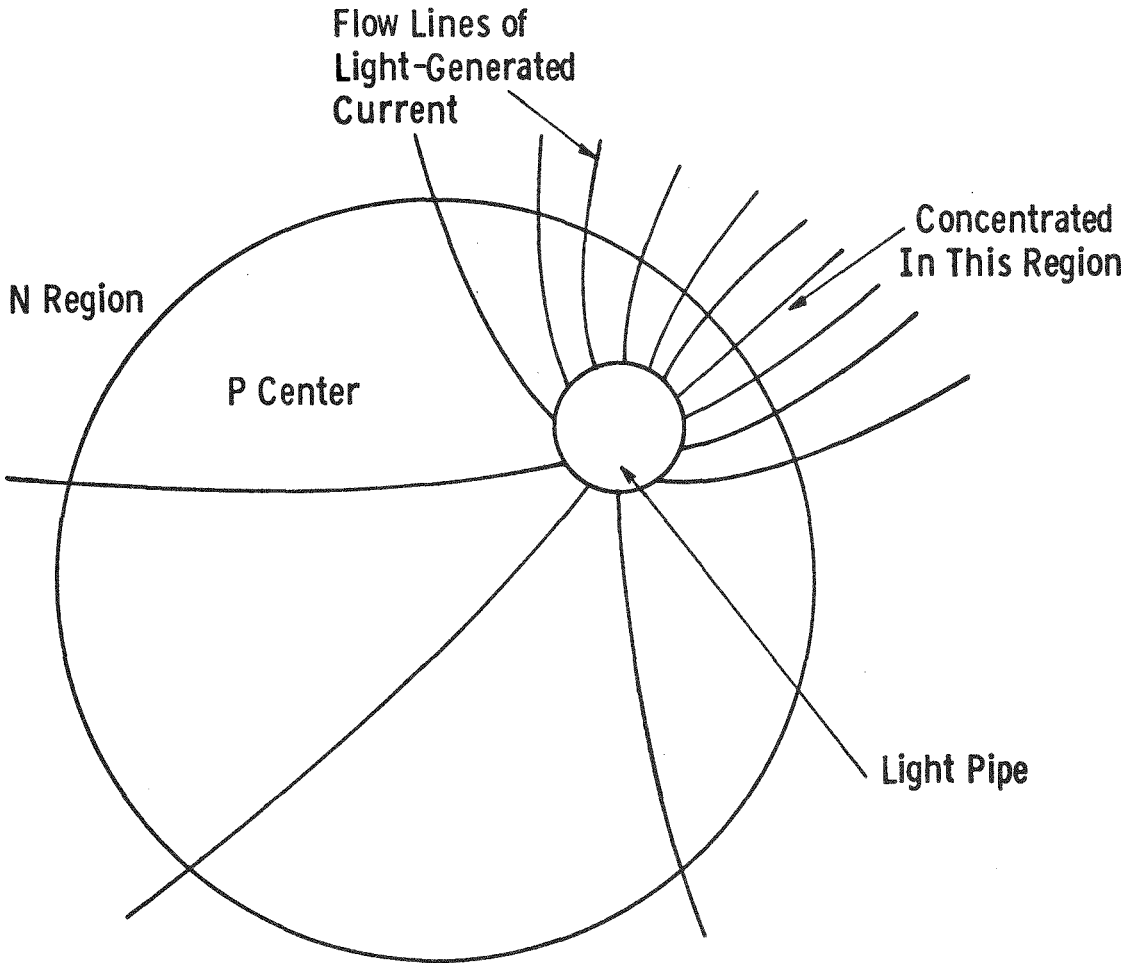

Fig. 2.18 – Concentrated current flow near the edge of a large light-sensitive region

Table 2.4

LATCHING CURRENTS

PATTERN NO.	LATCHING CURRENT P CENTER	LATCHING CURRENT N CENTER
1	20 ma	7 ma
2	30 ma	10 ma
3	35 ma	9 ma
4	30 ma	15 ma
5	32 ma	10 ma
6	30 ma	10 ma
7	30 ma	8 ma
8	30 ma	12 ma
9	46 ma	10 ma
10	20 ma	8 ma
11	48 ma	15 ma
12	32 ma	18 ma
13	32 ma	40 ma
14	55 ma	48 ma
15	78 ma	54 ma
16	80 ma	13 ma
17	95 ma	10 ma
18	85 ma	10 ma
19	85 ma	42 ma
20	55 ma	42 ma
21	90 ma	10 ma
22	75 ma	15 ma
23	65 ma	26 ma
24		47 ma
25		60 ma

di/dt = 0.01 A/sec V_A = 50 V 1.1 mm diam. light pipe

A somewhat similar consideration applies to the condition of the silicon surface in the light sensitive region. If the surface recombination velocity is high, light-generated carriers will be lost through recombination at the surface before they can diffuse to the depletion region and contribute to useful current. It is well known that the best (lowest) surface recombination velocity is obtained on thermally oxidized silicon surfaces.* Efforts to further improve the sensitivity of test patterns by removing part of the silicon have consistently decreased the sensitivity by about a factor of two, over a wide range of light intensities and angles of incidence. The effect is the same whether silicon is removed chemically or by mechanical polishing. At this time, it appears that removal of silicon will be neither useful nor necessary. If silicon removal is considered desirable at some later time, it should be done before the final thermally grown oxide is formed.

The minimum light energy required to fire the thyristor having been measured, it remained to be determined what value of light energy is required to cause thyristor firing with a practical, short, and reproducible delay time. A short and consistent delay time is desirable so that thyristors to be installed in a series string will operate well together.

Figure 2.19 shows photographs of anode voltage waveforms for a range of light levels. The anode supply voltage was 50 V. Circuit inductance was used to vary the current rate of rise to 0.01 A/μs or 0.5 A/μs. Data of this type showed that a light pulse energy of at least 300 nJ should be used to trigger a thyristor of this type.

2.4 CHARACTERIZATION OF FABRICATED THYRISTORS

Thyristors representing various processing variations were characterized. These characterizations were intended to furnish data useful to thyristor design considerations and were not always performed under those standard conditions which establish commercial specifications; measurements under standard conditions are discussed in Section 5.

---

*A. S. Grove, Physics and Technology of Semiconductor Devices, John Wiley and Sons, Inc., p. 222 (1967).

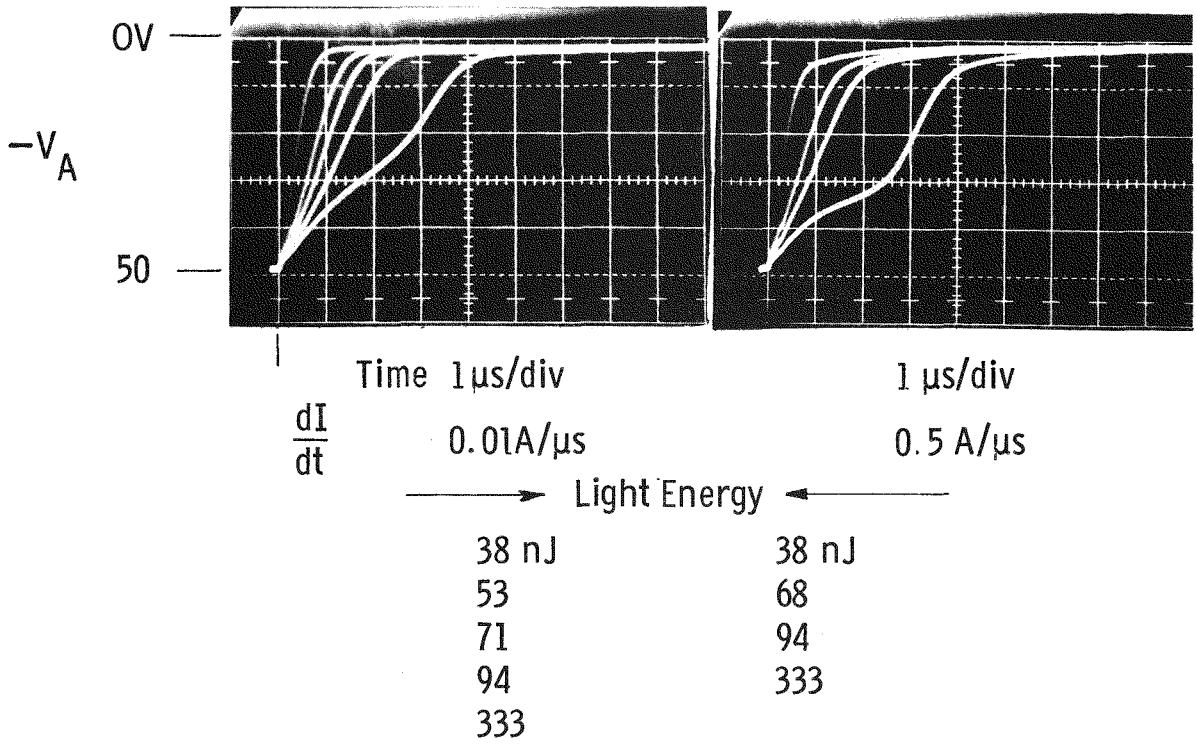

Fig. 2.19 – Turn-on delay time and light pulse energy

2.4.1 Turn-on

The most important concern of the designer of a high power thyristor to be triggered in series strings with a minimum of triggering light is that the turn-on be fast with a short delay time and low switching losses.

The turn-on behavior of the first lot of devices is shown in Fig. 2.20a and 2.20b. The target specifications (Section 2.1) call for a maximum delay time of 1.5 μsec and a maximum turn-on time of 3.5 μsec when turned on from 1100 volts at 25°C. The delay time is the time from the onset of the light pulse to the time when the anode voltage has fallen to 90% of its starting value. The turn-on time is the time from the onset of the light pulse to the time at which the anode voltage has fallen to 10% of its starting value. Figures 2.20a and 2.20b show that the thyristors having n-type light-sensitive regions have delay times of 0.85 to 1.2 μsec when 250 nJ of light energy is used. The delay is still only 1.3 μsec when the light energy is decreased to 140 nJ. This demonstrates that the objective for delay time can be easily met with the planned 300 nJ light trigger.

Figures 2.20a and 2.20b show that the turn-on time objective of 3.5 μsec is not so easily met when the anode voltage is low (600V). The turn-on time data were taken on a circuit that has a limited anode voltage capability. The objective specification calls for turn-on to be measured from an anode voltage of 1100V, but a test circuit with this capability was not available at that time. Data shown in Fig. 2.21 show that dynamic forward drop at 3.5 μsec is relatively insensitive to variations in the starting anode voltage. Thus if these data had been taken using a circuit capable of providing 1100V, the 10% voltage level would have been reached earlier and the turn-on times would have been significantly shorter. Note that this is observed both at high and low anode dI/dt levels (which were controlled by different values of inductance in series with the anode).

The light energy used in Fig. 2.21 was 950 nJ -- more than three times the 300 nJ planned for rated use. However, as is shown in Fig. 2.22, the triggering light energy has little effect on the anode voltage waveforms (other than to affect the delay time) for either high or low values of circuit-limited dI/dt. Thus it was concluded at that time (and was later shown to be true) that the turn-on time specifications would be met when the proper anode voltage and light energies were used.

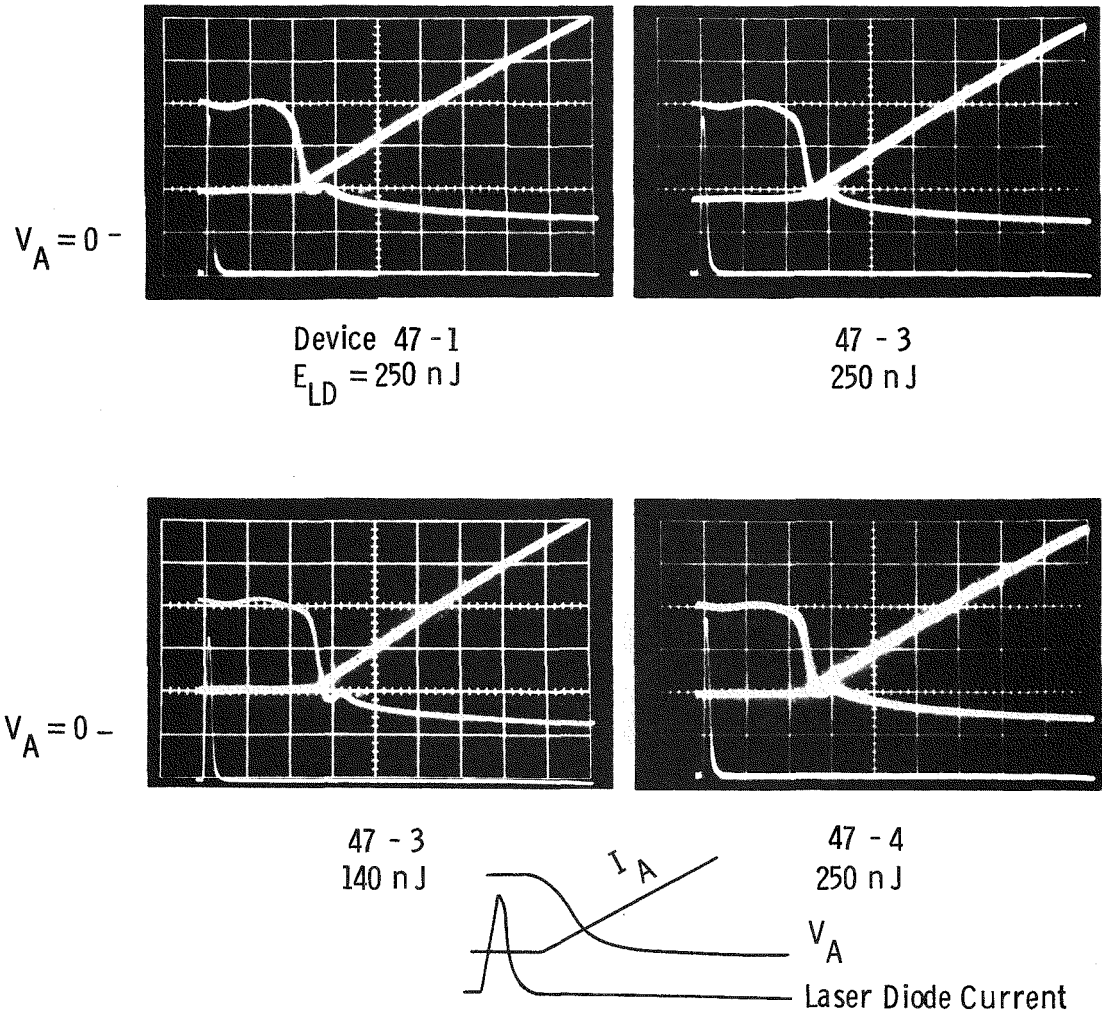

Fig. 2.20a – Turn-on, first lot (N centers, run 03236).
V_A = 200 V/Div, I_A and I_{LD} = 20 A/Div, Time axis = 0.5 µs/Div.
d I/dt = 25 A/µs. T = 25° C

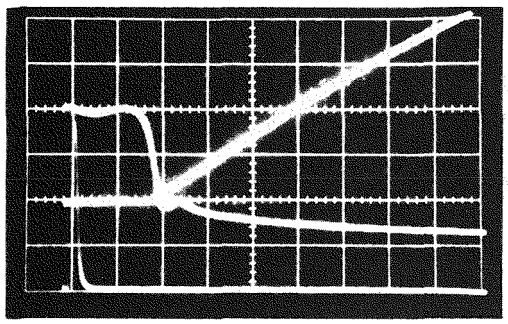

47 - 5
250 n J

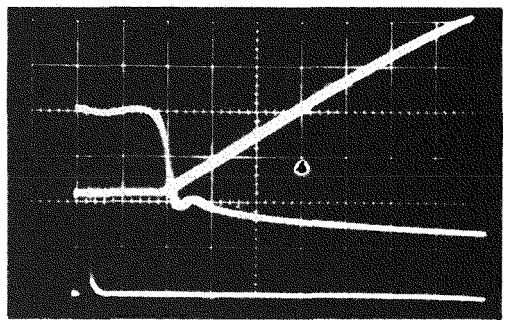

47 - 5
155 n J

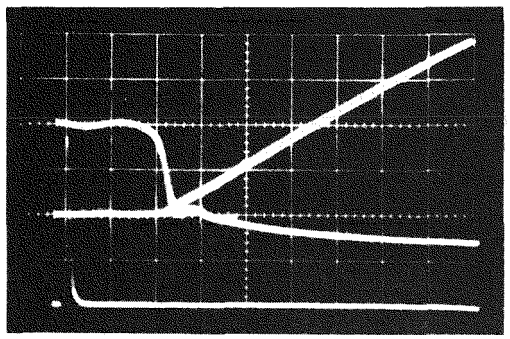

47 - 6
250 n J

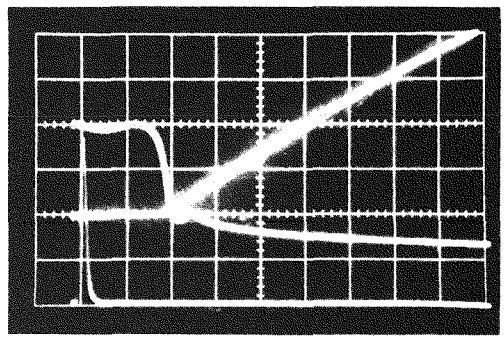

47 - 7
250 n J

Fig. 2.20b — Turn-on waveforms

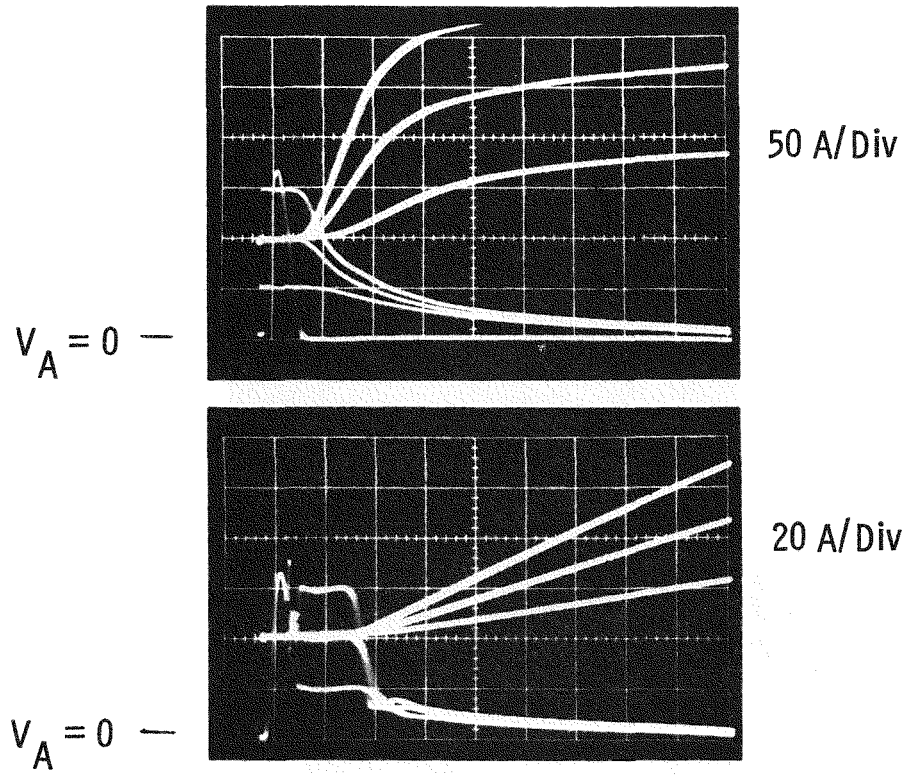

Fig. 2.21 – Turn-on, effects of V_A and dI/dt. V_A = 200 V/Div, Time Axis = 0.5 µs/Div. Light energy = 950 nJ. T = 25° C. Run 03236, device 47-7

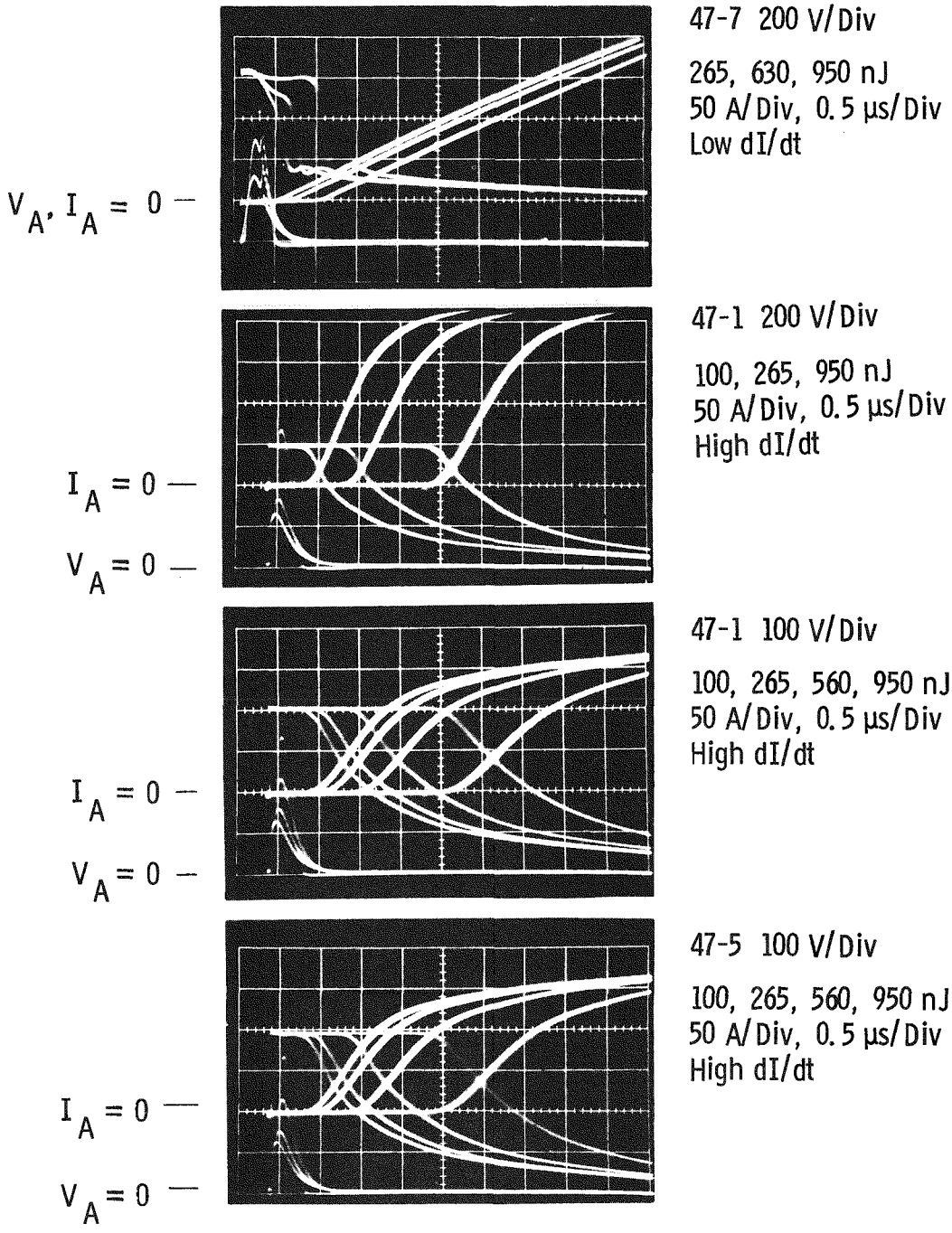

Fig. 2.22 – Turn-on, long light trigger (RCA source). T = 25° C. (Fastest response corresponds with highest light energy.)

In order to permit the determination of the light energy directly from subsequent figures, Fig. 2.23 is a calibration curve of the light energy per pulse from the end of a 1.1 mm dia. light pipe as a function of the peak laser diode current.

Figure 2.24 shows turn-on data taken on the thyristors from the second processing run. From Fig. 2.23, the 300 nJ of light energy corresponds to a peak diode current of 33A. Thus from Fig. 2.24 one can see that the delay times for 300 nJ of light energy were $\sim$ 0.9 μsec and the turn-on times were similar to those of Fig. 2.20. The same considerations concerning the anode voltage discussed above apply here.

Figure 2.25 shows additional data taken to compare the devices made with p vs. n-type light-sensitive regions for two sets of anode voltage and anode dI/dt conditions. All of the data support the view that p-centers are better. That is, for the same light energy, those thyristors with p-type light sensitive areas have a shorter delay time than those with n-type areas.

Figure 2.26 shows the waveforms of the turn-on of a device with a p-type center as a function of anode voltage demonstrating that for p-type centers as well as n-type centers (Fig. 2.21) the waveform of the dynamic forward drop after the region of fast anode voltage fall is fairly independent of the starting anode voltage.

The decision to use p-type light sensitive regions is based on the fact that more useful carriers are directly created by the light; therefore, the minimum light needed to fire the device is lower and the delay time for any given light input energy is shorter. There is, however, a potential disadvantage. As reported in Section 2.3, the effectiveness of the light is more sensitive to the alignment of the light spot to the light sensitive area of the thyristor when the light sensitive region is p-type. This calls for greater precision of light pipe-to-thyristor alignment in the case of p-type light sensitive regions. Typical waveforms showing the effect of different positions of a 1.1 mm diameter light pipe in a 1.8 mm diameter p-type light sensitive area are shown in Fig. 2.27. It is believed that the required alignment accuracy can be achieved in the thyristor package.

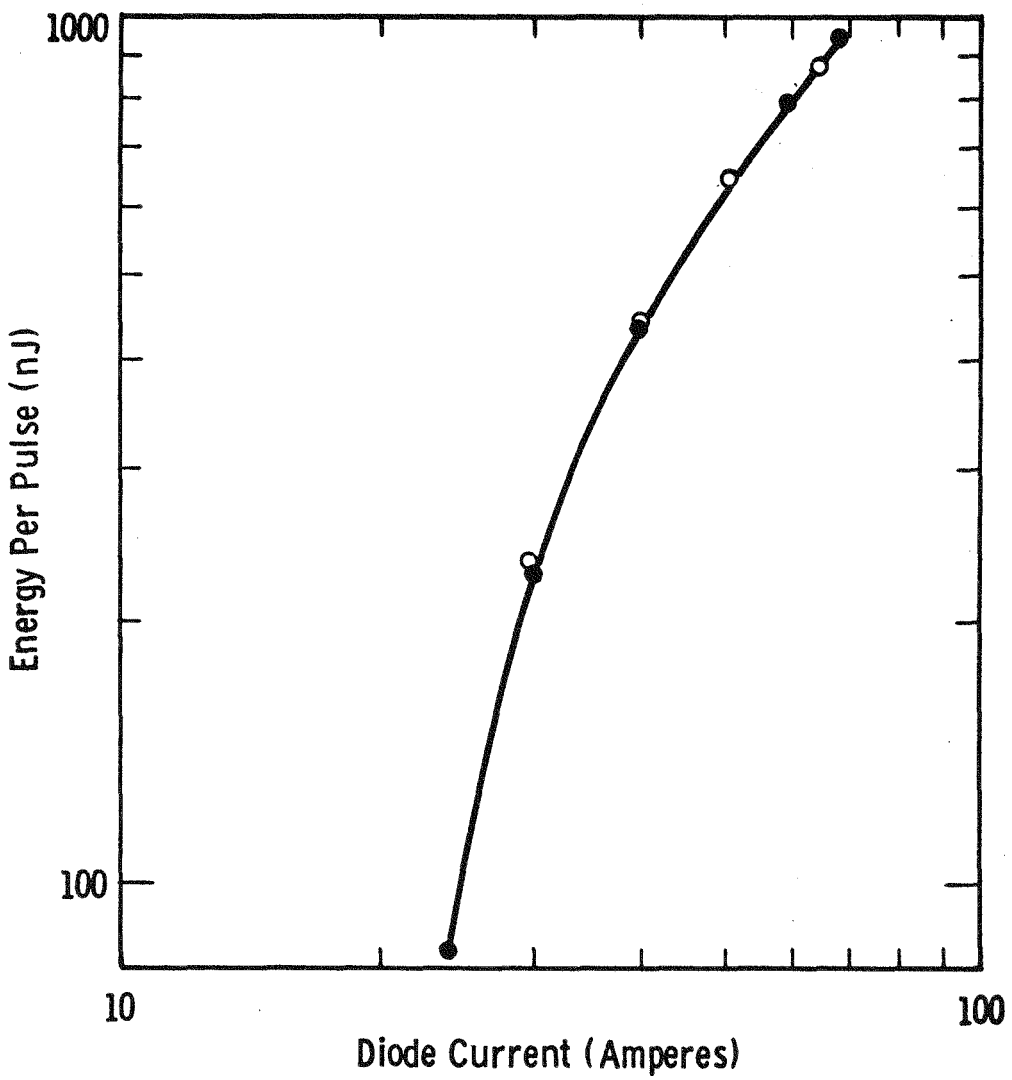

Fig. 2.23—Light energy per pulse vs laser diode current. RCA diode

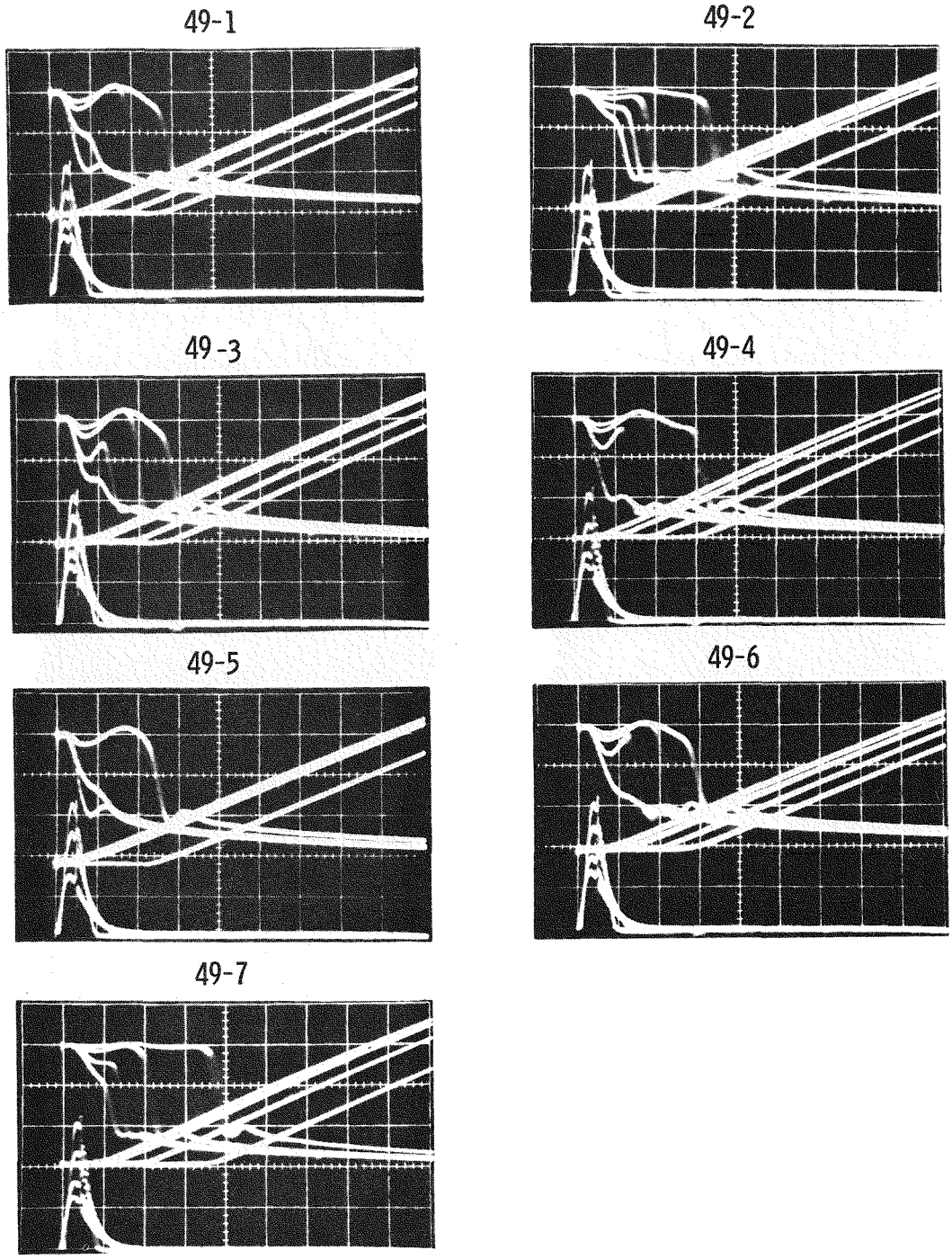

Fig. 2.24 — Turn-on, P centers. 200V, 20A, 20A, 0.5 μs/Div

N – Centers (47-7)

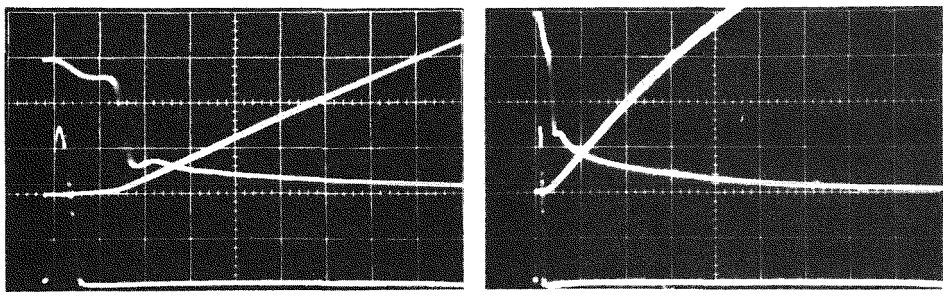

200 V, 20 A, 20 A,
0.5 μs/Div

100 V, 20 A, 20 A,
0.5 μs/Div

P Centers (49-3)

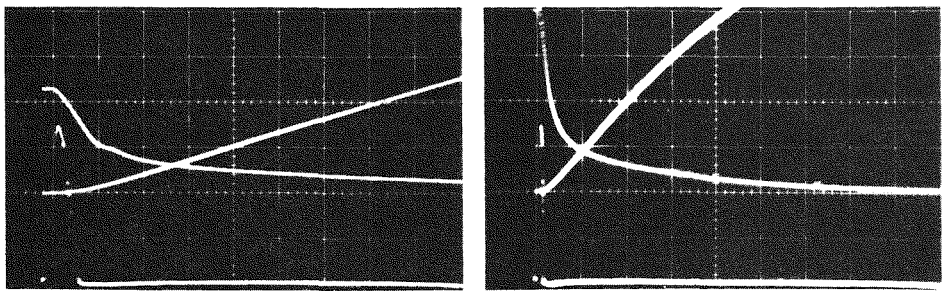

200 V, 20 A, 20 A,
0.5 μs/Div

100 V, 20 A, 20 A,
0.5 μs/Div

Fig. 2.25 – Turn-on, N center vs. P center

P Center (49-4)

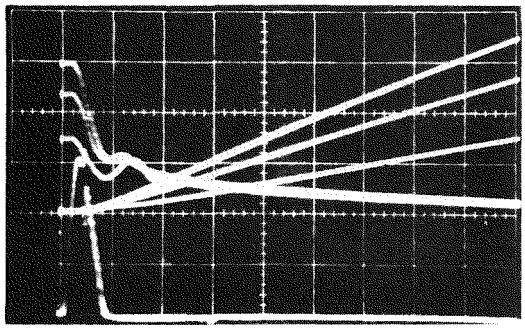

Fig. 2.26 – Turn-on wave-form at different anode voltage, 200V, 20A, 20A, 0.5μs/div

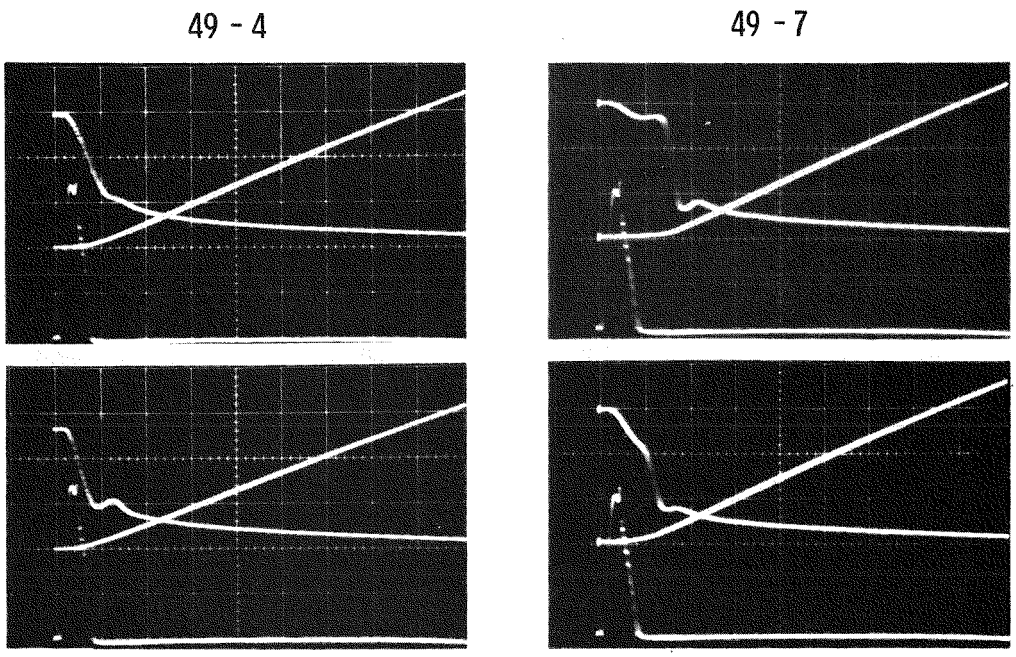

Fig. 2.27 — Turn-on, waveforms, variation of turn-on with light pipe position. 200V, 20A, 20A, 0.5μs/Div

Figures 2.21 and 2.26 indicate that for devices with either p- or n-type centers the turn-on time is insensitive to the anode voltage. This behavior is somewhat surprising and additional experimental and theoretical work should be undertaken to better define this relationship -- especially with lower level light pulses. This insensitivity is also exhibited in Fig. 2.28 which shows, for a thyristor having a p-type firing area, that the minimum light energy needed to fire is also insensitive to anode voltage above an anode voltage of 20 volts.

2.4.2 Latching Current

The design objective for latching current is $I_L < 400$ mA. Measurements on the first thyristor fusions show that those with n-type light sensitive areas have latching currents of 30-35 mA and those with p-type light sensitive areas have latching currents of 30-90 mA. (V_A = 50V, temp. = 25°C.)

2.4.3 Holding Current

The design objective for holding current is $I_H < 150$ mA. The data show $\sim$ 10 mA for the n-type light sensitive areas and $\sim$ 15 mA for p-type light sensitive areas.

2.4.4 Blocking Voltage

Blocking voltage was designed to be > 2000 V. Somewhat less than this was achieved on early runs. The problem was found to have two causes (1) contaminated silicon in the first run and (2) incorrect anode alloying in the second run. Two anode alloying techniques were subsequently shown to give good yield. One of them uses an aluminum-silicon eutectic preform and pre-evaporated aluminum on both the silicon slice and the molybdenum backing plate to prevent excessive alloy penetration. Good yield was also achieved, but with more difficulty, with an aluminum preform and without the pre-evaporated aluminum.

2.4.5 Turn-off Time

It is commercial practice in the Westinghouse Semiconductor Division to control turn-off time in high power devices by irradiating finished thyristors with high energy electrons. In this process, thyristors are first characterized for initial turn-off time, then each thyristor is irradiated with a measured dose of high energy electrons. The effect of the irradiation is to lower the minority carrier lifetime in critical areas of the device and thus decrease the turn-off time while slightly increasing the forward voltage drop. Empirical relations are used to determine what dose is appropriate to attain a required turn-off time while retaining an acceptable forward voltage drop.

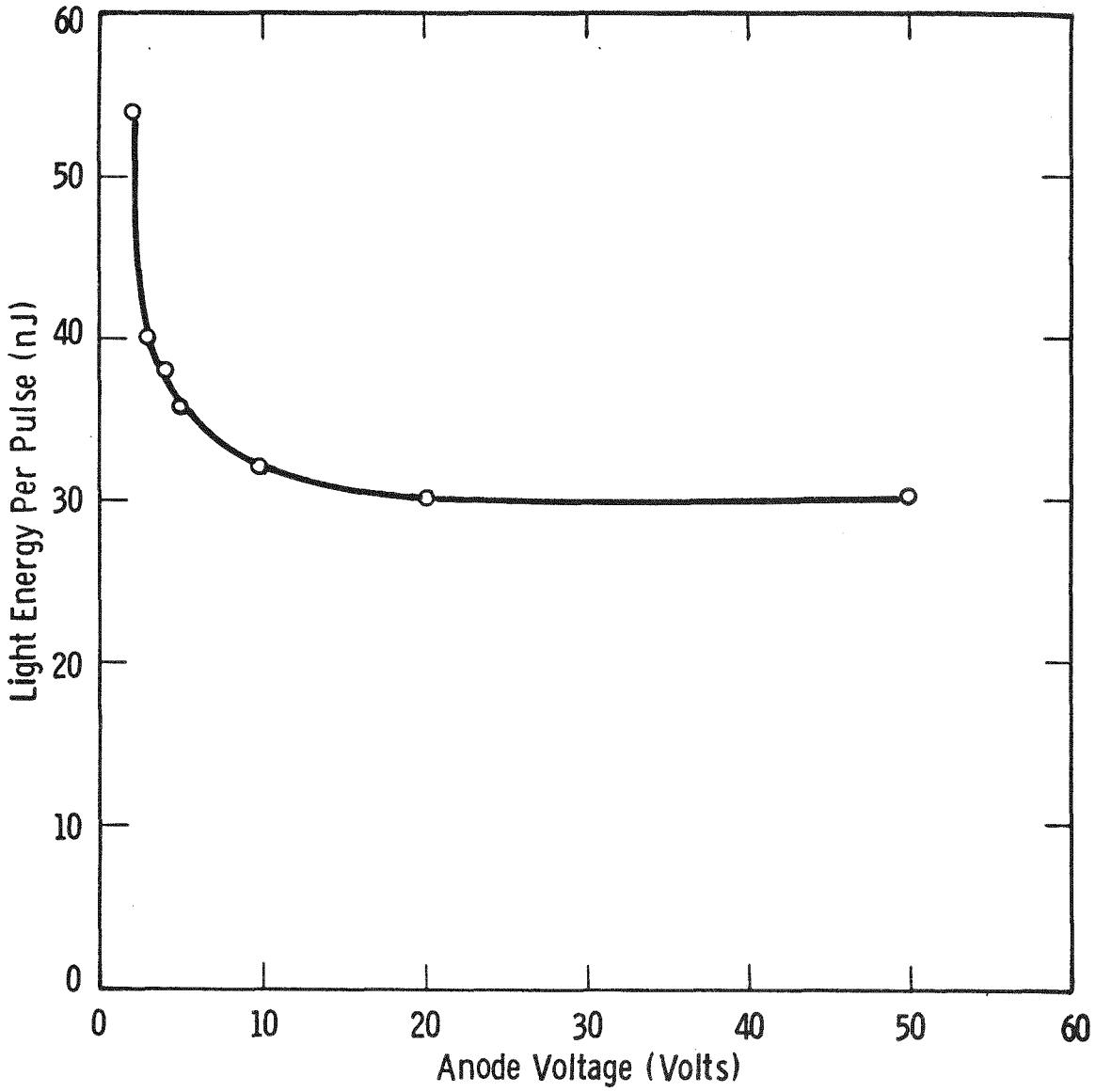

Fig. 2.28 – Minimum light energy to fire as a function of anode voltage. RCA laser diode

A sample group of thyristors representing n-type and p-type light sensitive regions was irradiated to demonstrate the validity of turn-off time control to light-triggered thyristors. The thyristors with n-type light sensitive regions had initial turn-off times of 160, 190, 360, 390, 440, and > 400 μs; those with p-type light sensitive regions had initial turn-off times of 420, 450, > 400, 530, 580, and > 600 μs. For both types, irradiation was successful in reducing the turn-off time to the desired value (t_{off} < 250 μs with I_{TM} = 250A, dI_n/dt = 50A/μs, dV/dt = 20V/μs, temp. = 125°C).

Because turn-off time is not a critical parameter in VAR generator applications, electron irradiation turn-off time control was not applied to all the devices used in the demonstration switch described in Section 6.

2.4.6 dV/dt

These devices have been measured to have dV/dt over 1000V/μsec from room temperature to 125°C, well above the guaranteed minimum value for this device. Typical waveforms observed in the dV/dt test are shown in Fig. 2.29.

2.4.7 Reverse Recovery

The type T920 thyristor, of which we are building a light-fired version, has no specified reverse recovery characteristics. Data taken on seven samples of electrically triggered T920's (-50A/μsec, 125°C) showed the values given in Table 2.5.

Table 2.5

REVERSE RECOVERY CHARACTERISTICS - T920

I_{rr}	t_{rr}	t_2
70A	3 μsec	2 μsec
120	5	3
95	3.5	2
95	4	2
100	4	3
90	3.5	2
100	4	3

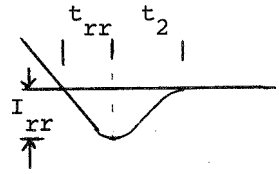

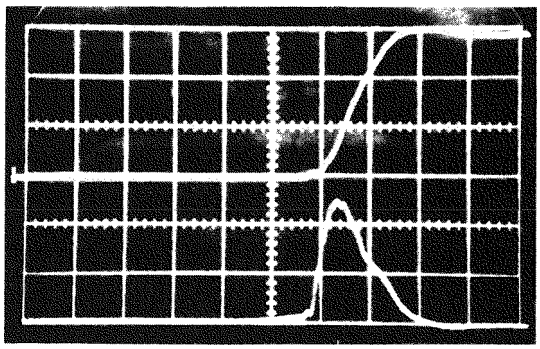

P Type
Firing Area

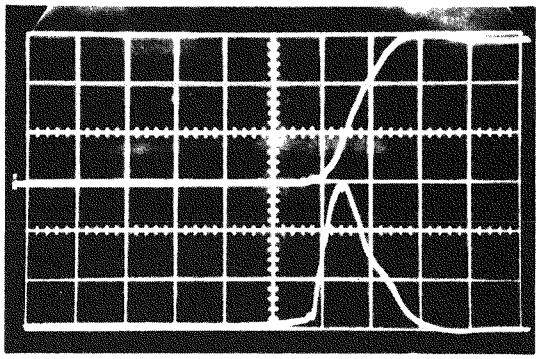

N Type
Firing Area

Fig. 2.29 – Waveforms observed during dV/dt test. Top trace V_A at 200V/div; Bottom trace forward recovery current at 1A/div, Time axis 0.5μs/div.

Similar data on the light-fired version (before the irradiation which will decrease these values) show (Table 2.6):

Table 2.6

REVERSE RECOVERY CHARACTERISTICS
LIGHT TRIGGERED THYRISTORS

	I_{rr}	t_{rr}	t_2
n-type	150A	4 μsec	3 μsec
	120	5	3
	120	4.5	2
	140	5	3
	120	5	2.5
p-type	160	5	2.5
	140	5	2.5
	135	5	2.5
	140	6	3
	140	5.5	2
	120	5	2.5
	125	5	2.5

Subsequent irradiation decreased the I_{rr} and t_{rr} to the same levels as those typical of the T920.

2.5 SUMMARY AND CONCLUSIONS OF THYRISTOR DESIGN

1) Except for the light-firing region, the light-fired thyristor developed in this program is very similar to the Westinghouse T92N electrically fired thyristor.

2) The thyristor is designed to be fired with a GaAs laser diode capable of providing 300 nJ of light energy per pulse at a wavelength of 0.904 μm. Pulse width will be 80-250 ns FWHM.

3) In order to optimize the light sensitivity of the thyristor, minority carrier lifetime in the p base of the thyristor is maintained at a high level (>5 μs).

4) In order to achieve maximum overall light sensitivity, the light sensitive region is not covered with an n region, and silicon is not removed from the light sensitive region.

5) In order to achieve a favorable combination of sensitivity and dV/dt capability, gate amplification is not used in the thyristor design.

6) The light-sensitive area is approximately 1.75 mm in diameter. The light pipe that illuminates this area will be approximately 1.1 mm in diameter.

7) Center firing is used in preference to edge firing.

Section 3

PACKAGE DESIGN AND FABRICATION

3.1 PACKAGE REQUIREMENTS

The package for the light-triggered thyristor must permit that thyristor to operate at least as well as does its electrically gated counterpart. That is, the package must provide low electrical resistance, low thermal impedance, high surge current capability, double sided cooling, compact size, and long creepage and strike paths. The package must be hermetically sealed to ensure high reliability. (Quantitative values of desired thermal impedance and surge current capability are given in Table 2.1 in Section 2.)

Since the designing of packages for high power devices is a somewhat empirical art, it was felt that a developmental program dedicated to a new package type for light-triggered thyristors was not warranted. Instead, it seemed prudent to retain all the essential characteristics of the commercially successful existing package while adapting it for the light-triggered thyristor. Thus the package used in this program is nearly identical to the package for the electrically gated thyristor.

3.2 OPTICAL COMPONENTS OF THE PACKAGE

Ideally, to obtain the most efficient coupling between the light source and the thyristor silicon, one would run a single flexible fiber optics cable from the light source to the silicon surface. This approach would not, however, provide a hermetically sealed package since air leaks would exist between the separate fibers of the fiber optics cable.

A design using a sealed window in the pole piece directly above the light sensitive area of the silicon would result in a hermetic package, but would not be efficient because of interface losses at both sides of the window and because of light spreading through the thickness of the window material. Further, any design using an optical path straight through the pole piece would not be compatible with proven mounting hardware and heat sinks.

Better efficiency could be attained by using a fused fiber bundle to conduct the light from the inside of the window to the optically active area of the silicon. A fused fiber bundle consists of a large number of optical fibers fused together into a strong, rigid rod. Such a bundle can be bent into desired shapes by heating the bundle to soften the glass. The losses due to bending are quite low since the bend radius will always be very large in comparison to the diameter of any individual fiber in the bundle. Significant losses would occur from partial reflection at both sides of the window, from light spreading through the thickness of the window, and from the fact that some light would impinge upon inactive areas (cladding glass and interstices) of the fused fiber bundle.

Losses due to the window could be eliminated by passing the fused fiber bundle completely through the package wall as shown schematically in Figure 3.1. This figure shows provision for accurately locating the thyristor inside the package to ensure proper alignment between the fiber bundle and the active area of the silicon, and shows a method by which a flexible fiber optic cable can be interfaced to the end of the fused fiber bundle. This concept appears very acceptable from every standpoint but one -- hermeticity. Leak checks performed on a number of fused fiber bundles showed that leakage existed through the interstices between the individual fibers. Since there appeared to be no practical way to overcome this problem, fused fiber bundles were not used in the final design.

The alternative to a fused fiber bundle is a single large diameter fiber used in the same way. Such a fiber should closely match the flexible fiber optic cable in diameter and in numerical aperture in order to keep coupling losses low and transmitted light intensity (watts/cross sectional area) high. A single large fiber has two advantages; it is, of course, hermetic and, because there are no interstices or cladding in the core, it can collect nearly all the light impinging upon it. The disadvantage of using a single large fiber is that light will be lost whenever the radius of a bend is not large with respect to the diameter of the fiber. Subsequent measurements have shown that this loss can be tolerated.

The material chosen for this application is Corning Glass 5000 series fiber optics cane in a 1.3 mm diameter. This diameter is compatible with the 1.1 mm diameter fiber optic cable and with the size of the light sensitive region of the thyristor. The numerical aperture of the cane is compatible with that of the fiber optics cable. The cane extends through the side of the package and terminates in a detachable connector for the convenience of the device user.

A Anode Pole Piece
B Cathode Pole Piece
C Teflon Locator
D Ceramic Body
E Flexible Fiber Optic
F Metal Sleeve
G Nut
H Alignment Tube
I Metal Sleeve
J Metal-Ceramic Seal
K Rigid Fiber Optic
L Thyristor
M Flange

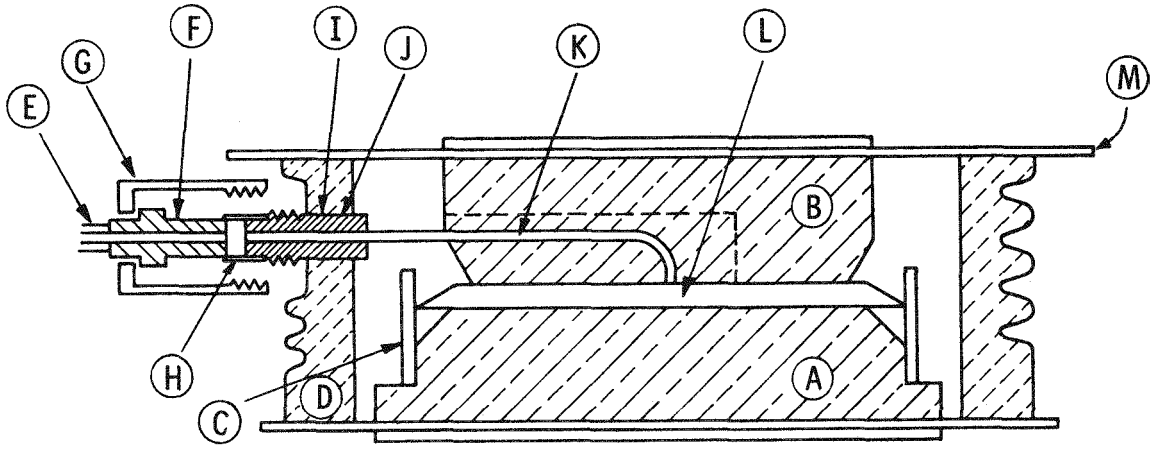

Fig. 3.1 – Schematic cross section of light-triggered thyristor package

3.2.1 Preparation of Fiber Optics Cane

As was previously mentioned, light loss will occur at the bend in the fiber optic cane. In order to minimize this loss, the bend should be smooth and as large as possible. Corning was asked to bend some sample pieces of cane for our evaluation; these bends were not as smooth as was required. Experimental bends were made in the Westinghouse glass shop with essentially the same result.

In order to obtain reproducibly smooth bends of the correct radius, a furnace controlled method was developed. In this method, pieces of cane were placed on a steel form in a furnace. As the temperature inside the furnace is slowly raised (to 650°C in 300 minutes) the pieces bend under the influence of gravity until their shape conforms to that of the steel form. Measurement of the transmission obtained in bent canes and in straight canes with and without an index-matching optical grease at the interface between flexible cable and solid cane give the results shown in Table 3.1. Application of a reflective metal film at the bend region did not measurably reduce the light loss due to the bend.

Table 3.1

TRANSMISSION THROUGH VARIOUS FIBER OPTICS CANES

Straight, dry	85%
Straight, with grease	94%
Corning, bent, dry	36 - 51%
Glass shop, bent, dry	43 - 49%
Furnace bent, dry	60%
Furnace bent, with grease	69%

The difficulty in obtaining smooth bends is in large part due to the fact that the cane consists of two different glasses, the core glass and the cladding glass, which have different softening temperatures (Table 3.2).

Table 3.2

SOME PROPERTIES OF CORNING 5000 SERIES FIBER OPTICS CANE

	Thermal Coefficient of Expansion	Softening Temperature	Strain Temperature
Core glass	9.1×10^{-6}/°C	593°C	380°C
Cladding glass	5.15×10^{-6}/°C	670°C	472°C

It was first planned that straight pieces of cane, cut to length and optically polished on both ends, could be bent as a last step. However, the differences in the core glass and cladding glass result in distortion of the core glass surface at temperatures high enough to allow the cladding glass to bend. Consequently, it was found to be necessary to first bend the canes, then subsequently trim and polish both ends. The preparation of the cane is described in detail in Section 3.3.

The light-triggered thyristor package contains a single fiber cane (light pipe) rigidly affixed at one end to the ceramic package wall and at the other end to the light sensitive region of the thyristor. Consideration was given to the possibility that fracturing of the light pipe might occur due to relative movement or thermally induced strain between the package wall and the thyristor. Measurements were made of the movement of the anode pole piece relative to the package wall during the application of maximum clamping force. This movement was found to be less than .03 mm. The strain induced in the light pipe due to the differential coefficients of thermal expansion of the package and the light pipe was calculated to be 0.14 mm for a temperature excursion of 250°C.

The strain required to cause fracture of a bent solid light pipe has been measured to be $>\pm$ 0.76 mm parallel to the length of the light pipe and $>\pm$ 1.3 mm perpendicular to the length. These data show that no light pipe failure due to relative movement between the package wall and the package pole pieces should occur. Nevertheless, light pipe fractures have been observed. The cause of these fractures is still under investigation.

3.2.2 Optical Coupling Between Light Pipe and Silicon

Some light loss will occur at the interface between the light pipe and the silicon surface of the thyristor. Because the refractive index of silicon is high, reflective losses at a silicon/air interface can be 35-45%, depending upon the angle

of incidence. An obvious way to reduce these losses is to grow a thermal silicon dioxide film of the proper thickness on the silicon surface. Figure 3.2 illustrates how the light transmission into the silicon is affected by the thickness of a silicon dioxide film. Even higher transmission can be achieved by using an antireflective film of silicon monoxide as shown in Figure 3.3. It is also worth considering the effect of filling the entire space between the end of a glass light pipe and the silicon surface with an epoxy. As is shown in Figure 3.4, the dependence of loss upon epoxy thickness is weak, varying between 15 and 20%. The practical implication of this is that the transmission into the silicon will be fairly high and will not depend to any great extent upon the attained epoxy thickness. Additionally, the epoxy can be used as a structural support and to hold the light pipe in alignment with the light sensitive region of the thyristor.

3.3 PACKAGING THE LIGHT-TRIGGERED THYRISTOR

Figure 3.5 shows a packaged light-triggered thyristor with the package cap removed to show the light pipe arrangement. The end of the light pipe is held to the light sensitive region with a small amount of transparent epoxy. Sealed packages are shown in Figure 3.6. The processes used in the packaging of the thyristor are summarized below.

1) Light pipes are bent to 6.35 mm.
2) Light pipes are trimmed to length and polished.
3) The end of the light pipe which will extend through the package wall is metallized with a silver-containing glass frit.
4) The metallized portion of the light pipe is copper plated.
5) The light pipe is soldered inside a nickel tube using a high temperature (220°C) solder.
6) The other end of the light pipe is bonded to the light sensitive region of the thyristor with a transparent epoxy.
7) The nickel tube containing the light pipe is soldered (using a 186°C solder) into a metallized hole in the ceramic package wall.
8) The package cap including the cathode pole piece is cold welded to the package body.
9) A threaded fiber optic cable coupling is placed over the protruding end of the light pipe and is epoxied to the outside of the package.

A brief description of the processes is given below.

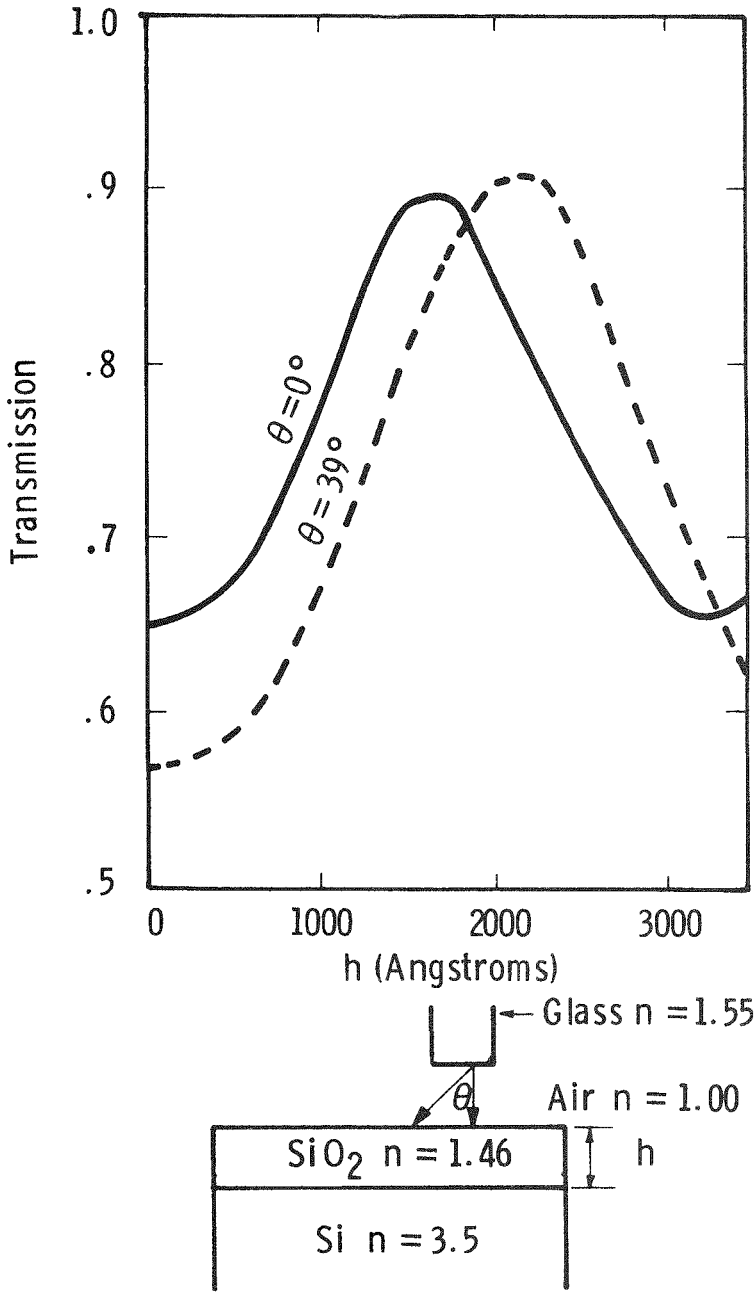

Fig. 3.2 — Light transmission from light pipe into silicon through a silicon dioxide film. n is the index of refraction

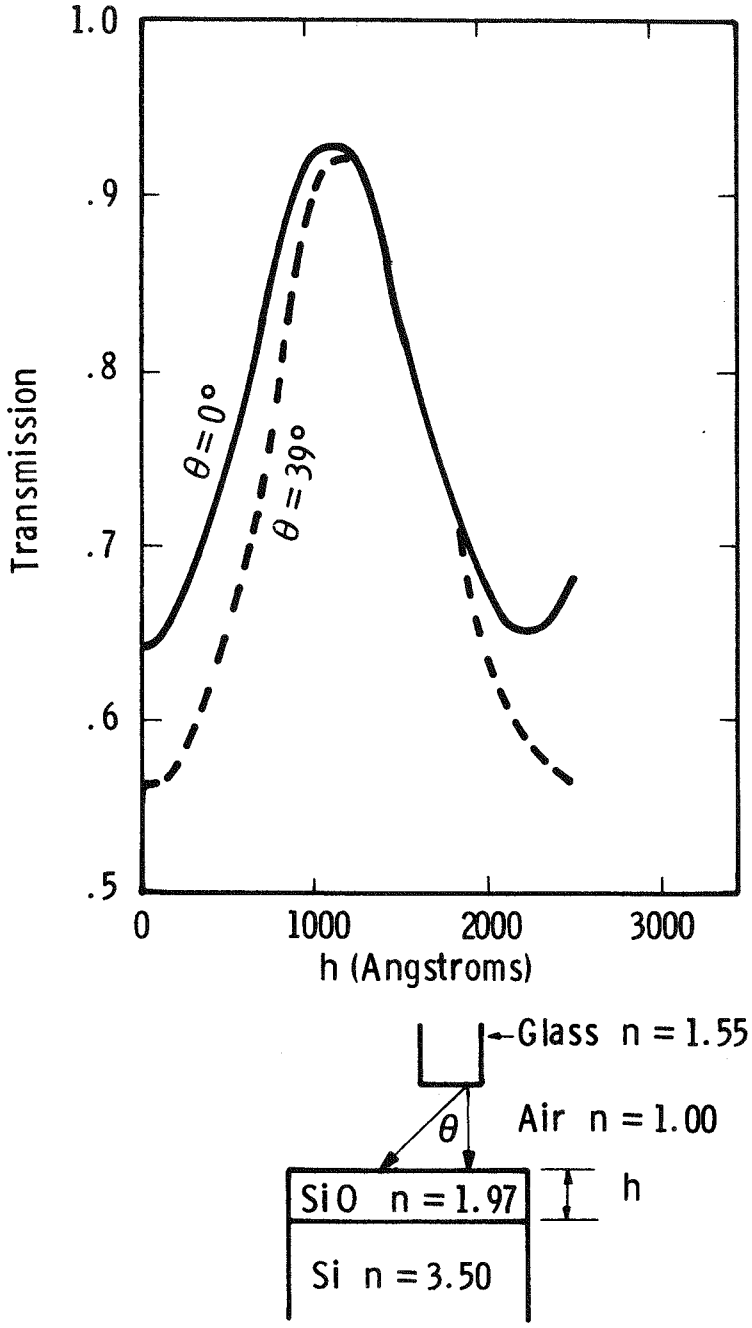

Fig. 3.3—Transmission of light from light pipe into silicon through a silicon monoxide film. n is the index of refraction

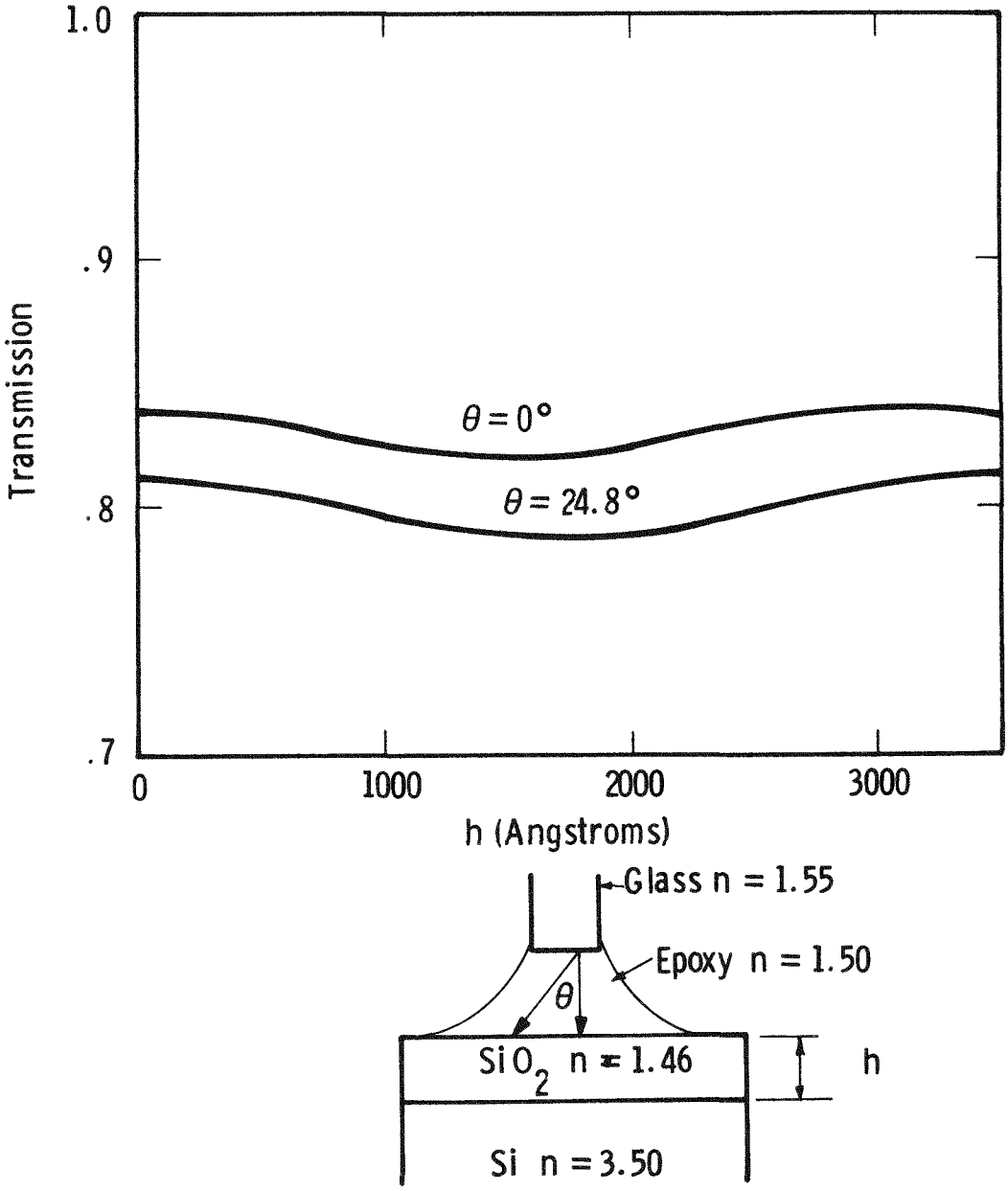

Figure 3.4. Transmission of light from light pipe into silicon through an epoxy medium n is the index of refraction.

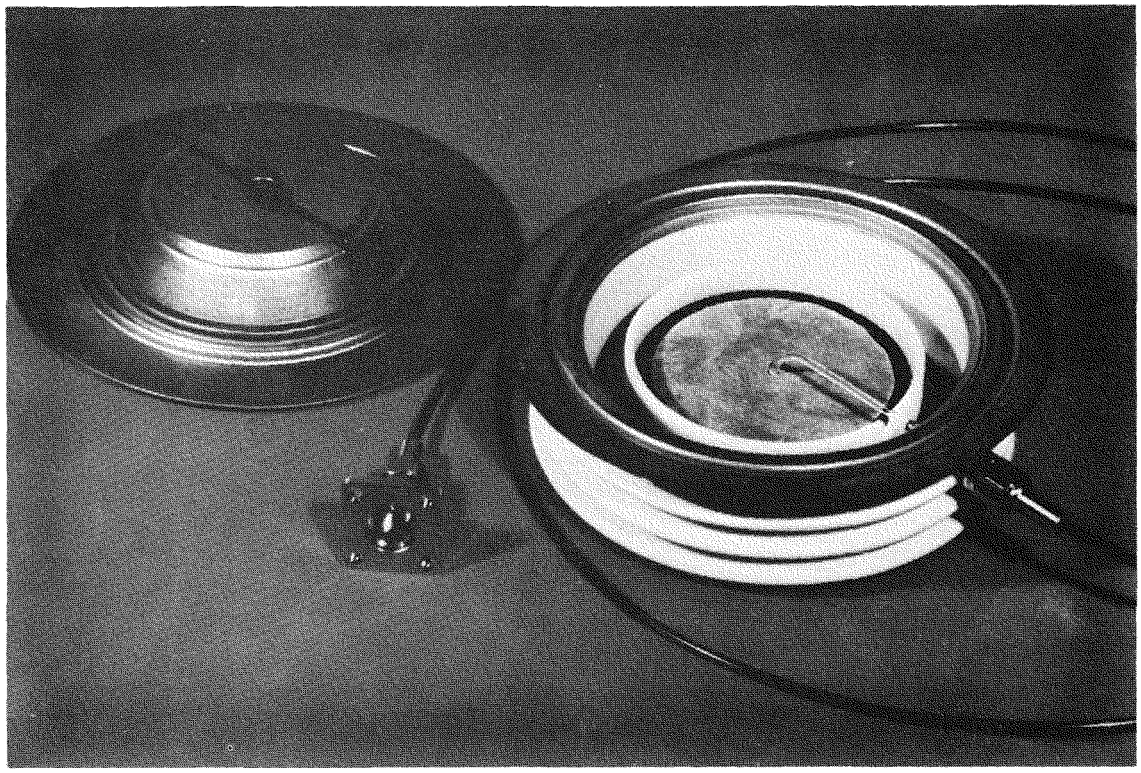

Fig. 3.5 Packaged Light-Triggered Thyristor with Cap Removed to Show Light Pipe

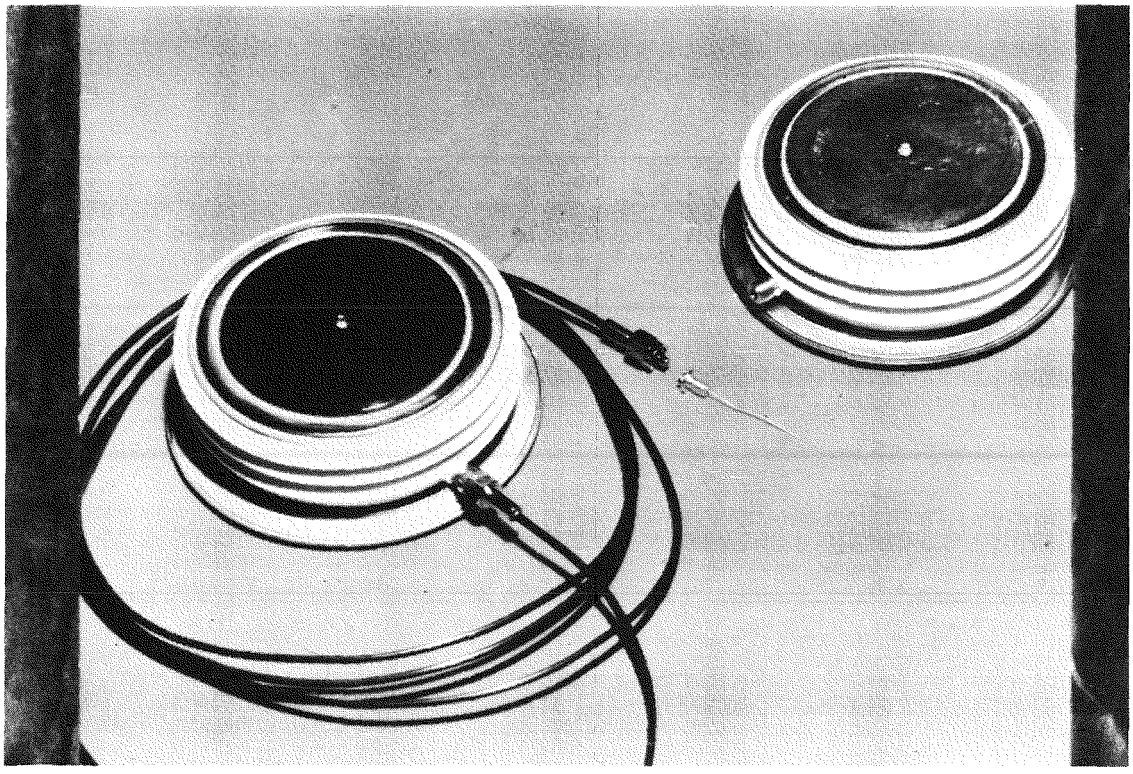

Fig. 3.6 Packaged Light-Triggered Thyristors Showing Method of Attaching Fiber Optic Cable to Package

3.3.1 Light Pipe Bending

The package design calls for a solid glass light pipe of ∿1.3 mm diameter with a 6.4 mm radius bend near one end. Some loss of light occurs whenever a light pipe is bent; but less light is lost when the radius of the bend is large and the 6.4 mm bend radius is a compromise between light loss and efficient package design. Measurements have shown that ∿68% of the light leaving a fiber optic cable is transmitted through such a bent light pipe.

3.3.2 Light Pipe Metalizing

The end of the light pipe which extends through the package wall is metalized in order to make a hermetic seal to the package wall. Metalizing consists of:

a) firing on a metal-containing glass frit,
b) copper plating the metalized area, and
c) solder-coating the metalized area.

A nickel sleeve is soldered over the metalized area to provide mechanical support for the light pipe end.

3.3.3 Cutting and Polishing Light Pipes

Good efficiency of light transmission into and out of the glass light pipe is dependent upon a good optical finish at each end. The finished dimensions of the light pipe must conform to the dimensions of the package. After the light pipes are bent, the end nearest the bend is first cut to length and polished. After the light pipe is metalized and sealed into the nickel sleeve, the other end is cut to length and polished.

3.3.4 Attaching Light Pipe to Silicon

The bent end of the light pipe is aligned by eye over the optically active area of the thyristor and is attached with a transparent epoxy. The epoxy serves the purposes of (a) keeping the light pipe properly aligned over the optically active area and (b) decreasing optical coupling losses between the light pipe and the silicon.

3.3.5 Soldering Light Pipe to Package

After one end of the light pipe is attached to the silicon, the other end, encased in a nickel sleeve, extends through a metalized hole in the ceramic body of the thyristor. The nickel sleeve is soldered to the metalized ceramic to complete the hermetic sealing of the light pipe into the package. A solder

with melting temperature lower than that used between light pipe and nickel sleeve is used so that the latter joint is not disturbed during the soldering to the package. A teflon plug is used to confine the solder during this operation.

3.3.6 Cold Weld of Package

The top electrode of the package is cold welded to the package body; this process is a standard one at the Westinghouse Semiconductor Division. The package, with top electrode in place, is first heated to approximately 120°C to drive off adsorbed moisture. It is placed in the dies of a hydraulic press. The dies are forced partially together, sealing the inside of the dies from the atmosphere. The interior of the die cavity is evacuated and then back-filled with $\sim$ 2 atmospheres of dry nitrogen. The dies are then forced against the flanges of the package body and the top electrode, compressing the flanges together and effecting the final hermetic seal of the package by cold welding.

3.3.7 Attaching the Fiber Optic Cable Connector

The dies which perform the cold welding operation do not have sufficient clearance to allow for the threaded fiber optic coupling; therefore, the attachment of this coupling is the last step in the package fabrication. The design of the fiber optic coupling is based upon the couplings manufactured by Amphenol Division of Bunker Ramo Corporation of Danbury, Connecticut, and is designed to mate with their fiber optic cable terminations. These terminations are manufactured to extremely close tolerances to maximize coupling efficiency. The light pipe in its solder-coated nickel sleeve extending through the package wall is not of the precise dimensions required for good coupling. The excess solder must be removed from this sleeve before the coupling is placed over it. Because the package has already been hermetically sealed before the coupling is added, the coupling need not be hermetically sealed to the package. A high strength epoxy is used to bond the coupling to the nickel sleeve and the ceramic package. Proper spacing of the coupling on the sleeve is obtained by using an empty cable termination as a gauge.

3.4 SUMMARY AND CONCLUSIONS

The package designed for the light-triggered thyristor has the same electrical, mechanical, and thermal properties as does the package for the analogous electrically-gated thyristor.

Light is guided to the light-sensitive region of the thyristor by a solid glass light pipe which is hermetically sealed into the ceramic package wall. Optical coupling between the light pipe and the fiber optic cable carrying the trigger signal is accomplished through a screw-on connector which is affixed to the outside package wall and to the light pipe where it extends through the side of the package.

Measurements and experiments indicate that the light pipe is sufficiently strong so that light pipe breakage should not occur in normal use. Nevertheless, a large number of light pipes have broken inside sealed packages. Investigative work to determine the cause and to eliminate this failure mechanism is continuing. It seems unlikely that major redesign of the package will be necessary.

Section 4

OPTICAL SYSTEM

4.1 SYSTEM REQUIREMENTS

As was shown in Section 2, reliable light-triggering of the thyristor can be achieved by approximately 300 nJ of light energy delivered in a time period of a few microseconds or less. A pulse repetition rate of at least 60 per second is required. In order for the light energy to be efficiently converted into effective electron-hole pairs, its wavelength must be in the range 0.90 - 1.10 μm.

The effectiveness of the light-created carriers increases as their density is increased. Thus the light-sensitive region of the thyristor should be as small as possible. This implies that the light should be guided to the thyristor by a fiber optics cable of small diameter.

The long term reliability of the optical system should be sufficient to assure operation over a period of years without major failures or need for major repairs or replacement.

4.2 LIGHT SOURCE

4.2.1 Light Source Characteristics

As was shown in Section 2, to obtain good efficiency of conversion from light into charge carrier pairs, the triggering light must have a wavelength greater than 0.900 μm but less than 1.10 μm. Only four practical light sources are available with principal emission in this wavelength region:

GaAs laser diode	@	.904 μm
GaAs light emitting diode	@	.940 μm
Nd: YAG laser	@	1.060 μm
Nd: Glass laser	@	1.060 μm

The light emitting diode is the least expensive single source and is the obvious first consideration. It suffers two disadvantages: (1) comparatively low light power emission ($\leq$ 1 watt); and (2) emission at wide angles (large angular aperture) which makes it impractical to collect all of the light output with a fiber-optics bundle. The second item is fundamental and cannot be expected to be significantly improved. This point is elaborated upon later.

Approximately 300 nJ of light energy is required by the thyristor to assure turn-on with an acceptable range of delay time. From Table 4.1, column 7, it is apparent that only one LED (the TI unit) is within an order of magnitude of delivering sufficient light; and, by projection, it would be a factor of 2 too low. On the other hand, a number of laser diodes are candidates.

A 1.1 mm dia. fiber optics cable has been selected because it provides a good compromise between the need for concentrated light at the thyristor end (small area) and the need to collect a high percentage of the light from the light source. This provides an upper limit for the effective area available for the light source per drive thyristor (e.g., a source must drive 2, 3 or more thyristors if it requires a larger fiber-optic cable for adequate coupling). Even the TI LED unit does not meet this requirement.

The conclusion is that the light emitting diode, in the present state-of-the-art, is <u>not</u> a viable light source to trigger the thyristor.

Nd:YAG (neodymium-YAG) and Nd:Glass pulsed lasers presently are available in ratings of 500 μJ per pulse and larger sizes. This is much more power than is needed for the light in the .900-.950 μm wavelength region for the intended applications. Also, calculations reported in Section 2 above show that light at 1.06 μm is poorly absorbed in the useful region of the thyristor, leading to lower overall efficiency of the trigger circuit. In addition, two disadvantages of present state-of-the-art Nd:YAG (or glass) lasers are their high initial cost and the comparatively short life of the pumping lamp. At the pulse rates required in a 60 Hz system, the replacement life of the lamps is measured in hundreds of hours. For these reasons the Nd laser group has been excluded as light sources for this program. However, the Nd lasers do have very attractive features that warrant further examination at a later date. For instance, the high power and highly collimated beam output will permit coupling one laser into a comparatively small fiber optics cable, so that more light can be supplied to

Table 4.1

COMPARISON OF SEMICONDUCTOR LIGHT SOURCES

Mfg.	Mfg. Identification	Half-Angle Beam Spread @ 50%; °	Peak Power W	Peak Current @ 5 µsec Width 60 Hz Rate (A)		Output µJ	Output at End of 1 m Long Fiber Optics Cable, 1.1 mm Dia.	
							Measured nJ	Estimated nJ
Light Emitting Diodes								
Spectronics	5453-4	15	0.180	6		0.90	37.5	--
GE	LED55C	8	0.210	6		1.05	32	--
TI	XL16X	75 (.072" dia.)	1.000	10		5.0	--	160
RCA	SG1009A	8*	0.185	6		0.925	37.5	--
Laser Diodes		Source Size mm	Peak Power W	Number of Diodes	Pulse Width µsec			
ALS	LD-65	Divergence = 0.25 rad.	12	1	0.08	0.96	250	--
RCA	C30038	.4 x .4 mil⁄	70	5	0.2	12	--	4×10^3
RCA	SG3001	.2 x .2	25	3	0.2	5	--	1×10^3
RCA	SG30041	.3 x .3	40	4	0.2	7	--	2.3×10^3
RCA	SG30010	.4 x .1	30	2	0.2	6	--	2×10^3
RCA	SG2009	.4 x .002	12**	1	0.25	3	1000	--
RCA	SG2010	.4 x .002	15	1	0.2	3	--	1×10^3
RCA	SG2012	.6 x .002	20	1	0.2	4	--	1.3×10^3

* Corresponds to 50% of total flux within ± 30° (± 40° = 60%).
** Corresponds to 50% of total flux within ± 13° (± 40° = 90%).
⁄ Half angle beam divergence of all RCA laser diodes is 9°.

an even smaller region of the thyristor, improving its sensitivity. The high power will permit triggering many thyristors (several modules) from one source; if delay time is critical, sufficient power is available to simultaneously fire (as distinguished from trigger) all of the thyristors in a string. In addition, the longer wavelength may prove advantageous when higher voltage (say 4000V or more) thyristors are light triggered in DC switching applications.

The remaining light source candidate is the laser diode. As can be seen from Table 4.1, there are several laser diodes that can deliver more than 300 nJ through a 1.1 mm diameter light pipe. The laser diode is thus the selected light source for this application.

4.2.2 Laser Diode Properties

NOTE: The following paragraphs on reliability are taken from RCA Application Note AN-4993 (November, 1975) and are quoted with the permission of RCA, Solid State Division, Electro-Optics and Devices, Lancaster, PA.

Laser diodes are available in a number of configurations: single heterojunction, double heterojunction, or double heterostructure, large optical cavity, stacked diode lasers, laser diode arrays, and stacked diode laser arrays. Operational temperatures vary from cryogenic to over 100°C. Devices of interest to this contract are limited to single heterojunction diodes and to stacked diodes operating in a normal temperature range. Arrays and stacked arrays may be useful in large systems.

Laser diodes require an optical cavity and high injection carrier density. The optical cavity is a Fabry-Perot type that is formed by cleaving opposite ends of the diode and sawing adjacent sides of the rectangular structure. Figure 4.1 describes the main features of the laser diode. Waveguiding in the plane of the p-n junction is required to minimize internal absorption and is obtained by controlling the profile of the index of refraction perpendicular to the junction plane. At room temperature, an injected carrier density of the order of 10^{18} cm^{-3} is required to achieve the necessary population inversion.

The three primary characteristics of the laser diode of interest to the user are the threshold current density, J_{th}, the radiant flux, and the far-field radiation pattern. The threshold current density is the minimum current density needed to obtain lasing at a given temperature. Above J_{th}, the radiant flux emitted is a reasonably linear function of the current as is shown in Figure 4.2. The

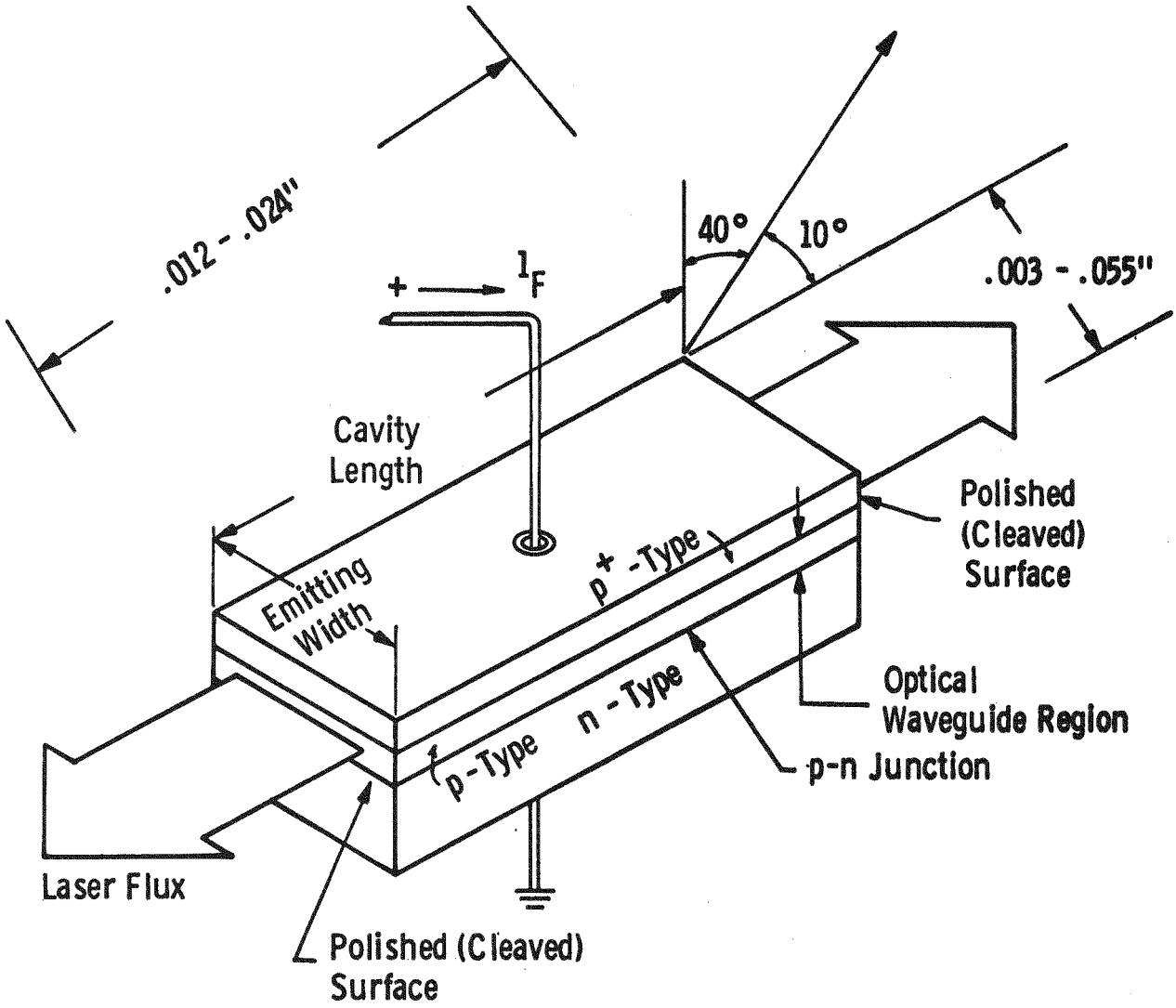

Fig. 4.1 – Injection laser diode structure

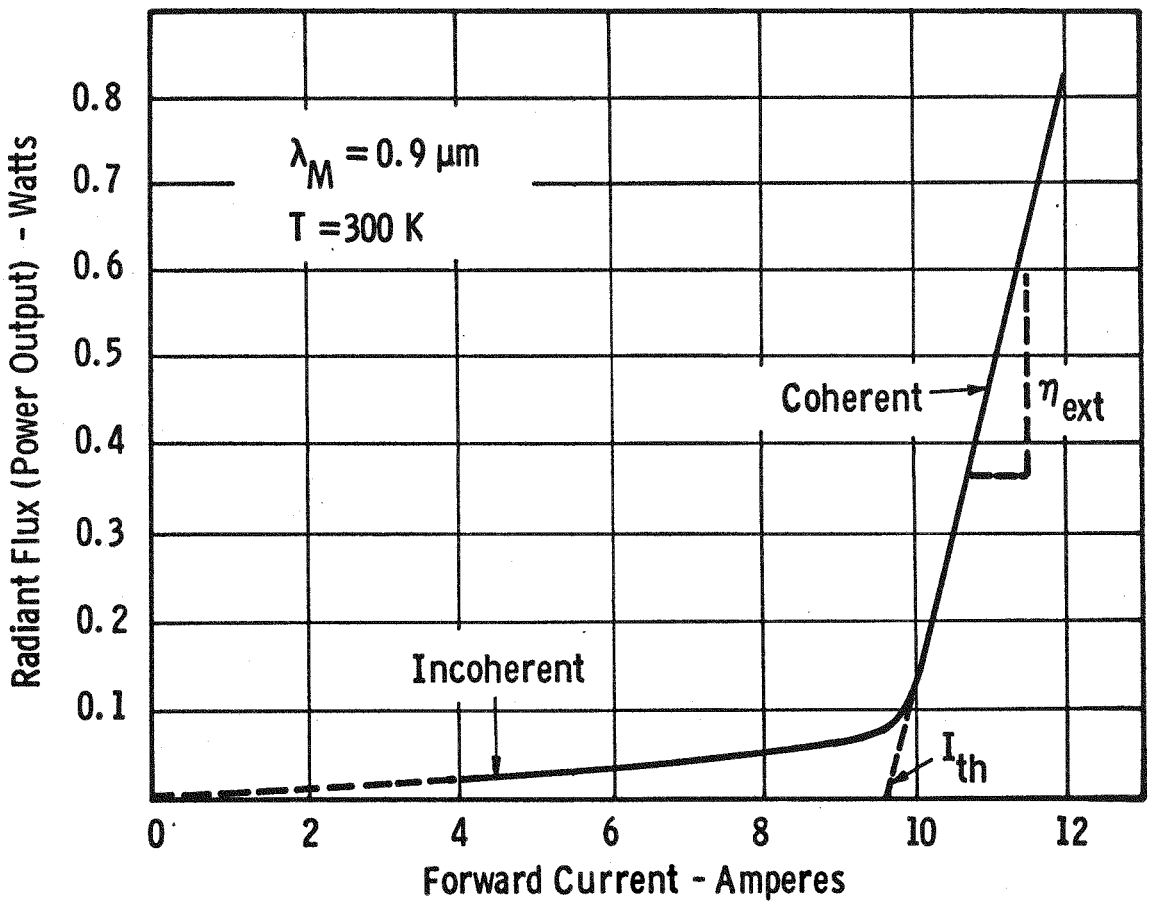

Fig. 4.2 — Output vs. forward current for a typical laser diode

far-field radiation pattern depends upon the nature of the internal waveguide of the laser diode. Threshold current densities are of the order of 10,000 A/cm^2 for single-heterojunction devices and 1000 A/cm^2 for double-heterojunction devices. For applications requiring high pulsed radiant flux emission, the double-heterojunction devices have three drawbacks that must be considered: (1) because the optical flux density is high, there is a greater danger of device failure by mechanical facet damage (see catastrophic degradation discussion below); (2) the far-field radiation patterns are broader, making it more difficult to collect the radiation into a fiber-optic system; and (3) largely for the above reasons, double heterojunction laser diodes are not readily available from suppliers.

Table 4.2 summarizes typical performance characteristics of single laser diodes.

Table 4.2

TYPICAL PERFORMANCE CHARACTERISTICS OF
COMMERCIAL SINGLE-HETEROJUNCTION LASER DIODES

Characteristics	Performance	Comments
Peak Radiant Flux	1 watt/mil of emitting facet	Limited by Catastrophic Degradation
Current Density	40,000-50,000 A/cm^2	Limited by Gradual Degradation
Power Conversion Efficiency	3 - 5%	12% (Best)
Duty Cycle	0.1% t_w = 200 ns; prr = 5 kHz	Can trade off pulse width and rep rate
Rise Time	< 1 nanosecond	--
Center Wavelength	904 nm	Temperature Sensitive 0.25 nm/°C
Spectral Width (50% point)	3.5 nm	Broad relative to other types of lasers
Half Angle Beam Spread (50% point)	9°	Total Collection requires F/1.0 optics
Source Size	0.08 mil x emitting width	Line Source

Figure 4.3 shows the typical peak radiant flux versus peak drive current for four RCA GaAs single heterojunction diodes as given in RCA Application Note AN-4993. Note that both the SG2007 and SG2010 will produce 10 watts of radiant power. However, for reliability and long life it is preferable to use the SG2010 at this output level because both reliability and long life are dependent upon current density -- longer life is obtained if the laser diode is operated well below the maximum rated current.

Changes in ambient temperature have significant effect on the output of laser diodes. Radiant output goes down as temperature increases for a constant drive current, and the trigger circuit designer must consider this. Figure 4.4 shows how the relative peak power output varies with the relative drive current for temperatures of -55°C, 27°C, and 75°C.

The relative radiant flux collected versus collection angle is shown in Figure 4.5. These are experimental data from RCA and were collected, as shown in the figure, by varying the spacing S for all other conditions fixed.

To increase the optical power density with practical drive currents, two or more laser diode pellets are stacked on top of one another to form a compact emitting source. This is actually a series of two or more line sources of light. Such stacked diodes also have output radiation patterns that are compatible with collection by fiber optics.

4.2.3 Life and Reliability of Laser Diodes

The following paragraphs on reliability are taken from RCA Application Note AN4993, dated November 1975.

> *"Reliable diode operation at room temperature for thousands of hours under pulsed conditions has been obtained when the operating current density, duty cycle, and optical flux density in the junction region are properly controlled. Two basic failure modes have been identified which must be considered when operating laser diodes.*
>
> *"(1) Catastrophic Degradation. The catastrophic failure mode occurs as a result of mechanical damage to the facet of the cavity when the optical flux density is excessive. A commonly used figure of merit is the emitted power per unit length of emitting facet (W/mil). The narrower the confined lasing region, the higher the internal optical flux density for a given value of power emitted per length of emitting region. Hence, lasers with larger waveguide region thicknesses can safely emit higher peak radiant flux than smaller cavity devices.*

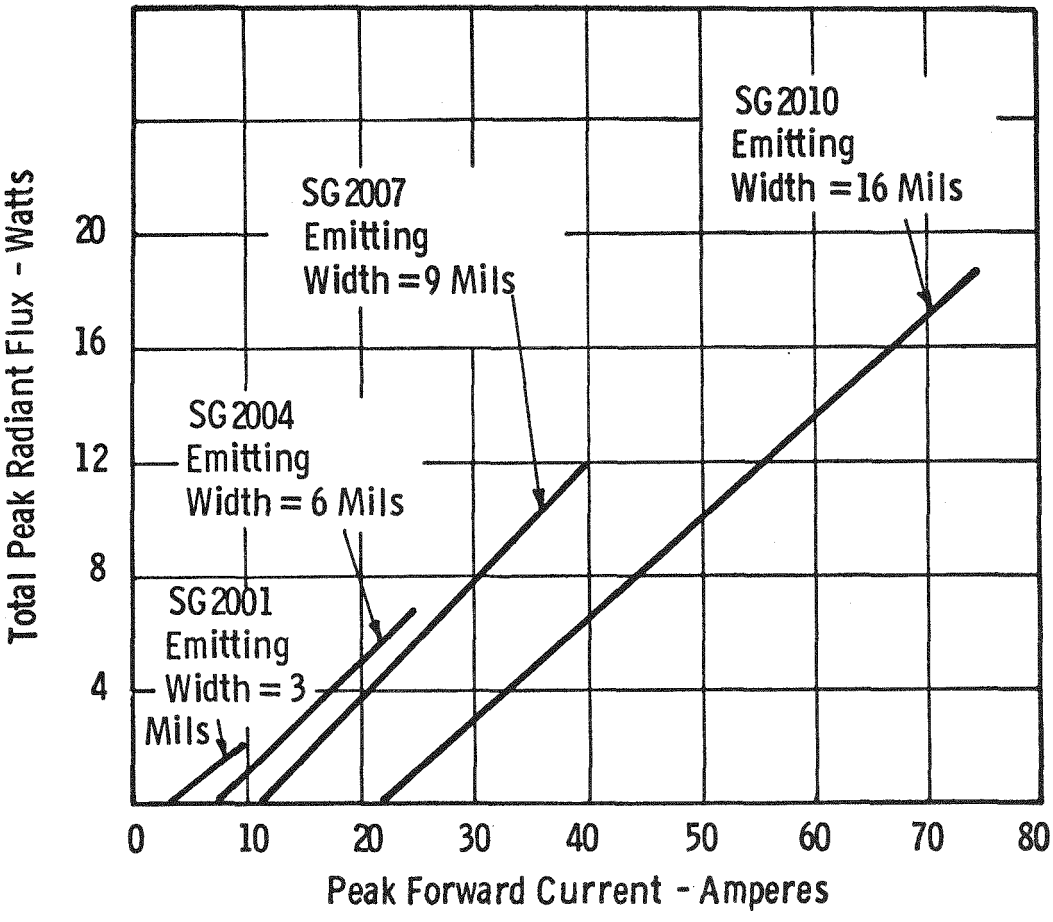

Fig. 4.3 – Peak radiant flux as a function of peak drive current for four typical laser diodes

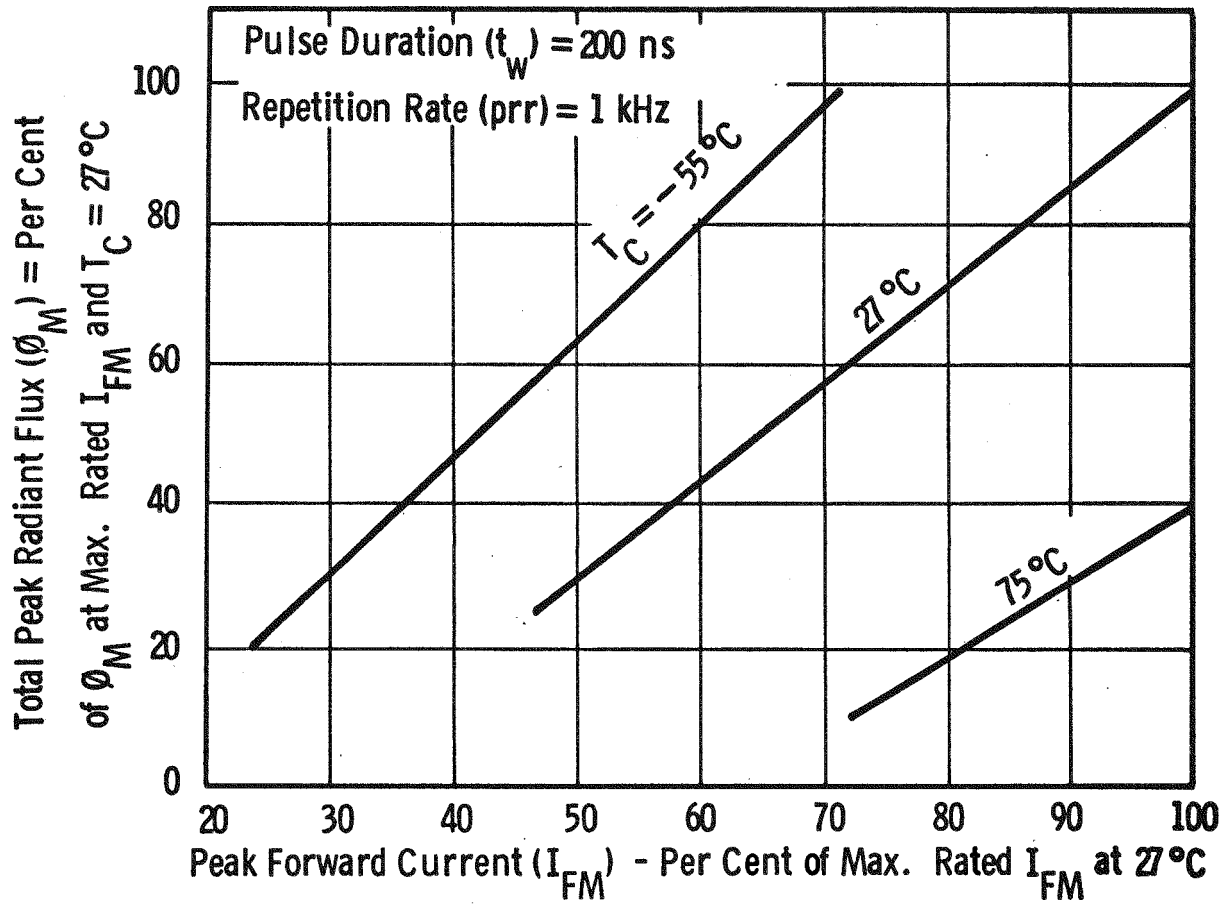

Fig. 4.4 — Temperature dependance of peak radiant flux vs. peak forward current for typical laser diodes

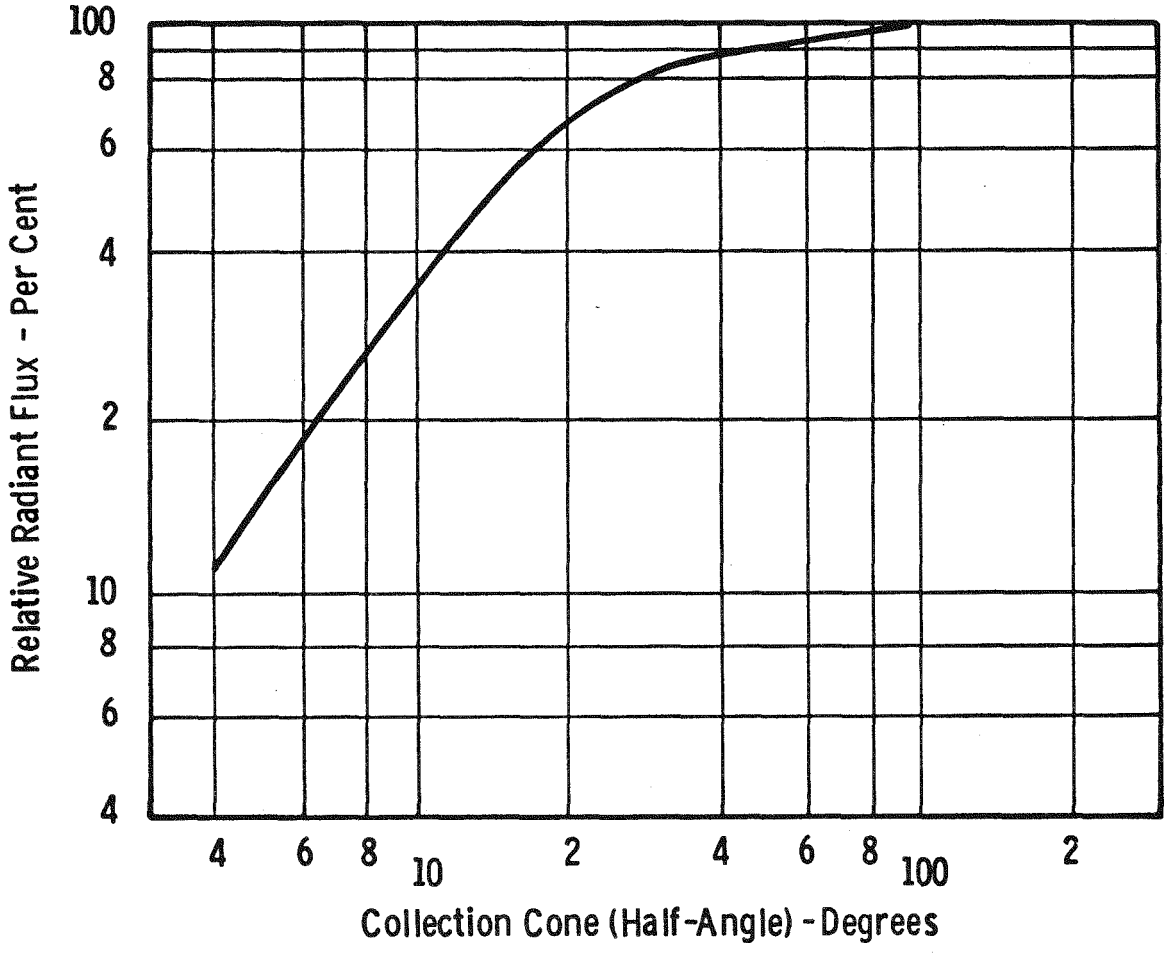

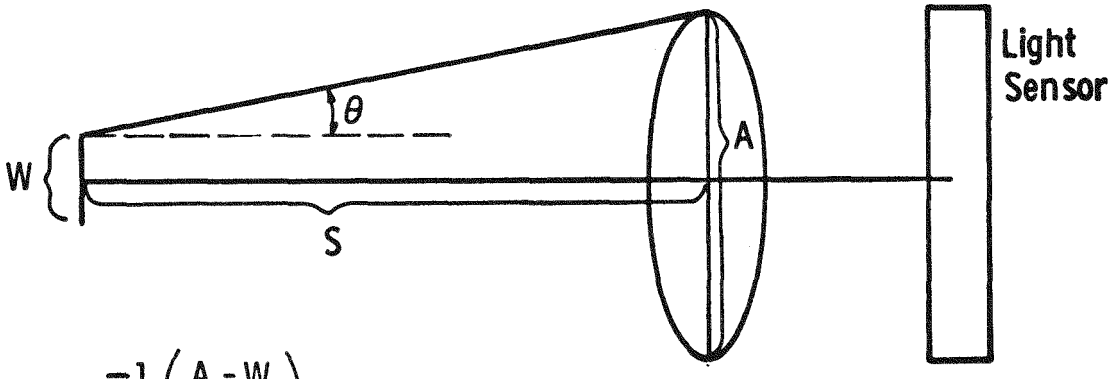

$$\theta = \text{Tan}^{-1}\left(\frac{A - W}{2S}\right)$$

Where

A = Aperture Diameter

W = Array Width

S = Aperture to Diode Spacing

Fig. 4.5 — Relative radiant flux collected as a function of collection angle

"Figure 4.6 is a plot of catastrophic damage threshold limit versus pulse width for typical single heterojunction laser diodes with optical cavity widths of 2 μm. The allowable peak power before the onset of catastrophic damage is highly dependent on pulse width and is affected to a lesser extent by pulse repetition rate. At pulse widths of less than 100 nanoseconds, the allowable peak power output increases exponentially. Allowable peak power output of a laser diode can also be increased by the application of antireflecting SiO films to the facet.

"(2) Gradual Degradation. A second failure mechanism, gradual degradation, depends on the operating current density, duty cycle, and diode fabrication technology. The degradation is believed to be due to the formation of the non-radiative centers and defect or impurity clusters which increase the internal absorption."

The operating life test data available from RCA on laser diodes have been extended to at least 5000 hours. This information is based on newer, larger diodes similar to those most likely to be used (SG2009) in a light triggered thyristor switch. The data are presented in Figure 4.7. In the letter from RCA that transmitted the information of Figure 4.7, it was pointed out that at present there is not "sufficient information to give definitive information about tradeoffs on pulse width, temperature and drive current as our tests are all conducted at room temperature and maximum ratings." However, Figure 4.8 shows that the pulse width could be increased by a factor of two without increasing the danger of catastrophic damage. This could increase the light received at a given thyristor by a factor of two; and, therefore, increasing the pulse width may have an important, favorable, economic impact.

It is obvious from the above that the trigger circuit must and can be designed to avoid catastrophic degradation. The data on gradual degradation, when converted to equivalent 60 Hz operation, indicate that over 417,000 hours (47 years) of operation can be expected to produce less than 25% loss in output. This is still a pessimistic extrapolation because the duty cycle at 5000 Hz is 80 times as large as at 60 Hz, meaning a higher operating temperature. Again, proper attention to the thyristor trigger circuit system design can incorporate derating of the laser diode to reduce the amount of degradation. This is an area that will require direct support to generate the needed design data.

Data given above are for laser diode operation at 25°C; actual operating temperature in a field environment could reasonably be expected to be higher. Because the cooling water for the thyristor stacks is expected to be 50°C or more, it is not feasible to cool the laser diodes with the same water. However, data from

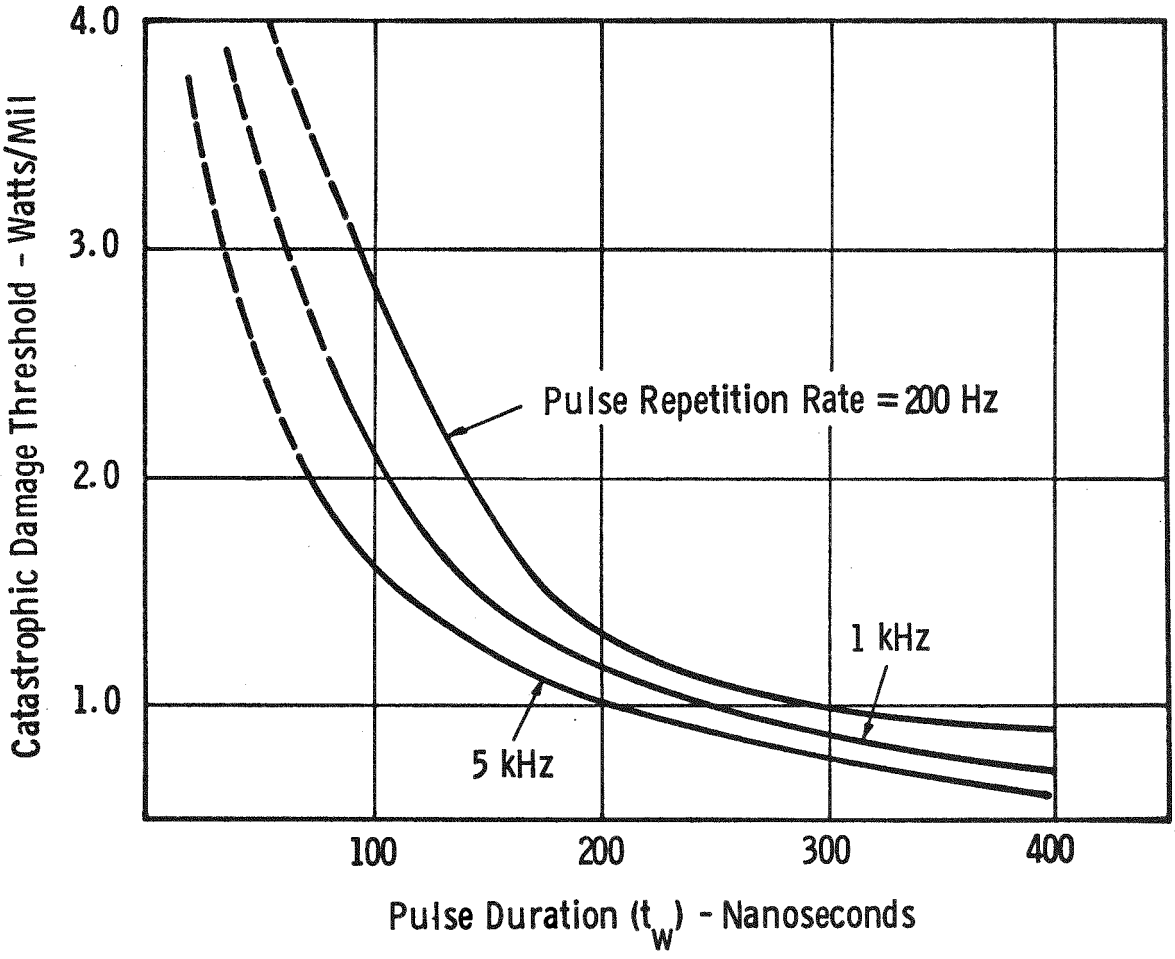

Fig. 4.6—Catastrophic damage limit as a function of pulse width

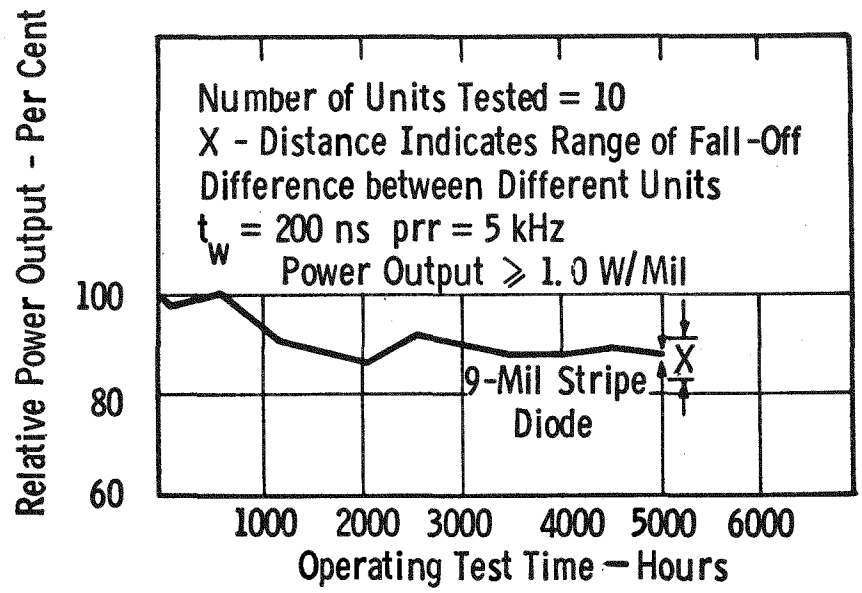

Fig. 4.7—Typical operating life of laser diode

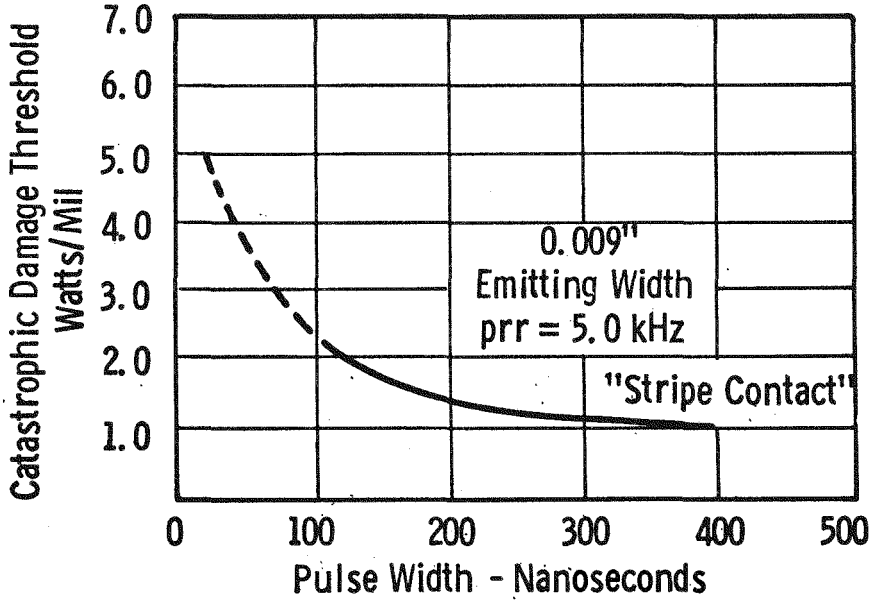

Fig. 4.8 — Catastrophic-damage threshold vs pulse width

thermoelectric cooler suppliers, when combined with the information from RCA and Laser Diode Laboratories, Inc. suggest that it will be economically feasible to use thermoelectric coolers to maintain the operating temperature of the laser diodes at approximately 25°C under all ambient temperature conditions. Then, the light output specified in the laser diode data sheets could be achieved, and the operating life and associated degradation would be expected to follow the curve of Figure 4.7. Only a small portion of the cooling water for the thyristors would need to be diverted to cool the heat sinks of the thermoelectric coolers.

The basic problem addressed here is really a systems problem which can be solved only by the designer of the user apparatus. The exercise above illustrates some alternative approaches. Quantitative analysis is not possible until more basic information becomes available relating laser diode life and degradation to temperature. At present, simple air cooling of the laser diodes is recommended for demonstration modules.

4.3 FIBER OPTICS CABLE

There are many possible sources of light with sufficient output to trigger a thyristor. The immediate problem is to collect this light and conduct it to the thyristor in an economical manner. For various systems reasons, the transmitting medium for this program was intended to be some form of light pipe or fiber optics cable. Two types are available -- plastic and glass. Plastic cables exhibit very high losses in the near infra red region, so the choice is limited to glass-based cable. The two varieties of glass cables are flexible fiber optics cables and rigid glass rod. Although rigid glass rod could in principle be used, the mechanical problems associated with manufacturing and installing many glass rods of irregular shape and appreciable length lead one to choose the flexible fiber optics cable if at all possible. In either case, the same problem of collecting the light from the light source exists. An additional constraint is that the light source and transmitting medium must be commercially available, or obtained by easily modifying commercially available parts of materials, or must be reasonably close to commercial availability.

Therefore, the problem is to collect enough output from a light source by a flexible fiber optics cable that, at the output end of the cable, sufficient light is transmitted to turn on a thyristor. One is up against two fundamental facts: most light sources emit over a fairly large area (do not have high watts/cm^2 output) and fiber optics cables can effectively accept light from only

a very small area. An additional restriction develops from the need for the light wavelength to be approximately 1 μm, which reduces the list of practical sources to three: the light emitting diode, the laser diode, and the neodymium lasers. Figure 4.9 illustrates the basic problem. Assuming reasonable dimensions for source, source to collector spacing, and collector size, the collection angle is relatively small. The glass fiber optics have acceptance angles (half cone angles) of approximately 40°, corresponding to numerical apertures of approximately 0.65. If the angle ψ is greater than 40°, light will pass through the wall of the cable and be lost. A practical minimum dimension for S, without development of special packaging, is 1.5 mm. Assuming that the source has zero dimensions and a 1.1 mm diameter light pipe, the maximum collection half angle is 20°. Using Figure 4.10 for an LED and Figure 4.5 for an LD (both figures from RCA), one can obtain the values shown in Table 4.3. It is to be expected that the calculated values for the light will be too high for two reasons: the size of the source is not zero, especially for the LED, so it would be expected that its measured transmitted value would be significantly less than its calculated value; and there are reflection losses at each end of the cable that were not considered. These losses should be comparable in percentage regardless of the source. This simple example shows how the laser diode, with its combined advantages of higher intensity output and more highly collimated beam than the light emitting diode, is a compatible light source for use with fiber optics cable for this application.

Table 4.3

LIGHT COLLECTED AND TRANSMITTED BY FIBER OPTICS CABLES
(POINT SOURCE 1.5 mm FROM CABLE END)

	A mm	θ Deg.	% Collected	% Transmitted	Source μJ	Transmitted Light Through 2 Meter Cable	
						Calc. nJ	Meas. nJ
LED	1.1	20	20	63	∿1	250	37
LD	1.1	20	65	63	∿1	410	250
LD	1.1	20	65	63	∿3	1230	1000

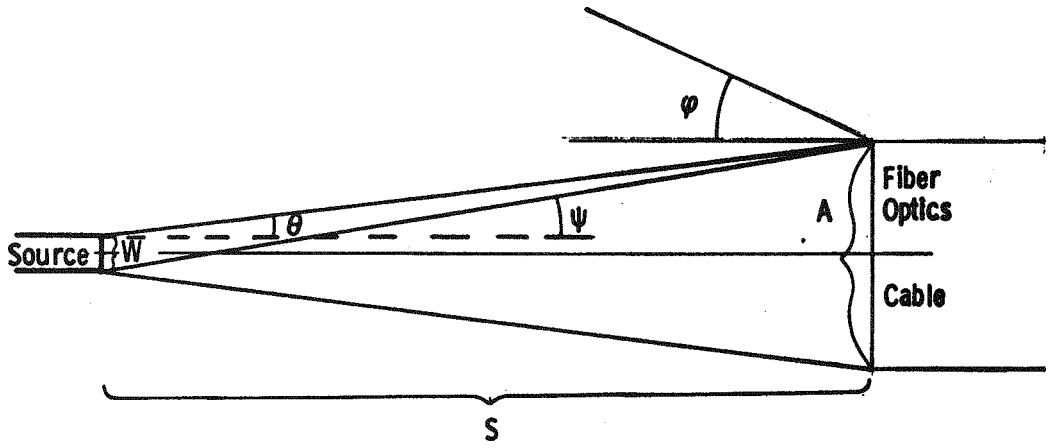

θ = Collection or Cone Angle
Numerical Aperture $\equiv$ Sin φ
$\varphi \approx 40°$ for Glass Cables
A = Diameter of Fiber Optics Cable
W = Diameter of Source
S = Separation of Source and Cable End

$$\theta = \tan^{-1}\left(\frac{A-W}{2S}\right)$$

Fig. 4.9 – Collection angle of a fiber optics cable

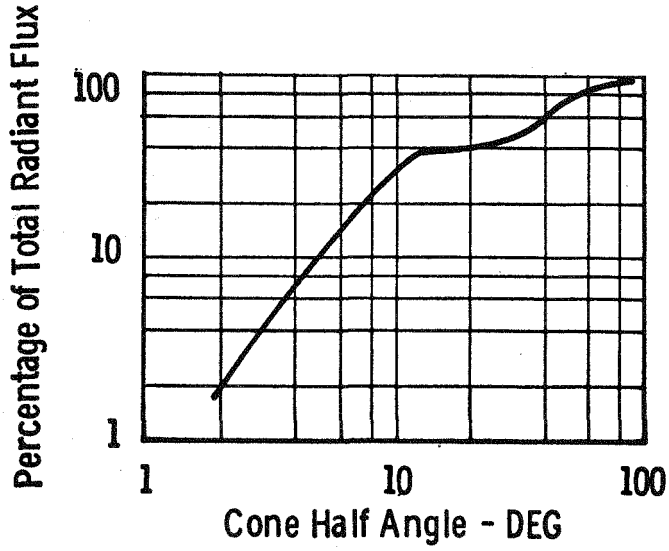

Fig. 4.10— Percentage of total radiant flux within a given cone angle for a light emitting diode

Some characteristics of commercially available fiber optics cables are listed in Table 4.4.

Table 4.4

PROPERTIES OF SELECTED FIBER-OPTICS CABLES

Mfg.	Type	Transmission in 2 Meters	N.A.	Active Dia., mm	Price per Ft.	6 Ft. with Ferrule Ends
Galileo	K2K	80%	0.66	1.1	$0.75	
Corning	5010	45%	0.63	1.1		$12
Valtec	101	74%	0.56	1.5		$16
Am. Optical		83%	0.66	1.1	$1.00	
Valtec	Quartz	97%	0.30	0.4	$3.00	
Corning	Optical Waveguide		0.15			

A system consisting of a series string of thyristors, each individually triggered by a separate laser diode is certainly possible. A significant disadvantage of such a system is that, should a single laser diode fail or degrade, the entire string of thyristors would become nonoperational.

Increased reliability can be achieved by using the output of a multiplicity of diodes to trigger the entire string. This can be accomplished by use of a multifurcated fiber optics cable. In such a cable, the individual fibers which collect the light from a single laser diode are separated and distributed in equal numbers to each of the outputs (the thyristor packages). Thus each thyristor sees a fraction of the light from each laser diode. In a variation of this arrangement, an extra output is provided so that the average light input of the bank of laser diodes can be monitored, providing a warning if several laser diodes should fail and the total light input to the thyristor stack should become dangerously low. (This variation is illustrated in Fig. 6.1.) Galileo Electro-Optics, Sturbridge, Massachusetts, was chosen to fabricate these multifurcated fiber optics cables.

4.4 OPTICAL COUPLING

As was discussed in Section 4.3, a major source of optical energy loss in fiber optics systems is losses due to inefficient coupling between components. The magnitude of these losses and some investigations into means of reducing these losses are described in the following.

4.4.1 Coupling Fiber Optics Cable to Laser Diodes

The discussion of fiber optics cables in Section 4.3 described the importance of numerical aperture and source-to-cable distance in determining optical coupling losses. An investigation was undertaken to see to what extent these losses would be reduced by decreasing the source-to-cable distance.

Three types of laser diodes, two types manufactured by RCA and one type manufactured by Laser Diode Laboratories, Inc., were investigated. The diodes were tested both with caps on and with the caps removed to permit better coupling to the fiber optics cable. The fiber optics cable used was the type selected for use in the demonstration module for this contract: a 1.2 mm diameter multistrand glass cable with Amphenol connectors. The results are summarized in Figure 4.11. Three different fiber optics cables (each 93 cm long including the connectors), three laser diodes of Laser Diode Laboratories Type LD-68, five of RCA Type SG2012, and two laser diodes of RCA Type C30042 were used to get some idea of the range of light values involved. The fiber optics cable showed a maximum difference of only 7 percent. One of the three fiber optics cables performed very near to the middle of the range, and the data of Figure 4.11 were taken with this cable. The effective range of output of the laser diode/fiber optics cable combination can be increased by minor screening if desired, but screening is not required for the contemplated application if the Laser Diode Laboratories Type LD-68 is used.

Only about 30 percent of the radiation emitted by the large (0.5 x 0.5 mm square) emitting area of the RCA Type C30042 laser diode was transmitted through the fiber optics cable; but even so the poorer of the two laser diodes evaluated produced sufficient light by itself to trigger eight thyristors. At the present state of knowledge, this type is believed to be much more powerful than is desired for the application, and was not pursued further. However, this type of unit could possibly be employed usefully in applications requiring very high voltage strings or very high current arrays of thyristors.

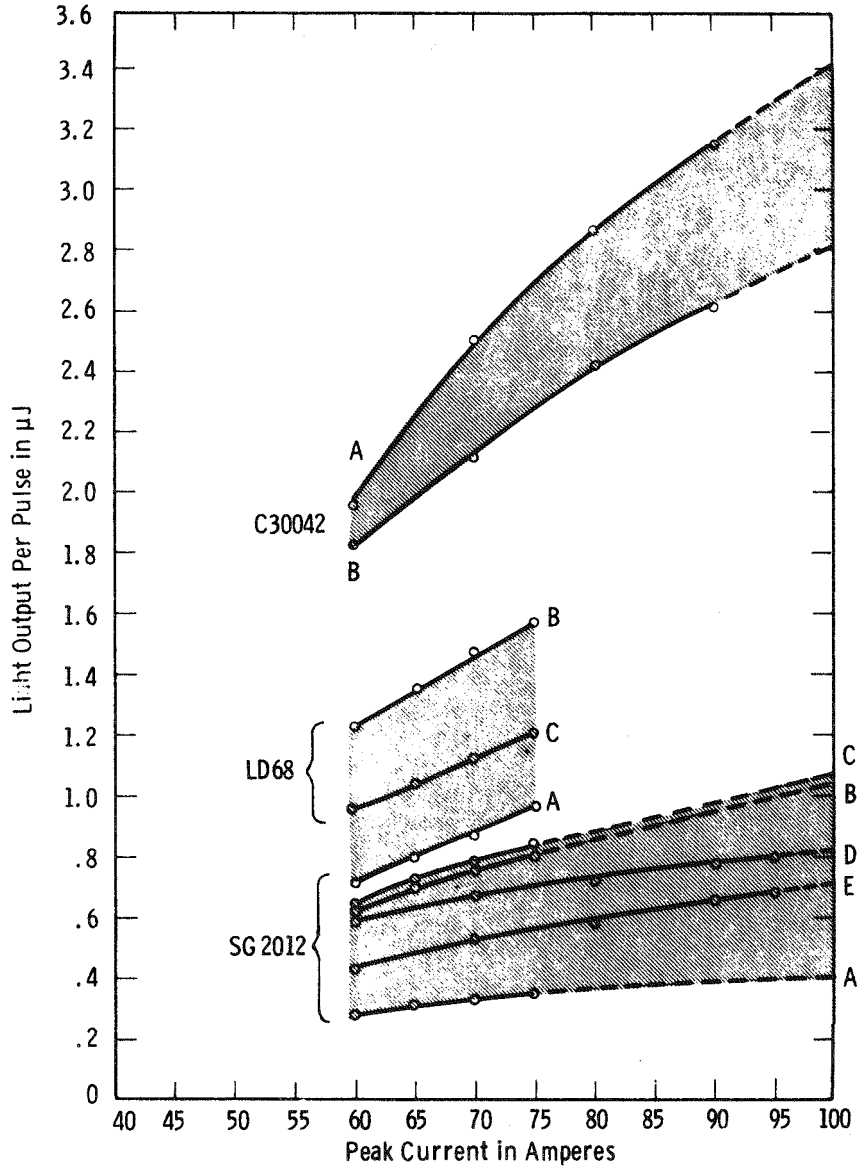

Fig. 4.11 Light output vs. peak current as collected and delivered by 93 cm of 1.2 mm diameter fiber optics cable from laser diodes as manufactured with the caps or case on and with the end of the fiber optics cable flush against the surface of the lens of the cap.

Figure 4.12 shows the results of removing the caps from the LD-68 and SG2012 laser diodes and butting the end of the fiber optics cable (FOC) snugly against the emitting region. Compare with Figure 4.11 and note that there is only a very small improvement in the effective light output from the LD-68/FOC combination, but there is a significant improvement in the SG2012/FOC combination. This is because the case design for the LD-68 is near optimum for use with the 1.2 mm diameter fiber optics cable (see Figure 4.13). Because of the problems anticipated with the laser diode operating in an uncontrolled environment, systems use of laser diodes without caps is not recommended.

4.4.2 Improvements in Laser Diode Current Waveform

Laser diode output data are derived from tests with power circuits that form the current pulse by simple capacitor discharge. The current pulse shape exhibits the familiar sharp rise to a peak value followed by exponential decay. Since the output of the laser diode is limited both by the maximum permissible peak flux (current) and by thermal considerations, the capacitor discharge circuit appears to make very inefficient use of the laser diode. By introducing a pulse forming network to obtain a more nearly rectangular wave, the light output should be increased without either damaging the laser diode facets (peak flux not exceeded) or overheating the laser diode. Figure 4.14 shows the current waveform for each type of circuit.

Measurements to assess the degree of efficiency improvement which might be attained were made with LD-68 laser diodes. Data were taken both with the cap on the unit and with the cap removed. In each case, the end of the FOC was placed as near as possible to the laser diode emitting surface. The package design of the Type LD-68 nearly meets the criterion of Figure 4.13(b); i.e., the FOC is close enough to the chip, even with the cap in place, to intercept nearly all of the light emitted. A small increase, about 15%, was noted in the amount of light collected when the cap was removed. The elimination of the two reflecting surfaces of the transparent plate accounts for most of this improvement. For interest, some optical grease was then applied to the end of the FOC and an additional 15% increase was noted in the amount of light collected. These results are summarized in Figure 4.15.

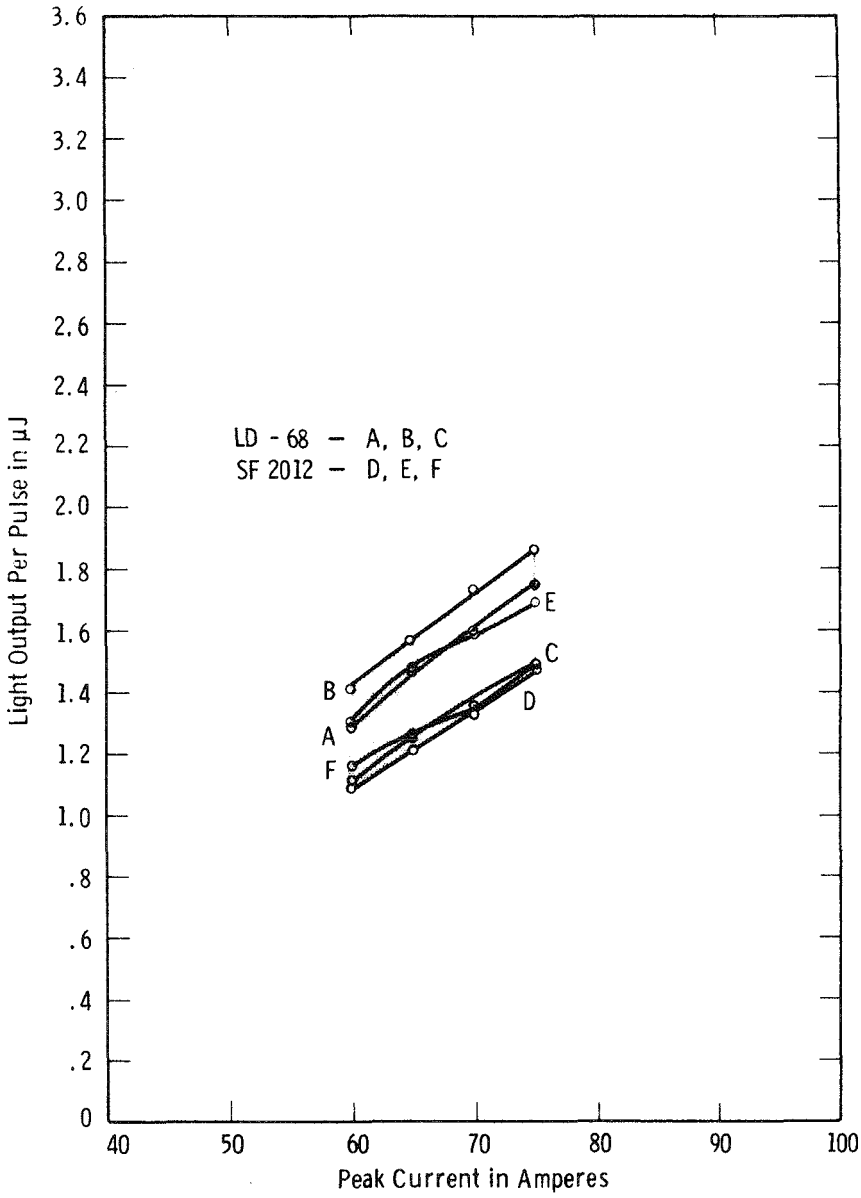

Fig. 4.12 Light output vs. peak current as collected and delivered by 93 cm of 1.2 mm diameter fiber optics cable from laser diodes with the caps removed and with the end of the fiber optics cable flush against the surface of the laser diode chip.

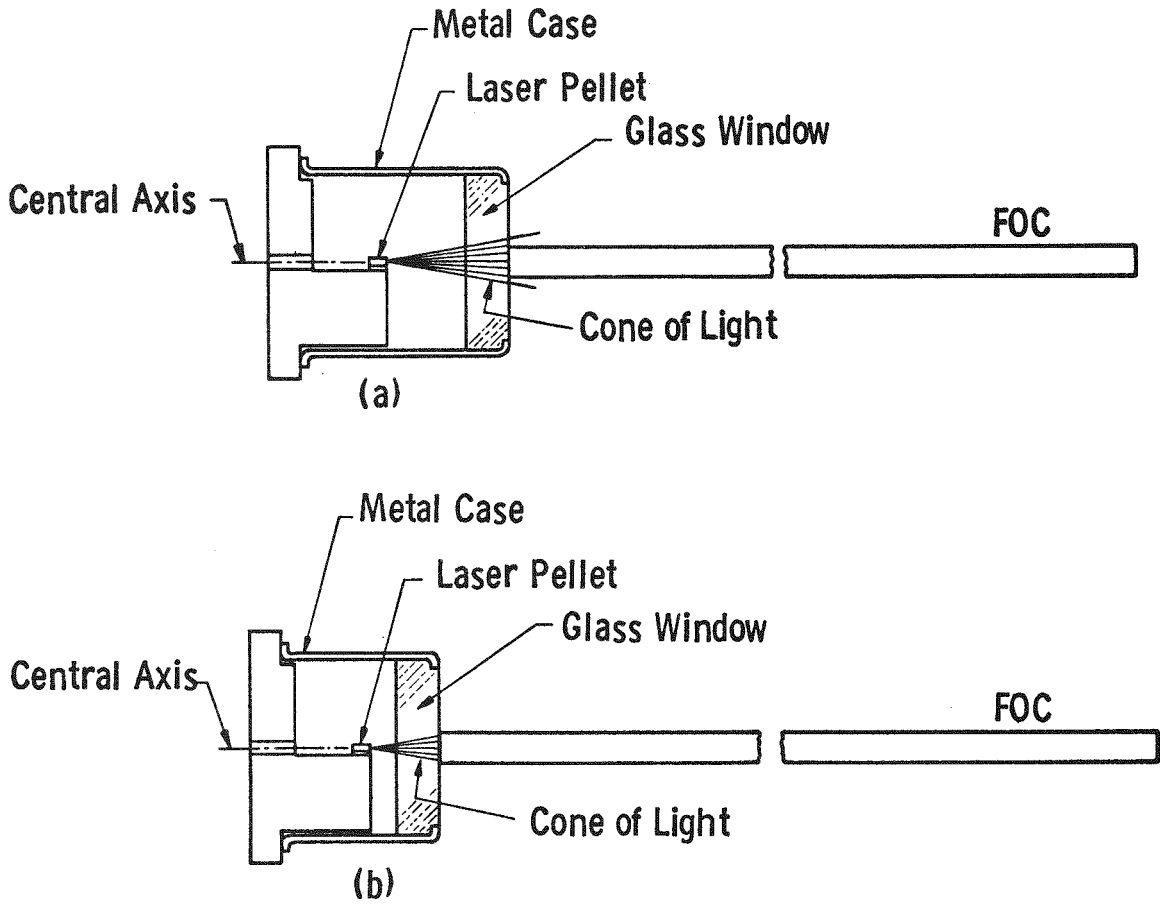

Fig. 4.13 — Cross-sections showing how the length of the laser diode metal case (cap) affects the amount of light coupled in the fiber optics cable (FOC)

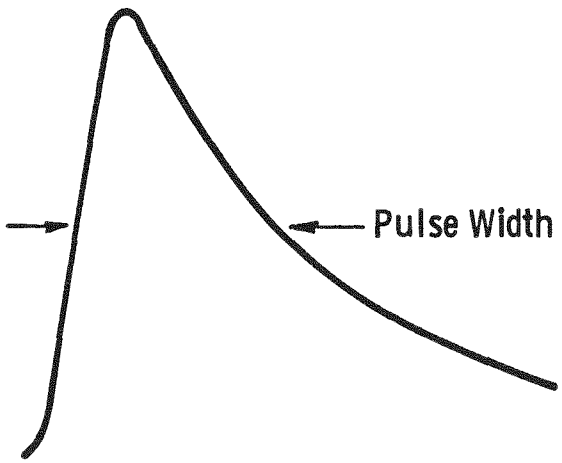

(a) Capacitor Discharge

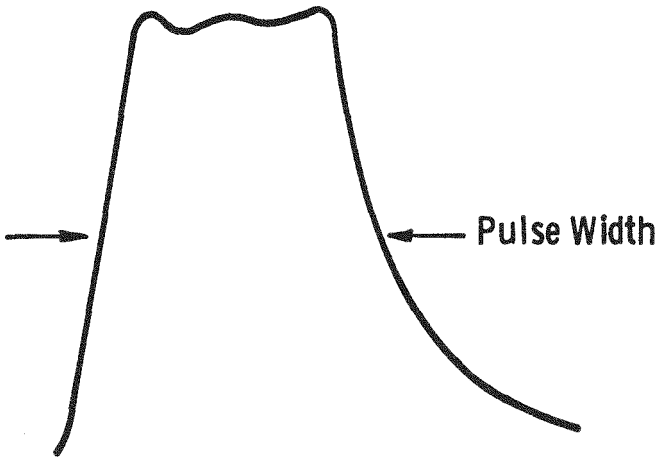

(b) Pulse Forming Network

Fig. 4.14 — Current waveforms of laser diode power circuits

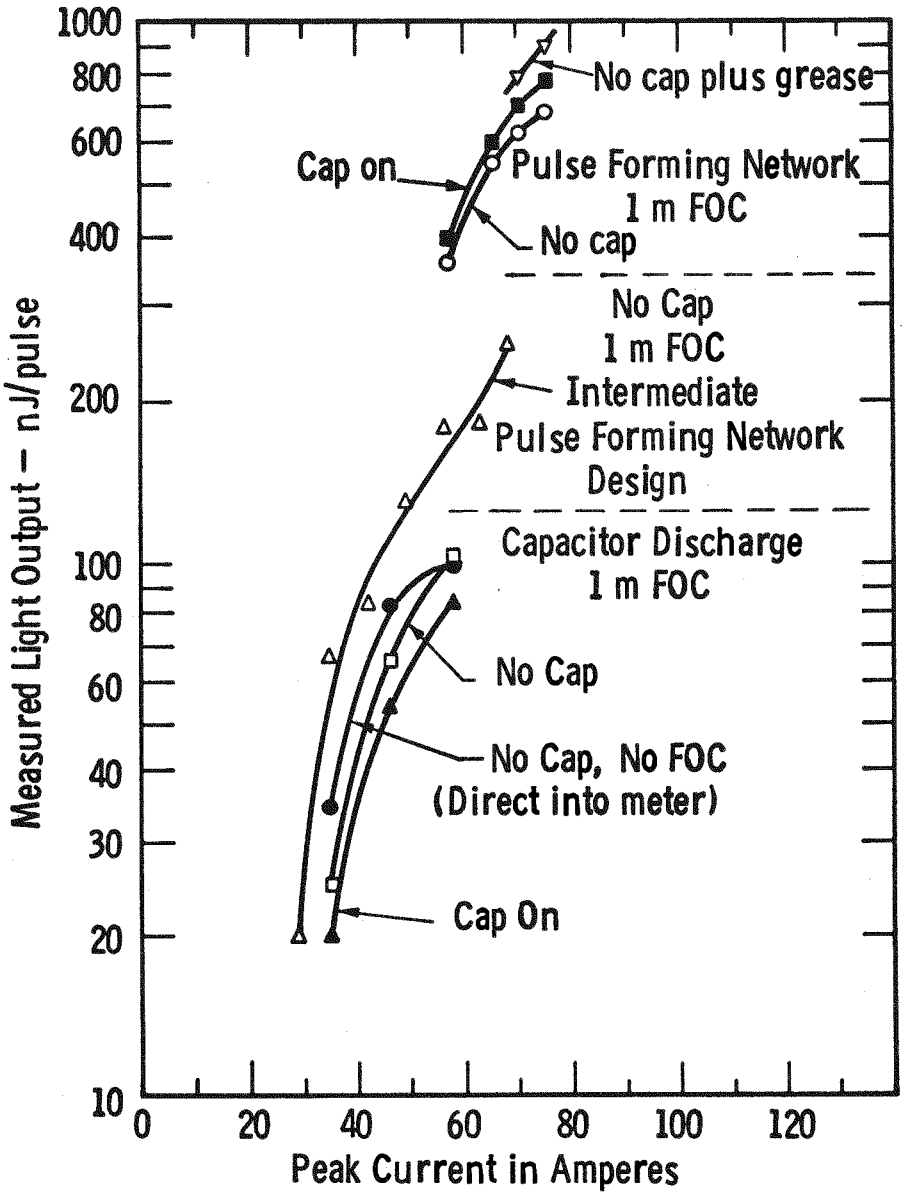

Fig. 4.15 – Details of experiments to increase the effective output of laser diode into fiber optic cable

The data show that significant improvements in light output can be attained through the use of a pulse forming network; however, because similar results can be obtained more easily and cheaply simply by increasing the width of a capacitor discharge, the pulse forming network is not recommended for this program.

Figure 4.8 in Section 4.2 shows that the pulse width could be safely increased from 200 ns to at least 400 ns if more optical energy is required.

4.4.3 Fiber Optics Connectors

Accurate axial alignment and carefully controlled spacing are essential to efficient coupling between fiber optics components. Demountable fiber optics cable connectors must possess a high degree of dimensional precision if coupling efficiency is to be maintained. Figures 4.16 and 4.17 are the suppliers sketches of the type of fiber optic cable connector that has been chosen for this program. This connector, made by Amphenol, is commercially available, and is the optical counterpart of a single lead electrical connector. The box receptacle accepts a standard laser diode package in such a manner as to ensure the best possible optical coupling between the laser diode and the fiber optics cable. Better coupling could be achieved with a special diode/fiber optic cable package, but the development of such a package is not considered necessary.

The sleeve of the light pipe of the thyristor package has been designed to mate with the cable plug so as to obtain near optimum coupling between the fiber optics cable and the light pipe.

4.4.4 Summary of Light Losses

Experiments have demonstrated that the total loss of light from the laser diode source to the silicon surface is 9 dB. This corresponds to an effective transmission of 12%. The losses break down as follows:

(1)	Laser diode into 1.1 mm flexible fiber optics cable (FOC)	4.3 dB
(2)	Attenuation in Corning FOC (1 db/m) 2m	2.0 dB
(3)	Flexible FOC to 1.25 mm dia. bent light pipe	1.6 dB
(4)	Light pipe-epoxy-silicon dioxide-silicon combination	0.84 dB

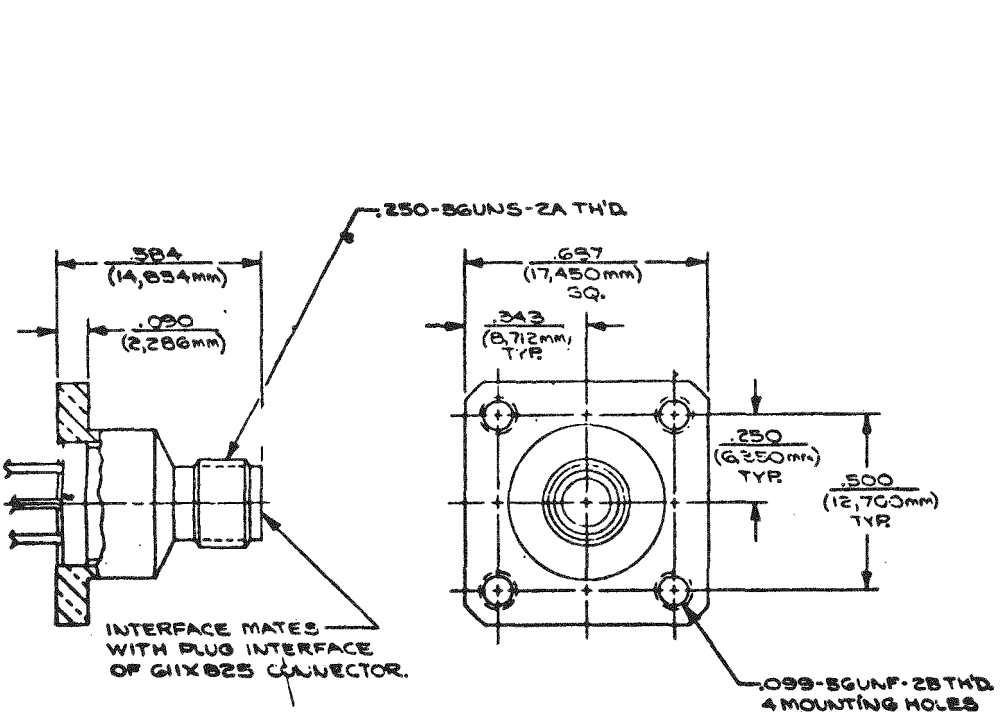

Fig. 4.16 — Amphenol connector for light source

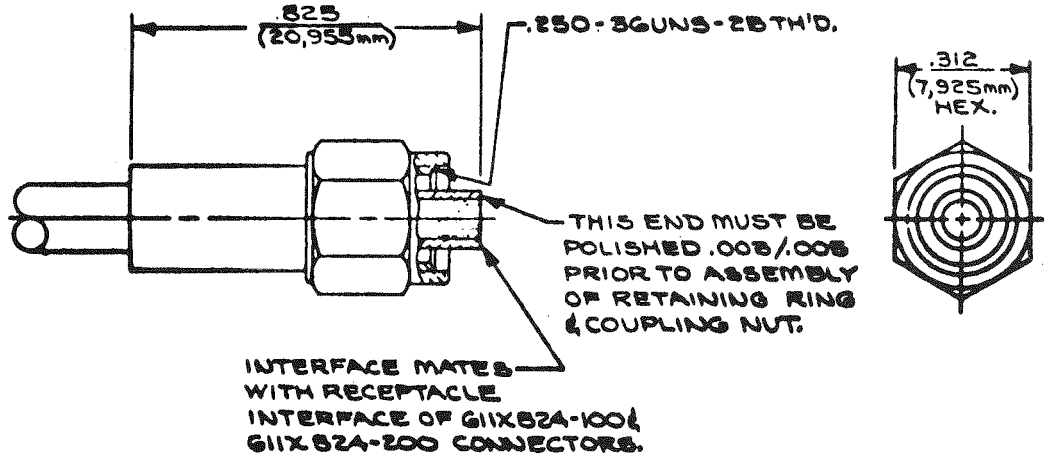

Fig. 4.17 — Amphenol connector for fiber optic cable

A total transmission of 10% was used for calculations in other portions of this report to allow for manufacturing variations.

Note that the above calculation is for a 2 meter length of fiber optics cable at an assumed attenuation of 1 dB per meter. From this one can project the transmission losses of longer lengths of cable. Furthermore, 1 dB/meter is the highest loss cable that is being considered. American Optical claims to have a cable with only 0.4 dB/meter losses in the near infra red region. This cable also has a slightly superior (larger) numerical aperture to that of the Corning cable. Such cables are not required for the present program, but may be of interest in larger systems with longer lead runs.

4.5 SUMMARY AND CONCLUSIONS

Considerations of practicality, efficiency, and reliability have led to an optical system design consisting of

- A bank of eight or nine GaAs laser diodes (LD-68 recommended).
- A multifurcated fiber optic cable which evenly distributes the optical output of the laser diodes between a string of eight light-triggered thyristors.
- Precision fiber optic cable connectors of the type available from the Amphenol RF Division of Bunker Ramo, Danbury, Connecticut.

Reliability and life projections based upon data supplied by RCA indicate that the light sources could be expected to operate for over forty years without serious degradation or failure. Optical power losses from laser diode source to the thyristor surface have been evaluated. An effective transmission of 12% (9 dB loss) is conservatively estimated.

Studies have shown that overall system improvements could be realized through improved laser diode packaging, special diode-to-fiber optic cable adapters, and through thermo-electric cooling of the laser diode bank. At this time, however, it is our feeling that the benefits to be realized do not justify the expenditure of the necessary additional development effort.

The state-of-the-arts of laser diodes and fiber optics cable are expected to continue to change rapidly for several years. As a result, for each new application an engineering analyses should be performed to determine the effect of

using the new technology available. More powerful laser diodes and lower loss fiber optics cable will make it possible to reduce the number of light sources to the minimum necessary to meet the overall system redundancy requirements. The present work has demonstrated that the present technology is adequate to develop a practical light triggered thyristor switch system. Improvements in the technology will result in even lower cost and more reliable systems.

Section 5

DEVICE TESTING AND EVALUATION

5.1 INTRODUCTION

In general, device testing was planned to measure those performance characteristics which are critical to any thyristor designed for low frequency applications, at the particular voltage and current level applicable to the target devices. Testing measured both static and dynamic performance to verify that the light-triggered thyristor performance was at least as good as that of an equivalent electrically gated device.

Other tests were designed to measure those properties which are unique to the light triggering process. The character of this group of tests was influenced by the light triggering source, and some testing procedures evolved as the need for better definition of the light-triggering process became apparent. Since some characteristics of the light-triggering process are without parallel in commercial practice, some test levels were arbitrarily chosen; others were guided by the desired device application.

Tests which were performed are described in the following subsections. Tests of characteristics which are common to all thyristors, regardless of the turn-on mechanism are described in 5.2; tests which are related to the light-triggered nature of the thyristors are described in 5.3. Test results are tabulated in 5.4.

5.2 STANDARD THYRISTOR TESTS

This section describes those tests which are relevant to all thyristors, regardless of the method of triggering.

5.2.1 Blocking Voltage (V_D @ I_D, V_R @ I_R, 25°C and 125°C)

In this test, the forward leakage current (I_D) and the reverse leakage current (I_R) are measured at prescribed forward voltage (V_D) and reverse voltage (V_R). In general, the voltages used in this test are the desired repetitive forward blocking voltage (V_{DRM}) and the desired repetitive reverse blocking voltage (V_{RRM}). Design values for these parameters are V_{DRM} and V_{RRM} > 2000V; I_{DRM} and I_{RRM} at 125°C < 50 mA.

During testing at room temperature, early production units exhibited good avalanche characteristics with low leakage currents at voltage levels between 2300 and 2700 V. Tests at 125°C at high blocking voltages showed leakage currents increasing in a normal manner. Several failures were observed when high avalanche currents were permitted at high temperature. In general, these failures were not catastrophic , but they were also not reversible. In a few cases, blocking voltage capability was reduced by one-half or more when devices were pulsed at high avalanche levels. It is believed that these changes were related to the edge preparation and passivation of the thyristors and did not relate to the light-triggered thyristor design. Subsequent units were therefore not tested at high avalanche current levels.

A blocking voltage level of 2000 V was selected as a reasonable and useful value at which all tests would be completed without losing devices because of destructive testing. In Table 5.1 all blocking voltage levels are presented as the forward leakage current (I_D) or reverse leakage current (I_R) at an applied voltage of 2000 V. Standard blocking voltage rating tests which measure the achievement of desired blocking voltage at < 50 mA leakage current, or the voltage at which leakage current exceeds 50 mA at 125°C, will not be performed until Phase II of the light-triggered thyristor project. The test circuit used in blocking voltage measurements is illustrated in Fig. 5.1.

5.2.2 Forward Conducting Voltage (V_{TM})

Forward conducting voltage is that voltage which exists across a thyristor while conducting a half sine wave 60 Hz pulse. The conducting voltage drop is an indication of the current capacity of the switch since a thyristor with a low voltage drop can carry a large current without exceeding the maximum allowed junction temperature. Most devices were tested at a peak forward current of 1500 A. In the test procedure, a large current pulse is drawn from a low voltage supply to avoid high power dissipation in the test apparatus. Thyristors

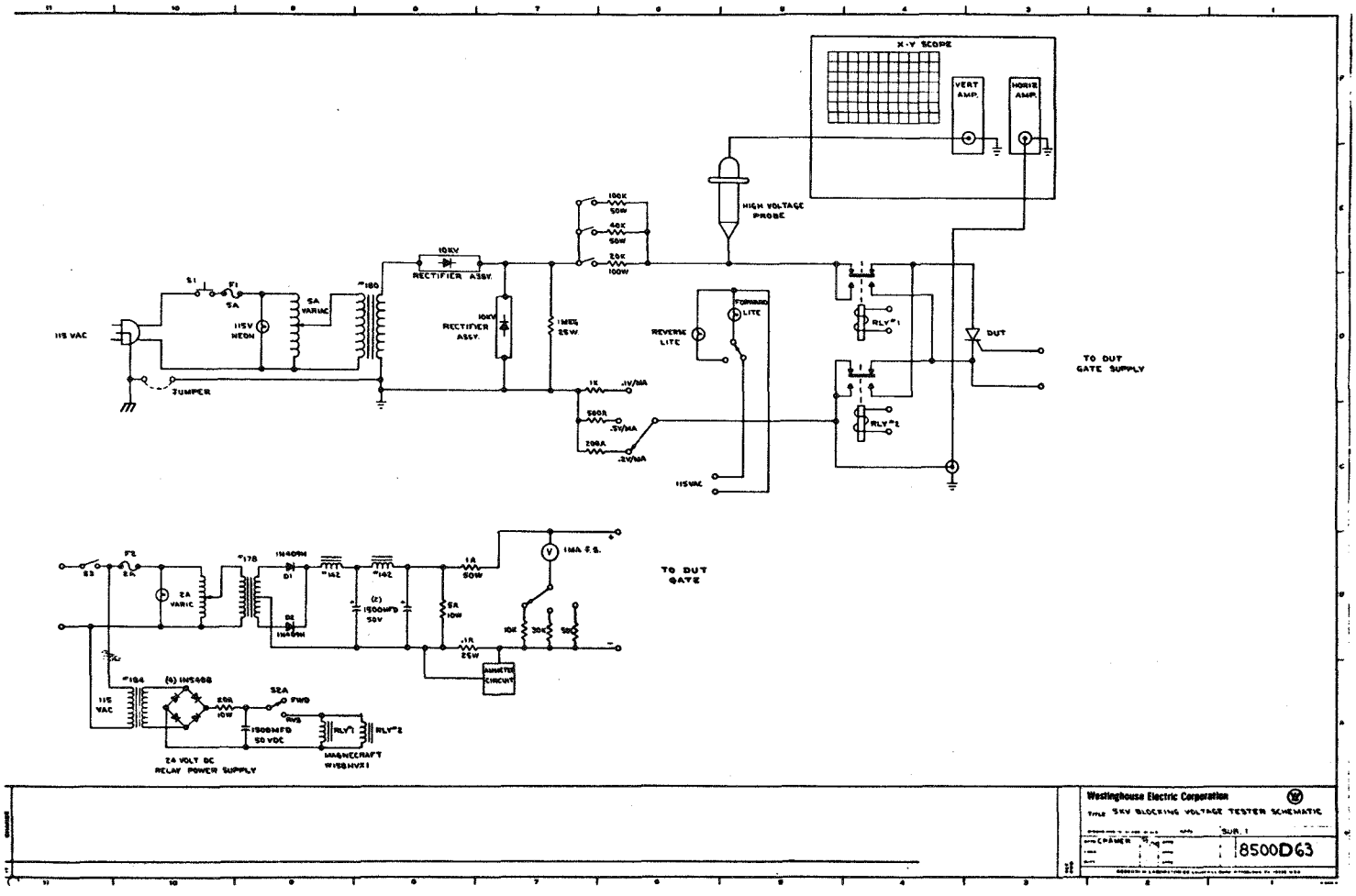

Fig. 5.1 Test Circuit for Measurement of Blocking Voltag

which did not turn on at the available low voltage were tested with a higher voltage apparatus which is not capable of delivering 1500 A; devices which were tested at less than 1500 A are indicated by an asterisk in Table 5.2.

5.2.3 Transient Tolerance (dV/dt)

Normal techniques for the measurement of dV/dt capability use a transient voltage which is 80% of the repetitive forward blocking voltage. For devices designed for 2000 V V_{DRM} this implies a peak transient voltage of 1600 V. A repetitive transient of this level is applied while the rate of voltage rise is progressively increased until forward turn-on occurs in a non-destructive manner. Test equipment available for this project had a maximum voltage capability of 800 V. Since it is possible for dV/dt turn-on to be destructive, the transient rate of rise was not increased to the maximum level tolerated by each device, but instead was increased only to a level which ensured that the device would meet its design specifications. Measurements were made at 125°C. Some devices were tested at the Westinghouse Semiconductor Division quality assurance laboratory to the maximum available dV/dt. These devices exhibited transient tolerance capability in excess of 1800 V/μs. The test circuit which was used in the dV/dt measurements reported here is illustrated in Fig. 5.2.

5.2.4 Turn-Off Time (t_q)

Turn-off time is a measure of the time necessary for a switch to regain forward blocking capability after the end of a forward current pulse. Parameters which influence turn-off time are

a) Peak forward current during the pulse
b) Forward current decay rate
c) Peak re-applied voltage after the current pulse
d) Rate of rise of the re-applied voltage
e) Thyristor junction temperature

Test apparatus capable of 1600 V re-applied voltage was not available for this test so initial tests were performed at the available 800 V level. All other aspects of this test were standard. Measurements were made at 125°C with a forward peak current (I_T) of 250 A decaying at a rate of 10 A/μs. The test circuit used for measuring t_q is illustrated in Fig. 5.3.

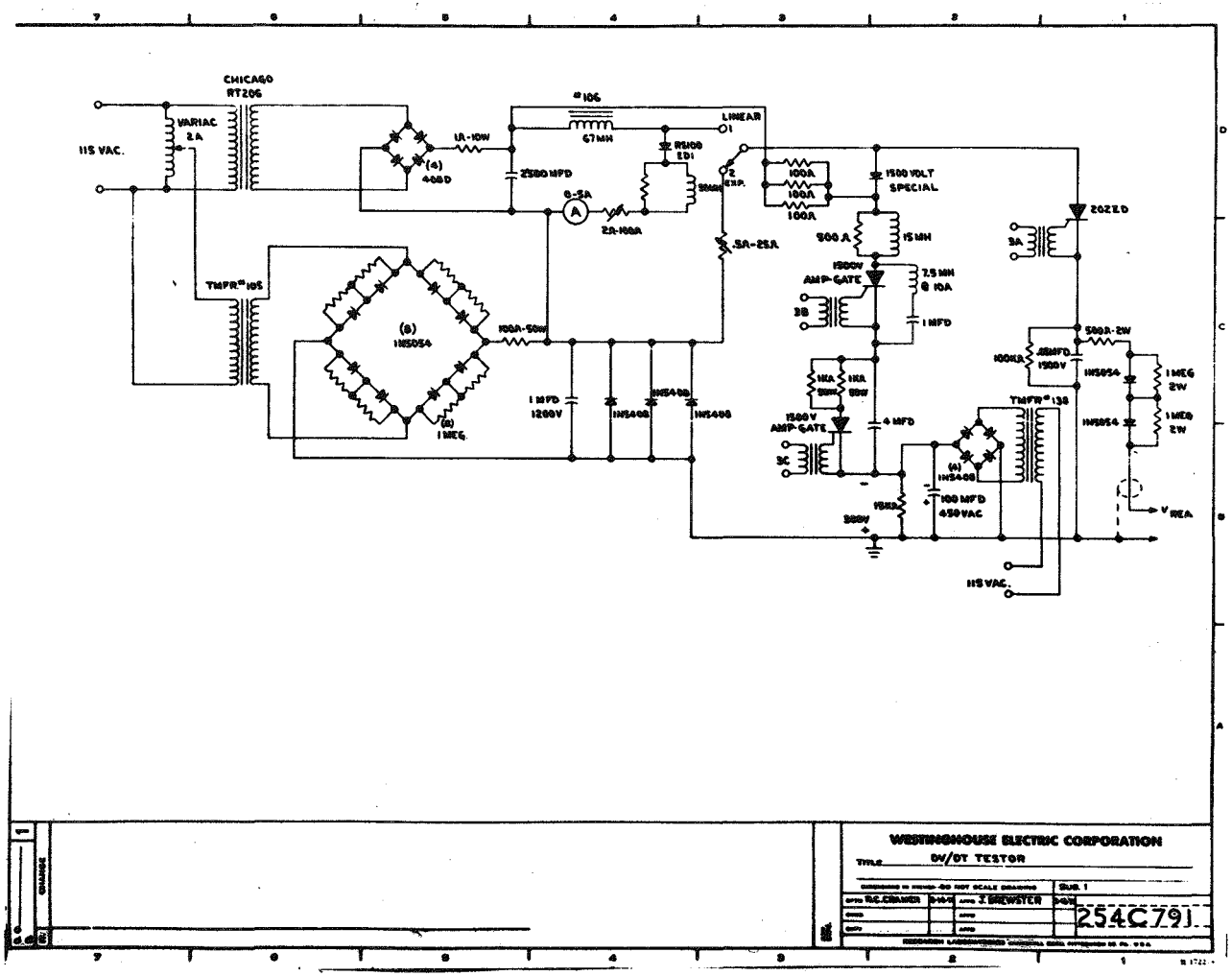

Fig. 5.2 Test Circuit for Measurement of Transient Tolerance (dv/dt)

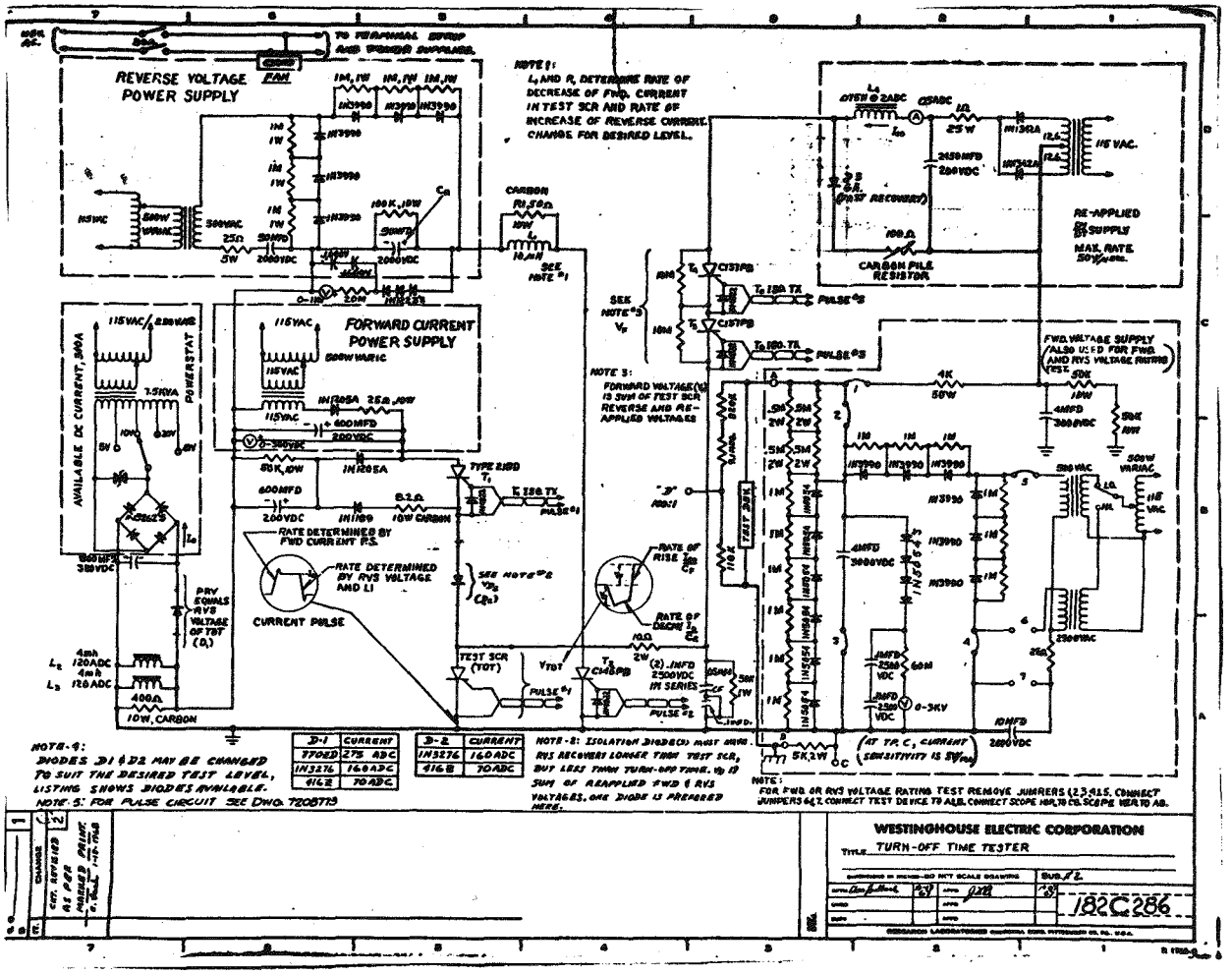

Fig. 5.3 Test Circuit Used for Measuring Turn-Off Time (t_q) and Reverse Recovery Charge (Q_{rr})

5.2.5 Reverse Recovery Charge (Q_{rr})

Immediately after conducting forward current, a thyristor does not block reverse voltage but will conduct a small reverse current until the excess holes and electrons generated by the forward current are removed by reverse current sweep-out. The reverse current which flows through a thyristor after forward conduction is dependent upon

a) The peak forward current
b) Carrier lifetime in the thyristor
c) Forward current decay rate
d) Junction temperature
e) Magnitude of the reverse voltage

"Reverse recovery charge" is the measured time integral of the reverse recovery current. Typical test conditions were selected for the Q_{rr} test to give results comparable to those of electrically gated thyristors. Results of this test are used in the selection of suppression components for a switch consisting of several series connected thyristors so that dynamic voltage sharing will be achieved during reverse recovery of the switch. Measurements were made at 125°C with a forward current of 350 A decaying at a rate of 3.5A/μs. The circuit used in the measurement of Q_{rr} is illustrated in Fig. 5.3. Waveforms observed in the measurement of Q_{rr} are shown in Fig. 5.4.

5.2.6 Holding Current (I_{HO})

Holding current is the minimum current required to maintain a device in its forward conductive state after all external gating influence has been removed. Most high power thyristors exhibit holding currents of 50-150 mA at 25°C. At currents below these levels, the carrier regeneration processes end and the forward blocking condition is restored. Holding current was measured at 25°C with the test circuit illustrated in Fig. 5.5.

5.3 LIGHT-TRIGGERING RELATED TESTS

All turn-on and switching tests performed on the light-triggered thyristors were performed with a laser diode trigger source. The laser diode was an RCA SG2003 driven with a current pulse of 80A peak current and 200 ns pulse width. A typical switching event is shown in Fig. 5.6.

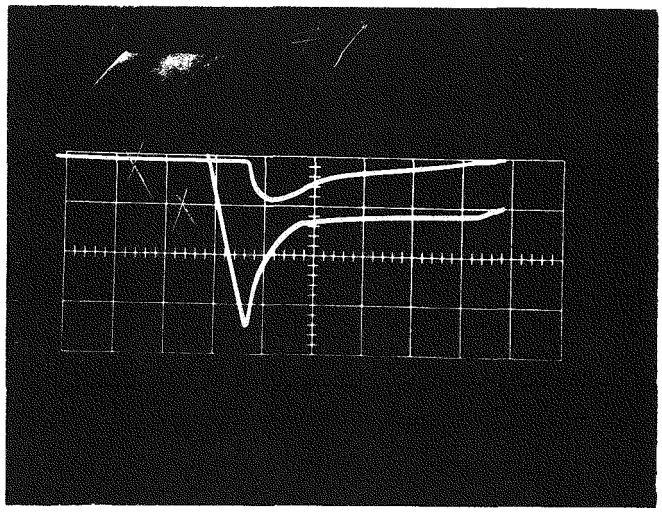

Fig. 5.4 Observed Waveforms in the Measurement of Reverse Recovery Charge (Q_{rr}). Horizontal: 20 μs/div. Vertical: I_A (lower trace) 10A/div., V_A (upper trace) 200V/div. Pulse width 300 μs, peak anode current 350A, temperature 125°C

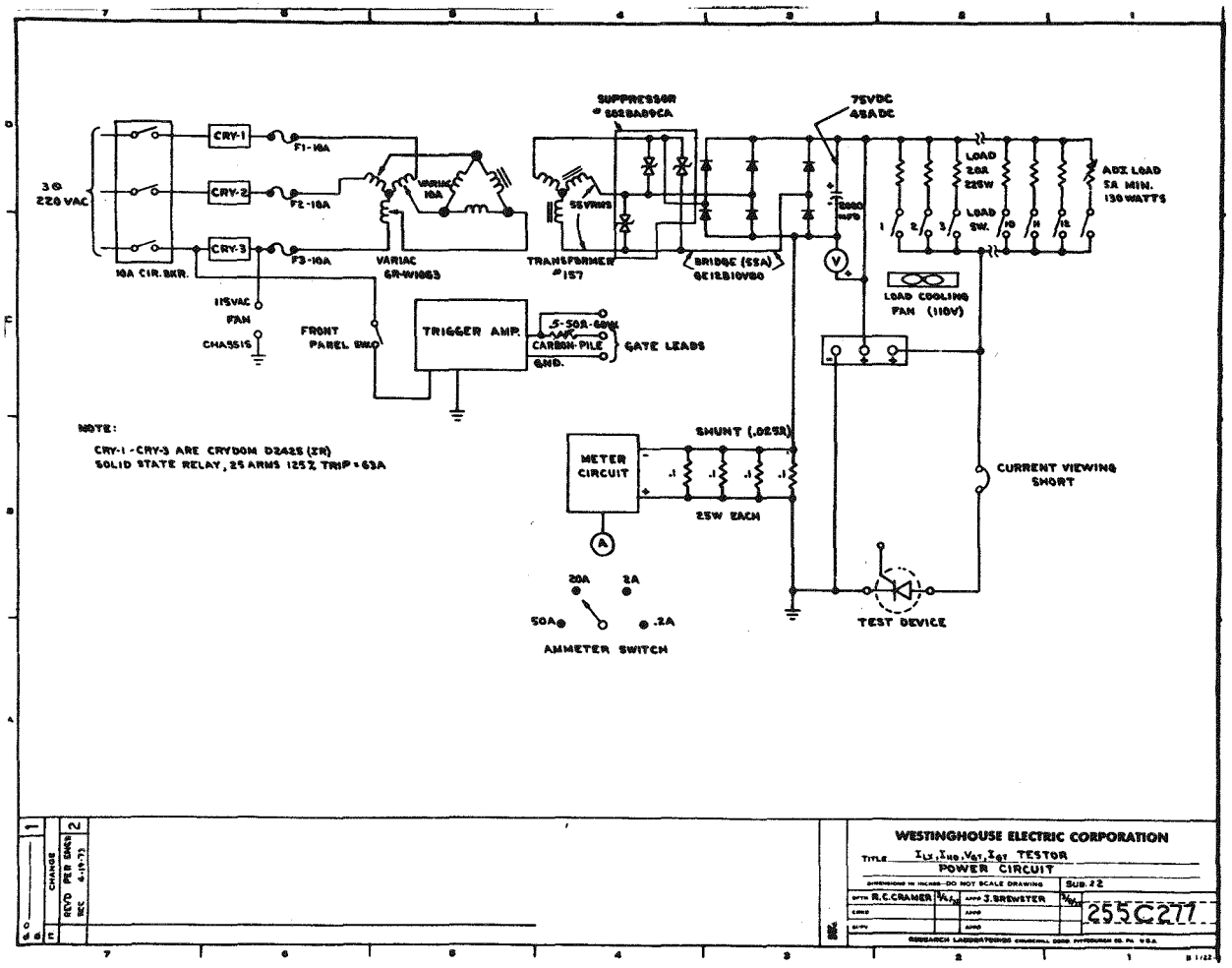

Fig. 5.5 Test Circuit Used in the Measurement of Holding Current (I_{HO}) and Latching Voltage (V_{LX})

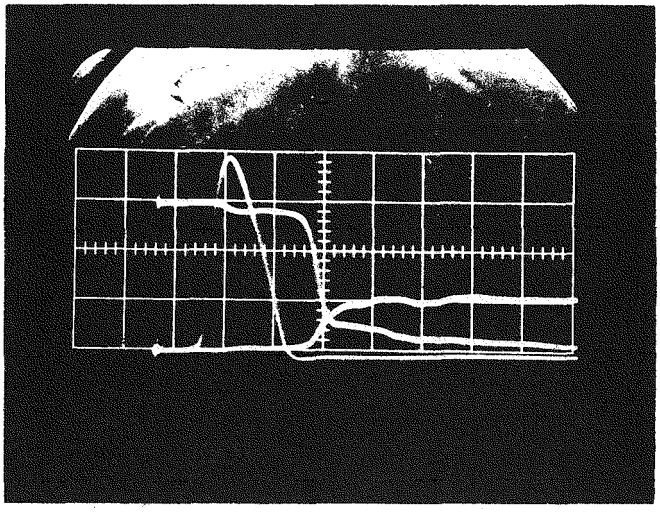

Fig. 5.6 Typical Switching Event. The three curves show laser diode current (20A/div.), anode voltage (400V/div.), and anode current (20A/div.). Time axis is 200 ns/div.

The light output energy generated by each laser diode pulse was measured to be 360 nJ at the output end of a 1.0 meter long fiber optic cable. All thyristor measurements were made with optical pulses of this energy.

5.3.1. Latching Current (I_{LX})

"Latching current" is the minimum current required by a thyristor to remain in the "on" condition immediately after gate excitation is removed. After the thyristor is turned on, current can typically be reduced below the latching current level with the thyristor remaining on until the current decreases below the holding current level. Problems sometimes occur in electrically gated thyristors when the anode current fails to reach the latching current level before the termination of a very short gate pulse. It was anticipated that similar problems might occur in the light-triggered thyristor because of the short duration (200 ns) of the laser diode light pulse. Consequently, two types of latching current test were performed.

In the first test, a battery and a resistive load network in the anode circuit were used to allow a fast rise of anode current so that the expected latching current level would be achieved before the disappearance of the light trigger pulse.

In the second test, in order to be more certain of the latching characteristics of light-triggered thyristors, a base condition test was devised; all thyristors were tested against this condition. This test anticipates that, for the expected device application (series connected string), the thyristors would be shunted by a series combination of resistor and capacitor used for transient voltage suppression and for transient voltage sharing. It was assumed that the suppression network could be represented by 0.5 μF and 100 ohms, and that this network would be charged to at least 75V before turn-on was attempted. Thus when turn-on is attempted, an immediate current provided by the charged suppression capacitor flows through the thyristor; this current is in addition to a circuit-limited anode current (provided by a 60 μF capacitor in series with an inductor) with a rate of rise of approximately 0.1 A/μs. All devices tested latched on properly under the base condition latching test. This test is called the "low voltage latch test" in subsection 5.3. The test circuit used for this measurement is the circuit illustrated in Figures 5.7 and 5.8. Typical observed waveforms in this test are shown in Figure 5.9.

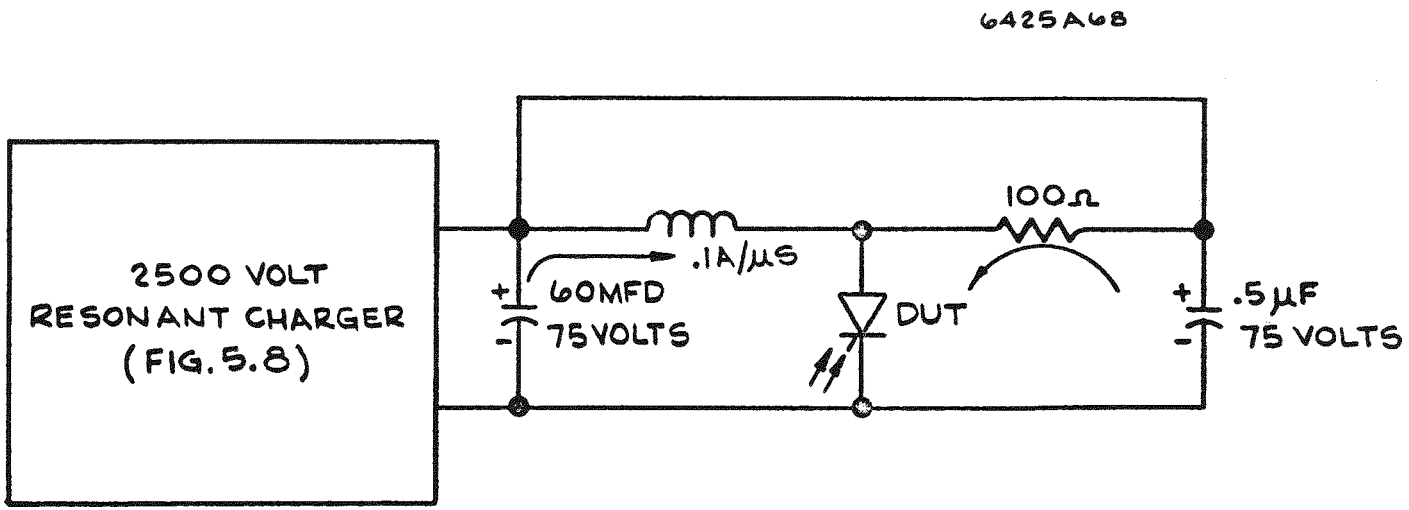

Figure 5.7. Circuit for base line switching test.

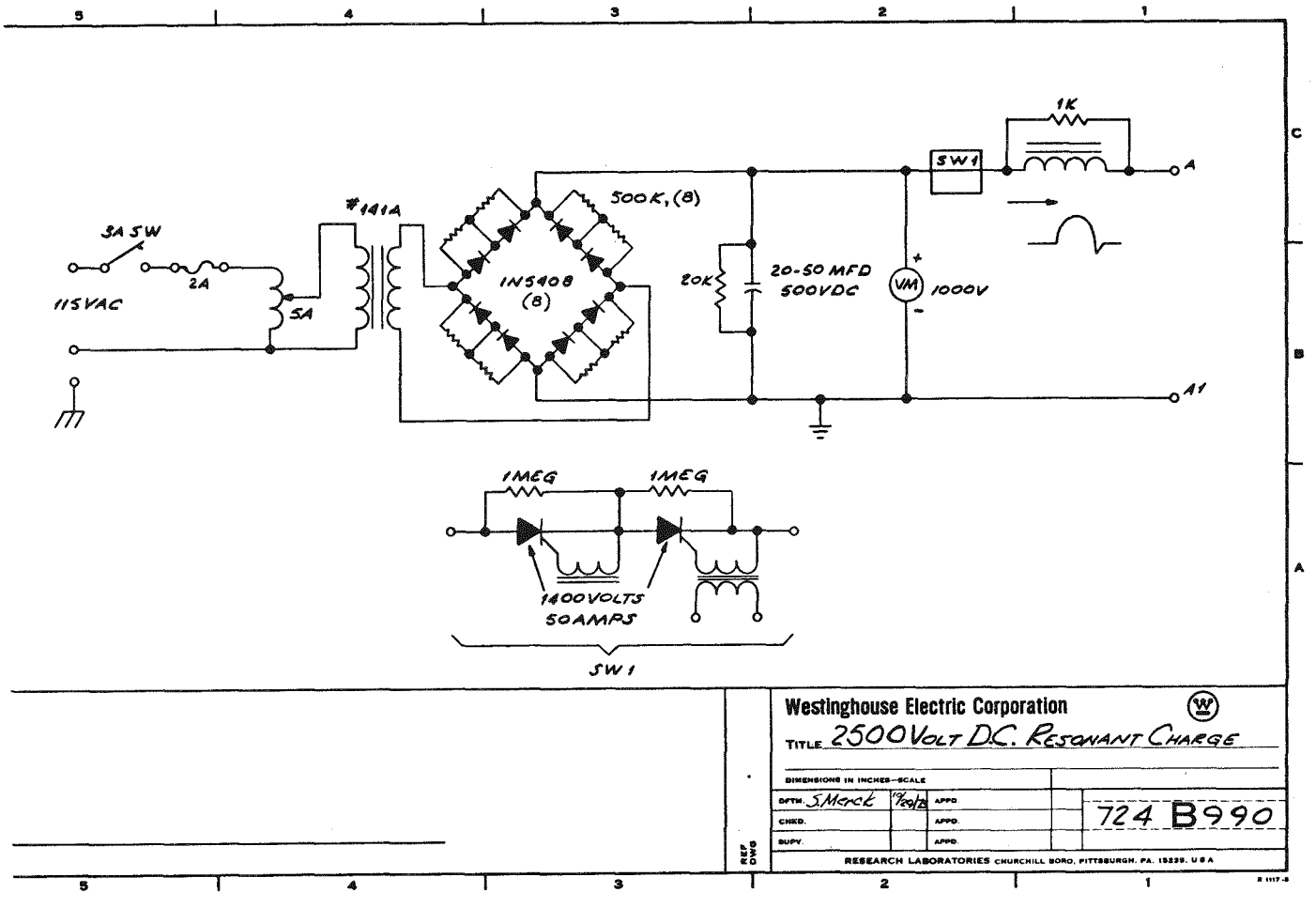

Fig. 5.8 2500V D.C. Resonant Charger Circuit

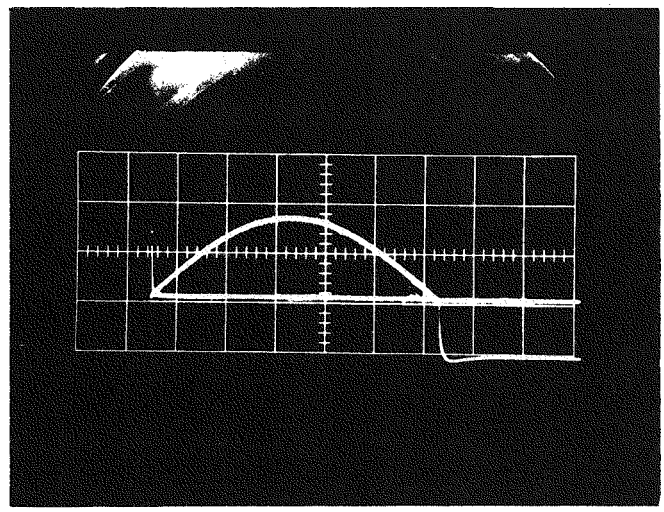

Fig. 5.9 Waveforms Observed in Base Line (Low Voltage) Latching Test. Horizontal: 100 μs/div. Vertical: I_A (upper trace) 10A/div.; V_A (lower trace) 50V/div. I_A is the sum of 0.5 μF discharging through 100 ohms and an 0.1 A/μs follow current.

5.3.2 Latching Voltage (V_{LX})

During measurement of latching current, some thyristors were found that did not latch on at the voltage (50 V) supplied by the test equipment, but would latch on at a somewhat higher voltage. Further, it was discovered that as the energy of the triggering light pulse was decreased, all thyristors required an increase in anode voltage in order to latch on. These observations indicate that latching voltage is indicative of the effectiveness of the light triggering pulse and can be used as a test for possible optical component problems. Therefore, a latching voltage test was devised and was used on all thyristors. In this test, the available anode current was set at a level at least ten times the normal latching current. Using a fixed value of triggering light energy (360 nJ) the anode voltage was decreased until latching no longer occurred. An acceptance level of latching voltage was chosen to be 5.0 V (electrically gated thyristors typically latch on at anode voltages as low as 2.0 V). In a few cases, thyristors with latching voltages as high as 10.0 V were accepted for further tests.

It is believed that the V_{LX} test is useful in screening completed thyristors for optical component inadequacies. Although there is no industry standard for latching voltage, a test of this parameter appears to be useful in identifying units which are likely to fail prematurely in use. For example, it has been observed that in some units with high latching voltage, switching action is sluggish (anode voltage rate of fall is slow). This presents a condition of high power dissipation in the device during switching; such a unit would probably fail during a high di/dt turn-on condition. It is anticipated that only those thyristors which latch on at mode voltages of 5.0 V and above will be accepted for series stack applications and that this specification can be easily met. The circuit used in the measurement of latching voltage is that circuit shown in Fig. 5.5.

5.3.3 Turn-on Time (t_{on})

Waveforms observed during the turn-on time test are illustrated in Fig. 5.6. Test conditions call for the device to be turned on from a 1200 V blocking level with anode current supplied by a network in parallel with the device. This network is composed of a 0.5 μF capacitor in series with a 50 ohm resistor. The time from which turn-on is measured is the time at the peak of the laser diode current.

Turn-on time is the sum of "delay time" and "fall time". The delay time is the time from the peak of the laser diode current to the time when the anode voltage has decreased to 90% of its initial value. The fall time is the time required for the anode voltage to decrease from 90% to 10% of its initial value. The current for the turn-on test is that supplied by the 0.5 μF capacitor discharging through the 50 ohm resistor and through the device under test. The test circuit used in the measurement of t_d, t_f, and t_{on} is illustrated in Fig. 5.10.

5.3.4 Reverse Photocurrent

If, because of a circuit timing error, a light pulse trigger should be applied to a thyristor in its reverse blocking state, a reverse leakage current pulse would be observed. There is no possibility that the thyristor will turn on, and only a small photocurrent representing the light-generated carriers will flow. Figures 5.11 and 5.12 show the magnitude of this effect for several anode reverse voltages at room temperature and at 125°C. The figures show that the magnitude of the reverse photocurrent increases with increasing anode reverse voltage and decreases with increasing temperature. In no case does this current represent a significant energy loss.

5.4 TEST RESULTS

The results of the tests described in 5.3 are given in tabular form in Tables 5.1, 5.2, and 5.3. Those devices described here are those judged suitable for incorporation into a switching module composed of eight series thyristors (see Section 6).

5.5 SUMMARY AND CONCLUSIONS

In general, the characteristics of the devices reported here successfully meet the target specifications and qualify them for incorporation into the series switch described in Section 6. Some of the characteristics; in particular V_{TM}, Q_{rr}, and t_q; are not as uniform as could be desired. This is attributed to the fact that the thyristors were chosen from separate runs with a small number of thyristors in each run. Better uniformity among thyristors is to be expected when a large number of thyristors is processed simultaneoulsy.

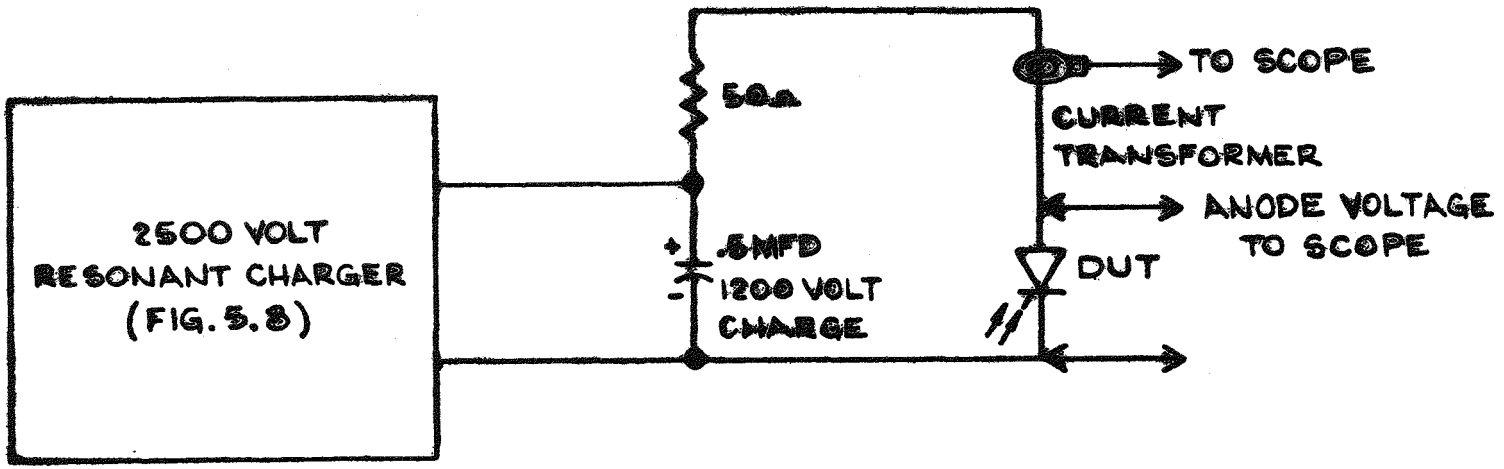

Figure 5-10. Circuit used in the measurement of t_d, t_f, and t_{on}.

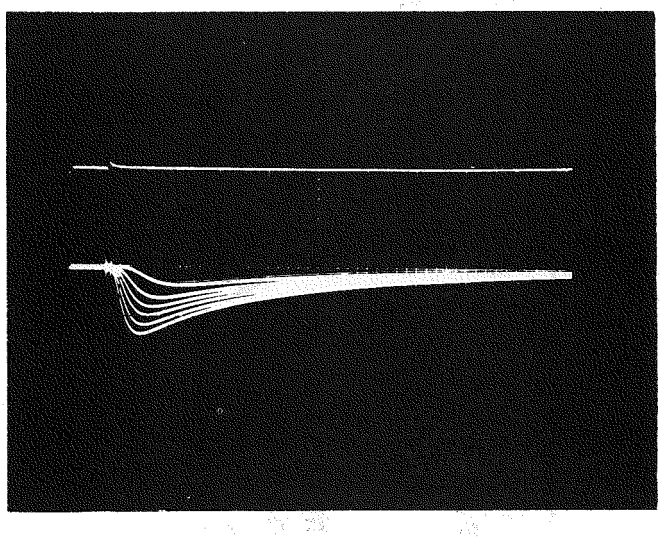

Fig. 5.11 Reverse Photocurrent at 25°C. Horizontal: 10 μs/div. Vertical: 5 mA/div. Anode reverse voltages are 0, 200, 400, 600, 800, and 1000V. The light pulse occurs at t = 7 μs.

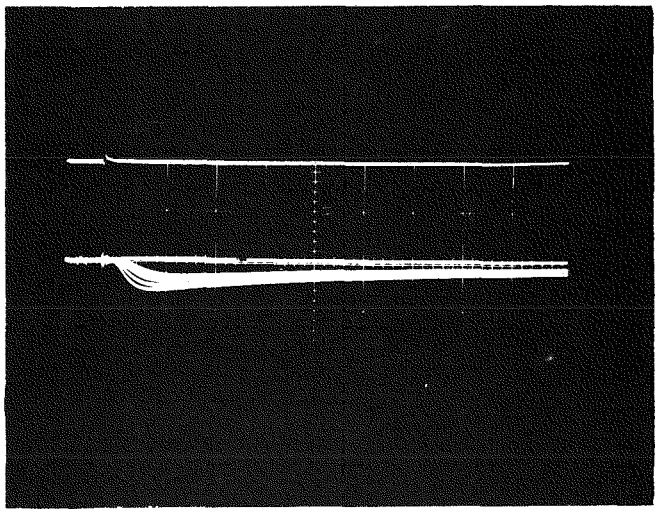

Fig. 5.12 Reverse Photocurrent at 125°C. Horizontal: 10 μs/div. Vertical: 5 mA/div. Anode reverse voltages are 0, 200, 400, 600, 800, and 1000V. The light pulse occurs at t = 7 μs.

Table 5.1

BLOCKING VOLTAGES

Device Number	25°C				125°C			
	V_D (V)	I_D (mA)	V_R (V)	I_R (mA)	V_D (V)	I_D (mA)	V_R (V)	I_R (mA)
1	2650	2.0	2000	2.0	2000	13	2000	20
6	2000	0.5	2000	3.5	2000	16	2000	26
7	2000	4.0	2000	8.0	2000	22	2000	30
9	2000	0.1	2000	9.0	2000	14	2000	32
10	2700	2.0	2000	4.4	2000	38	2000	17
20	2000	0.5	2000	0.5	2000	8	2000	9
22	2000	0.5	2000	0.5	2000	4	2000	7
28	2000	0.5	2000	0.5	2000	9	2000	10
30	2000	0.5	1700	2.0	2000	12	2000	13
32	2000	0.5	2000	0.5	2000	14	2000	12
33	2000	0.5	1700	2.0	2000	10	1900	10
24	2000	0.5	2000	0.5	2000	11	2000	11.5
25	2000	0.5	2000	0.5	2000	15	2000	13

Table 5.2

CONDUCTION AND SWITCHING PARAMETERS

Device	V_{TM} (V) @	I (A)	tq (µs)	dV/dt (V/µs)	I_{HO} (mA)	I_{LX} (mA)
1	1.40	1500	680	>400	20	32
6	1.75	1500	550	>400	55	100
7	1.60	1500	450	>400	50	70
9	1.55	1500	380	>400	35	40
10	2.80	1500	380	>400	25	42
20	1.85	1500	260	>400	40	60
22	2.10	1500	250	>400	42	65
28*	2.30	1400	85	>400	45	100
30	1.85	1500	280	>400	42	70
32	2.30	1500	130	>400	40	55
33	2.10	1500	240	>400	20	60
24*	1.65	1200	130	>400	40	85
25*	1.90	1200	350	>400	40	65

* Measured at 1200A forward current instead of the standard 1500A.

Table 5.3

SWITCHING PARAMETERS

Device	t_d (μs)	t_f (μs)	t_{on} (μs)	Latching Voltage (V)	Low Voltage Latch Test	Q_{rr} (μC)
1	0.6	1.0	1.6	<5	Pass	650
6	0.2	0.8	1.0	<5	Pass	740
7	0.2	0.8	1.0	<5	Pass	750
9	0.1	0.7	0.8	<5	Pass	740
10	0.5	0.6	1.1	4.0	Pass	330
20	0.5	0.5	1.0	5.0	Pass	320
22	0.5	0.7	1.2	10.0	Pass	320
28	0.5	0.7	1.2	16.0	Pass	175
30	0.4	0.8	1.2	16.5	Pass	360
32	0.45	0.75	1.2	8.0	Pass	250
33	1.2	0.70	1.8	8.0	Pass	285
24	0.44	0.40	0.84	9.5	Pass	180
25	0.90	0.36	1.26	15.5	Pass	280

Section 6

FABRICATION AND EVALUATION OF AN 8-THYRISTOR STACK

To demonstrate the suitability of using light-triggered thyristors in electric utility applications, an 8-thyristor module was fabricated and tested. Tests performed on the module followed those used in testing conventional electrically gated thyristor modules. The module includes associated emitter networks, heat sinks, and triggering circuit. A discussion of the trigger circuit, module fabrication and test program follows.

6.1 TRIGGER CIRCUIT

The triggering circuit consists of two parts

a) the light transmission system and

b) the laser diode pulse power supply.

6.1.1 Light Transmission System

Included in the light transmission system are the solid state light sources (laser diodes) and the optical cable harness necessary to transmit the optical energy to the thyristor string.

To guarantee that a sufficient amount of optical energy is delivered to each thyristor and to provide a degree of reliability in the event of a catastrophic failure of one or more single laser diodes, the following steps were implemented:

a) A laser diode, Type LD-68, manufactured by Laser Diode Laboratories, was selected as the light source.

b) Nine laser diodes were used in series to provide optical energy for eight thyristors and a sensing output.

c) The optical cable harness shown in Figure 6.1 was designed to have each output contain an equal number of fiber strands from each input (each output would then be equal to the average of all inputs).

d) Constant monitoring and display (meter) of the average optical energy delivered to the thyristors is provided.

6.1.2 Laser Diode Pulse Power Supply

The laser diode pulse power supply circuitry is shown in Figure 6.2 and consists of four basic sections: (1) the discharge circuit, (2) the charging circuit, (3) the trigger circuit, and (4) the optical energy monitoring circuit.

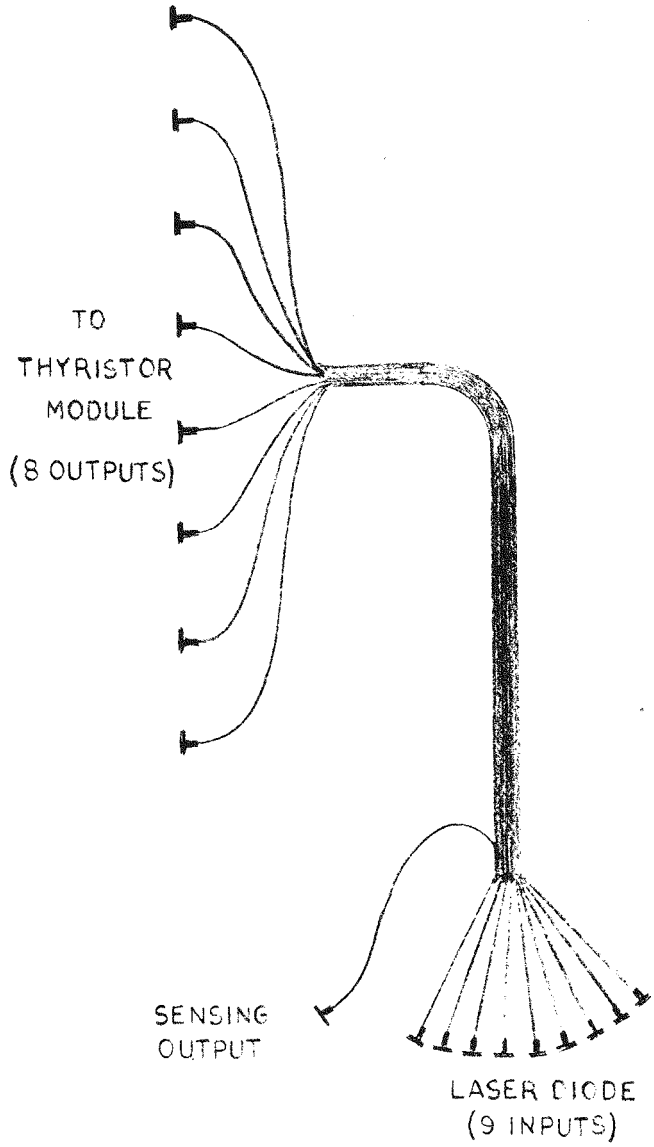

Fig. 6.1 Optical cable harness.

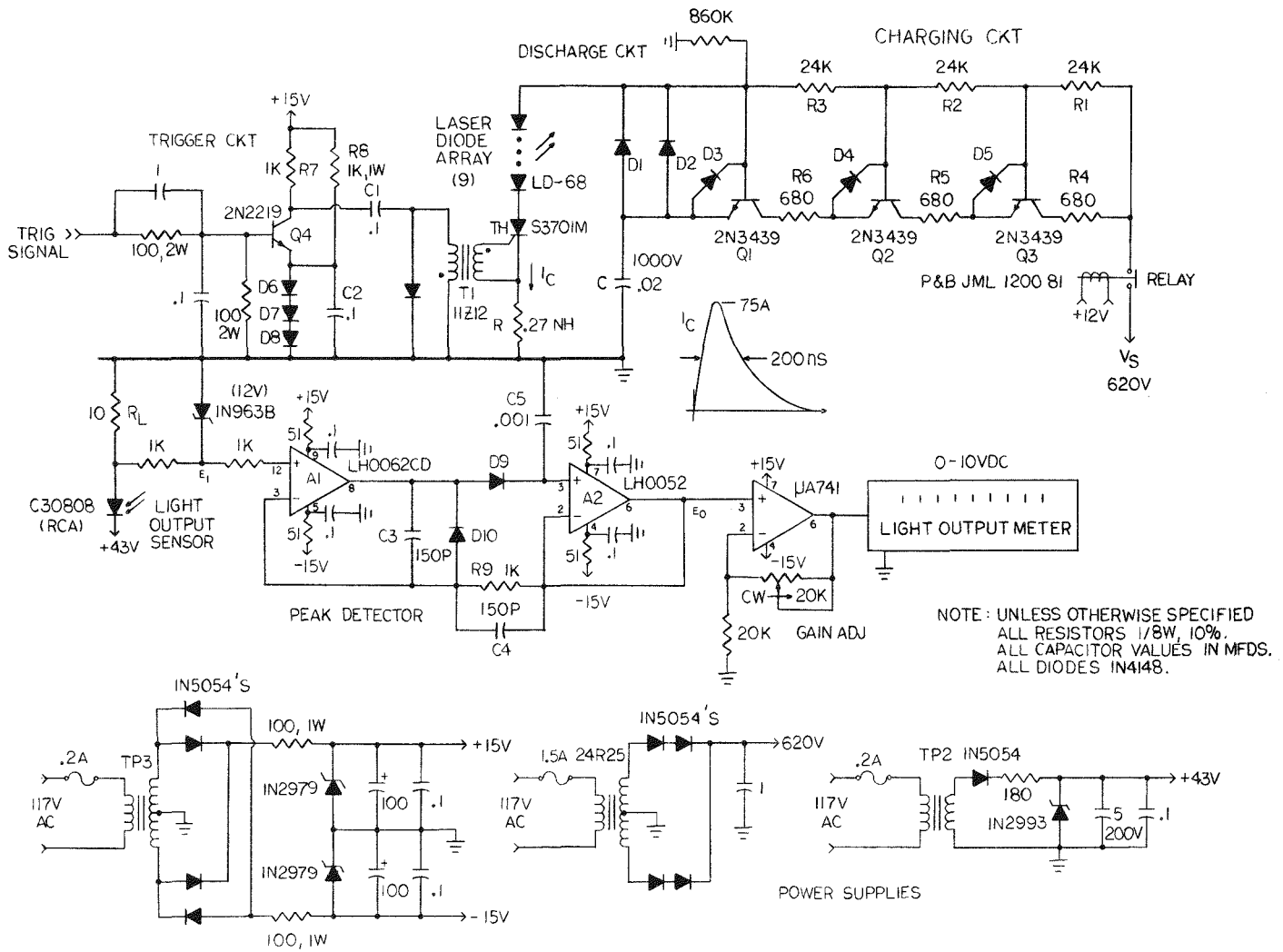

FIGURE 6.2 LASER DIODE PULSE POWER SUPPLY.

6.1.2.1 Discharge Circuit. The discharge circuit generates a 75 ampere, 200 nanosecond current pulse in the laser diode array. This current pulse is generated by discharging the storage capacitor C through the switching thyristor, TH, (RCA 53701M) and laser diodes. The rise time of the current pulse is determined by the turn-on characteristics of the switching thyristor, while the fall time is determined by the capacitor value and total resistance in the discharge circuit. Oscillographs of the capacitor voltage, V_c, and laser diode current, I_c, are presented in Figure 6.3. Monitoring of the laser diode current is accomplished using a noninductive resistor, R, placed in the discharge circuit.

6.1.2.2 Charging Circuits. The charging circuit charges capacitor C to the supply voltage, V_s, during the time interval between laser current pulses and isolates the supply voltage from the discharge circuit during the laser current pulse, allowing the switching thyristor, TH, to recover to the blocking state.

Capacitor C charges to the supply voltage (620V) when thyristor TH is not conducting. Diodes D1 and D2 are in the OFF state because zero current flows through them. At the onset of a pulse trigger, the impedance of the thyristor drops rapidly and capacitor C discharges toward ground potential. During the period when current is flowing through diodes D1 and D2, transistors Q1, Q2, and Q3 are reversed-biased by a diode voltage drop. Thyristor TH continues to conduct until the current in the loop drops below the required holding current. This condition determines the values of resistors R1, R2, and R3.

The voltage across capacitor C then begins to recharge toward the supply voltage, V_s. During this period, diodes D3, D4, and D5 do not conduct and transistors Q1, Q2, and Q3 are forward-biased into saturation. The time required for recharging (0.2 ms) is determined by the values selected for R4, R5, R6, and C.

6.1.2.3 Trigger Circuit. The trigger circuit responds to a positive voltage (approximately 7V) applied to its input terminals. This voltage forward biases transistor Q4 into saturation and connects capacitor C1 (previously charged with the polarity indicated) to ground potential. When this occurs a negative pulse is generated in the primary of pulse transformer, T1, which subsequently produces the appropriate polarity pulse to thyristor TH located in the discharge circuit. Resistor R8, capacitor C2, and diodes D6 through D8 provide approximately 4 volts noise immunity in the trigger input.

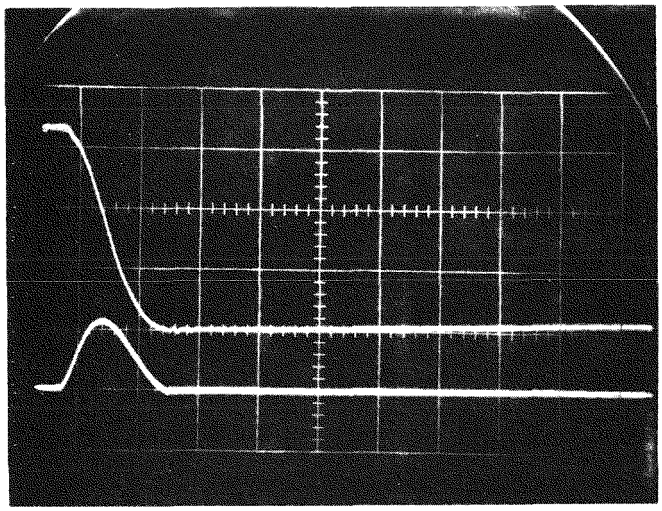

Fig. 6.3 Capacitor voltage and laser diode current.

6.1.2.4 Optical Energy Monitoring Circuit. Means of monitoring the average optical energy delivered to each thyristor in the module is provided by including an additional sensing output on the optical cable harness (see Figure 6.1). The monitoring circuitry consists of a light sensor (photodiode and load resistor, R_L), a peak detector, and a dc voltage meter. Under nominal conditions the meter is adjusted to give full scale deflection when all (nine) laser diodes are operational. In the event of a failure of one or more laser diodes, the scale deflection is reduced proportionately.

In the peak detector circuit shown in Figure 6.2, amplifier A2 operates as a unity gain follower inside the overall feedback loop. Amplifier A1 serves two purposes. First, the input signal (from the light sensor) needs to supply only the input bias current of A1. Second, the output rise time is not determined by the time constant of the ON resistance of diode D9 times C5, but is dependent only on the output current capability I_M of amplifier A1 (the output slew rate is given by $\Delta E_O/\Delta t = I_M/C5$).

When E_1 is less than E_O, C5 charges through D9 and the output of A2 rises. When E_1 becomes less than E_O, D9 becomes reversed-biased and C5 is prevented from discharging (the input impedance of A2 must be high if long decay times are desired). The output of amplifier A2 is therefore maintained at its previously high level. During this period, D10 conducts and supplies feedback for A1, thereby preventing it from overloading. Capacitors C3 and C4 are required for loop stabilization.

6.2 THYRISTOR MODULE FABRICATION

The thyristor module is shown in Figure 6.4. The assembly was fabricated for a unidirectional string of 8 thyristors. This assembly includes heat sinks, provisions for liquid cooling, and snubber networks. The assembly is essentially the same as those modules presently being used in VAR generator applications except it has been modified to accommodate only the single unidirectional thyristor string (whereas conventional modules also include a reverse thyristor string) and contains no electrical gate drive components. The snubber network for each thyristor is given in Figure 6.5, with the component values selected for a typical VAR generator application.

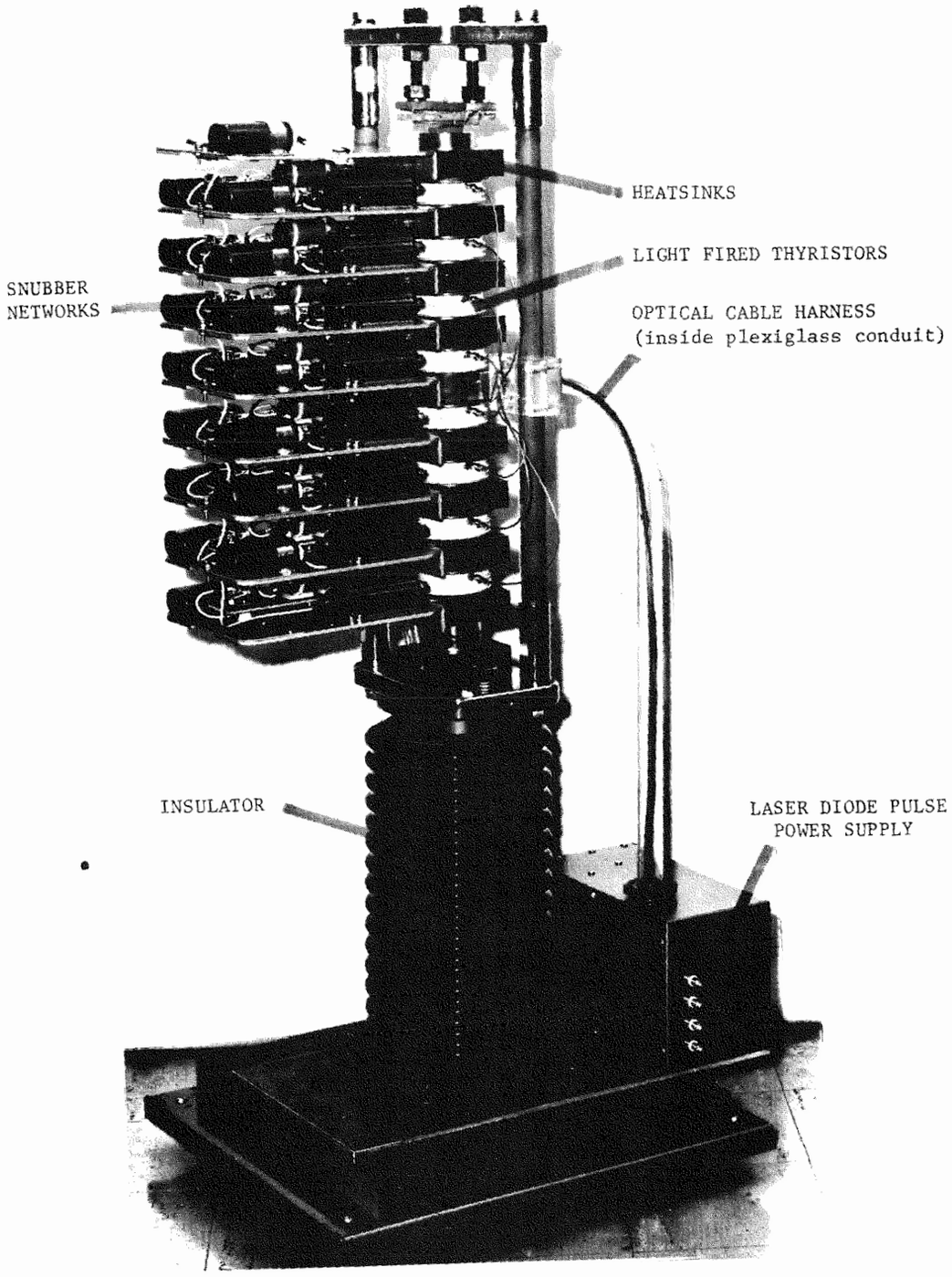

Fig. 6.4 Thyristor module assembly.

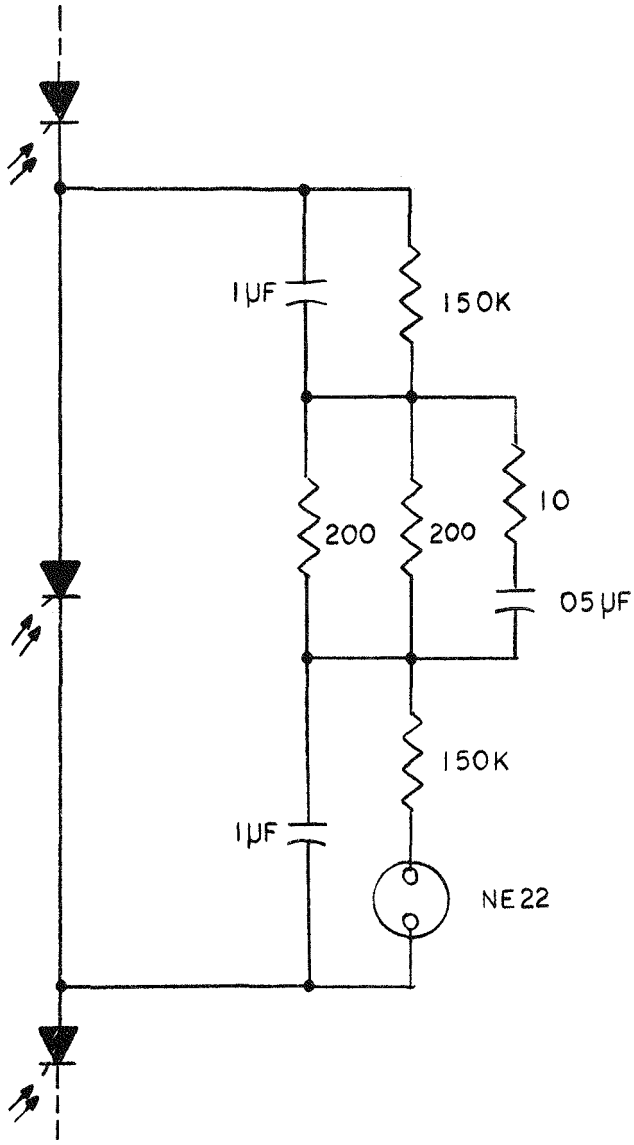

Fig. 6.5 Snubber network (one per thyristor)

6.3 THYRISTOR MODULE TEST PROGRAM

6.3.1 Trigger Circuit

Prior to the testing of the thyristor module, measurements of the amount of optical energy available at each fiber optics cable output were made. These measurements were made by disconnecting the appropriate fiber optics cable output at the input of each thyristor. The results are summarized in Table 6.1.

It is to be noted that the light energy transmitted into the silicon is ∿ 57% of the light available at the end of the fiber optics cable (Section 4, p. 4-27) so that to provide the 0.3 μJ required for reliable thyristor triggering, a minimum of 0.53 μJ should be available at each FOC output. The output at one thyristor position (position 8) is not quite at this value. Additionally, the variation in individual FOC outputs was greater than anticipated (a variation of 2 to 1 is observed). This variation was traced to nonequal numbers of input fiber strands in each output and to fiber strand breakage. The manufacturer of the harness (Galileo Electro-Optics) maintains that the observed variation in outputs is not typical and that much higher uniformity should be expected. Further discussion with Galileo Electro-Optics concerning methods of improving harness fabrication for future use is being conducted.

Table 6.1

OPTICAL ENERGY DELIVERED TO EACH MODULE THYRISTOR

Thyristor Position	Thyristor Serial Number	FOC Output Energy, μJ
1 (top)	1	0.61
2	25	0.92
3	7	0.63
4	32	0.98
5	10	0.67
6	20	0.65
7	22	0.94
8	24	0.51

In spite of these difficulties, all thyristors in the stack were triggered normally, with acceptable delay times.

6.3.2 Thyristor Module

The tests conducted on the thyristor module to demonstrate the performance achieved were as follows:

a) Static voltage division within the module
b) Thyristor turn-on time
c) Module steady state operation
d) Module dynamic operation

The results of these tests are summarized below.

6.3.2.1 Static Voltage Division Within the Module. To verify proper functioning of the snubber networks, a 4000V rms, 60 Hz, voltage was applied across the module and the voltage measured across each thyristor. During this test the module thyristors were not triggered. The results are presented in Table 6.2. The observed variation in voltages was 1.8 percent, well within expectation.

Table 6.2

STATIC VOLTAGE DIVISION WITHIN MODULE

Thyristor Position	Thyristor Voltage VRMS
1 (top)	502
2	501
3	502
4	504
5	498
6	495
7	496
8	499
	(3997V total)

6.3.2.2 Thyristor Turn-On Time. A 500V peak, 60 Hz voltage, with a series resistance of 100 ohms was connected across each thyristor. The module was then triggered using the laser diode power supply circuitry presented in Figure 6.2. The turn-on time of each thyristor was measured using the laser diode current pulse as the reference. To illustrate the procedure an oscillograph of the

thyristor voltage V_{THY} and the laser diode current I_C for a single thyristor (position No. 2) is shown in Figure 6.6. The results are presented in Table 6.3.

This test verified that the light emitting devices were operating, the optical cable harness connections were properly made, the thyristors were operable after mounting in the module, and that all turn-on times were within allowable tolerances.

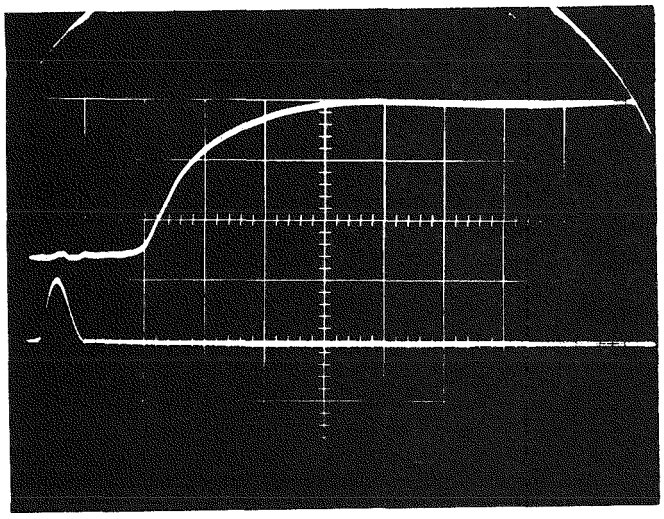

Figure 6.6 -- Thyristor turn-on time

Table 6.3

THYRISTOR TURN-ON TIME

Thyristor Position	t_{delay} (μs)	t_{fall} (μs)	t_{on} (μs)
1 (top)	0.7	1.1	1.8
2	0.8	1.1	1.9
3	0.5	1.1	1.6
4	0.2	1.0	1.2
5	0.2	1.1	1.3
6	0.4	1.0	1.4
7	0.1	1.1	1.2
8	0.5	1.0	1.5

6.3.2.3 Module Steady State Operation. A 6500V peak, 60 Hz voltage (corresponding to rated module voltage for the Minnesota Power and Light installation)* was connected across the module as shown in Figure 6.7. The voltage, LRC network components, and firing angle were selected to ensure that the module voltage rating was not exceeded, damping was adequate, and sufficient latching current was obtained during the light triggering pulse interval. The module voltage V and current I are shown in Figure 6.8. The module voltage with reference to the laser diode current is also presented in Figure 6.9. The module turn-on time was approximately 1.6 microseconds.

This test verified proper steady state operation of the module and provided a limited amount of burn-in time (40 hours) under rated voltage, reduced current conditions.

6.3.2.4 Module Dynamic Operation. Full scale voltage (6500V) and current (1600A pk), corresponding to rated module voltage and current in the MP and L installation, was applied to the module to verify proper voltage sharing by the thyristors during line switching, turn-on, and turn-off transients.

The test circuit is shown in Figure 6.10. Inductor L and capacitor C form a 60 Hz resonant discharge circuit selected to produce a peak current in the module equal to that anticipated in the MP and L installation when C is charged initially to rated module voltage. The saturating inductor L_S limits initial dI/dt during discharge of the bus-bar capacitance.

Line switching tests were performed on the module by charging capacitor C to 6500V and then operating the closing switch SW to apply this voltage to the module, which for this test was not triggered. Oscillographs of the module voltage V and the voltage across one half of the module $V_{1/2}$ are shown in Figure 6.11.

---

*In order to further evaluate the feasibility of light-triggered thyristors in commercial applications, EPRI is sponsoring work (Research Project 567) in which three modules (containing bidirectional switches) will be connected in series. This system will operate under actual use conditions at MP&L for a time period sufficient to further assess technological and commercial aspects of direct light firing.

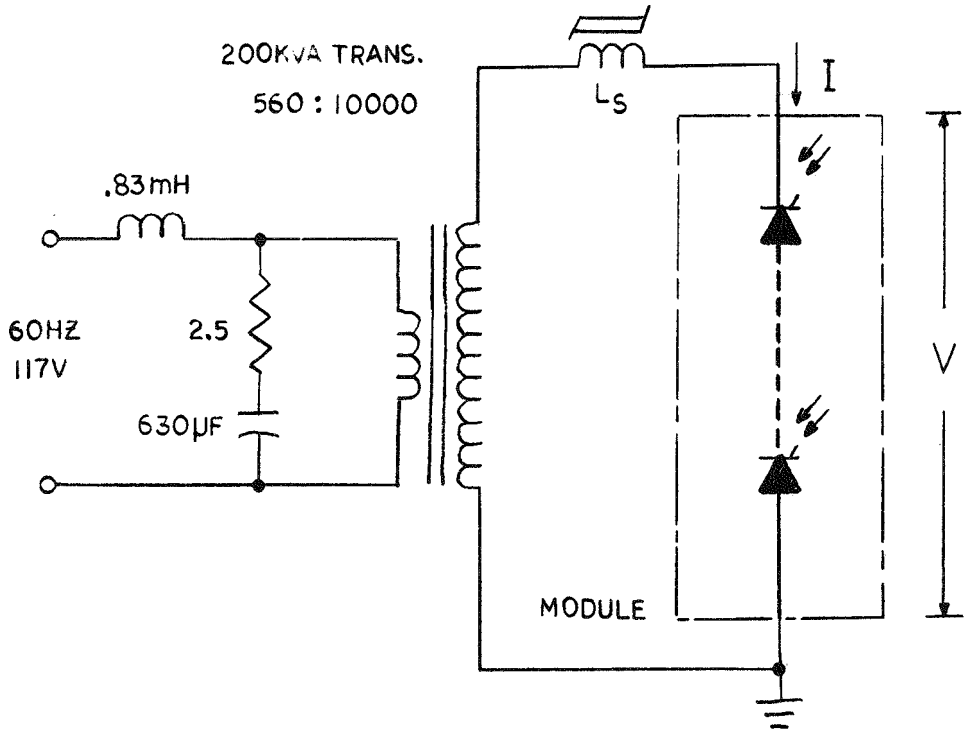

Fig. 6.7 Module steady state operation test circuit.

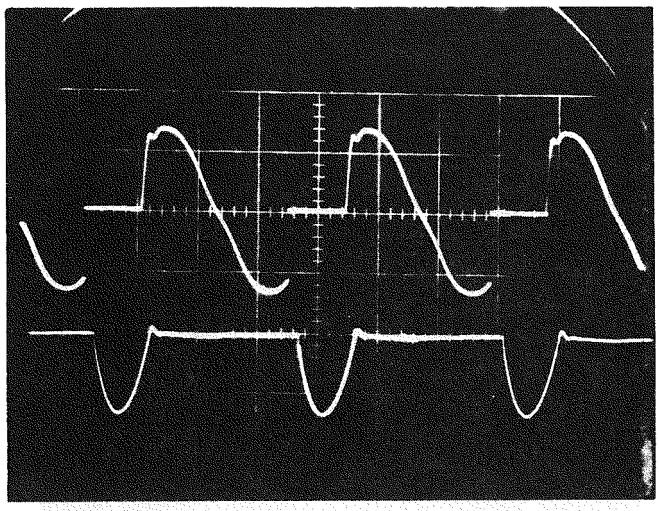

Fig. 6.8 Module steady state operation.

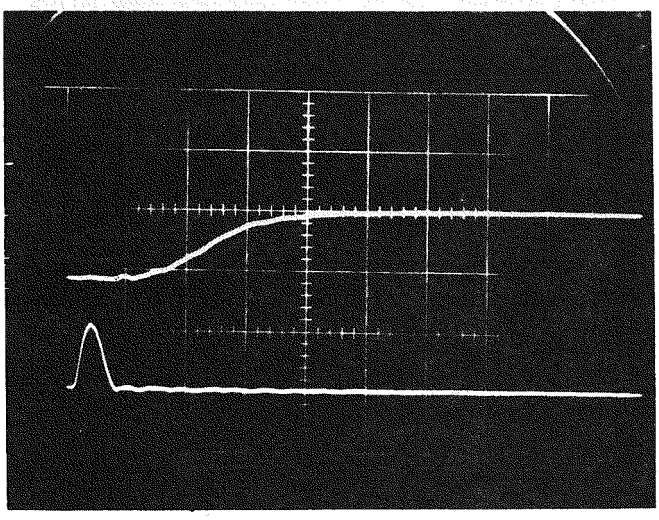

Fig. 6.9 Module voltage with reference to laser diode current (turn-on).

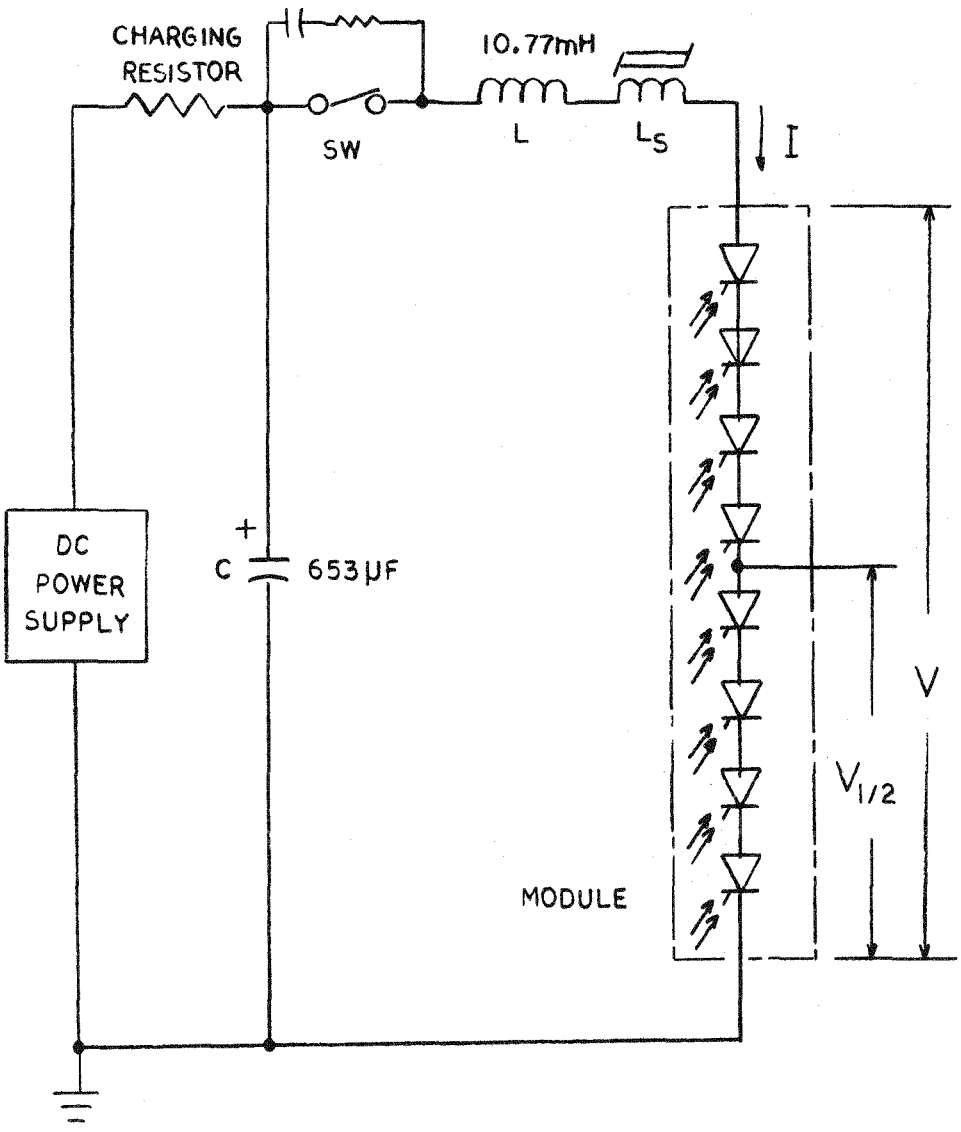

Fig. 6.10 Module dynamic operation test circuit.

Module switching tests were conducted by charging capacitor C to 6500V, operating the closing switch, allowing the transient voltage swing to settle, and then triggering the module. The module voltage V and the current I, for one cycle of operation, are shown in Figure 6.12. Since the module thyristors are arranged as a unidirectional switch, current is conducted for a half cycle only, leaving capacitor C with a reverse charge.

Turn-on and turn-off transients, under the same operating conditions, are presented in Figures 6.13 through 6.15 respectively.

After completion of the above set of tests, using MP&L rated module voltage (6500V pk), the tests were repeated with the voltage increased to 8500V (an increase of 30 percent). These tests were also successful and the results are presented, without further comment, in Figures 6.16 through 6.20.

6.4 STACK EVALUATION SUMMARY AND CONCLUSIONS

Tests performed on the 8-thyristor module, to verify the suitability of using light fired thyristors in electric utility applications, were completely successful. In each instance the performance of the light fired thyristor module was the same as that observed under similar test conditions with modules employing conventional electrically fired thyristors.

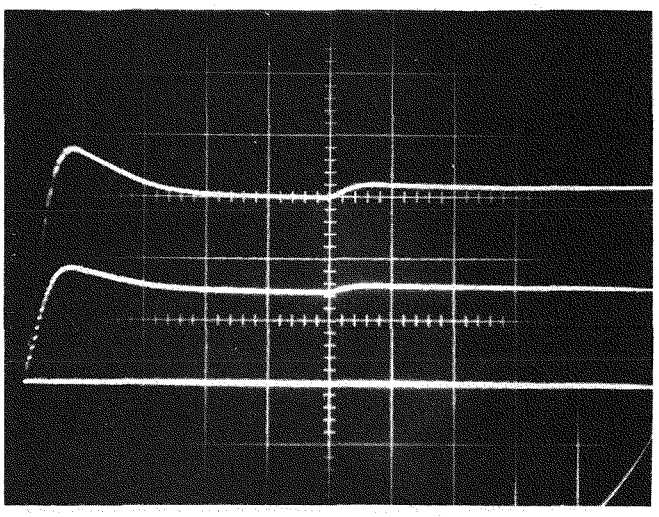

V 2kV/div.

$V_{1/2}$ 2kV/div.

- 0 50μs/div.

Fig. 6.11 Module voltage division during line switching (thyristors not triggered).

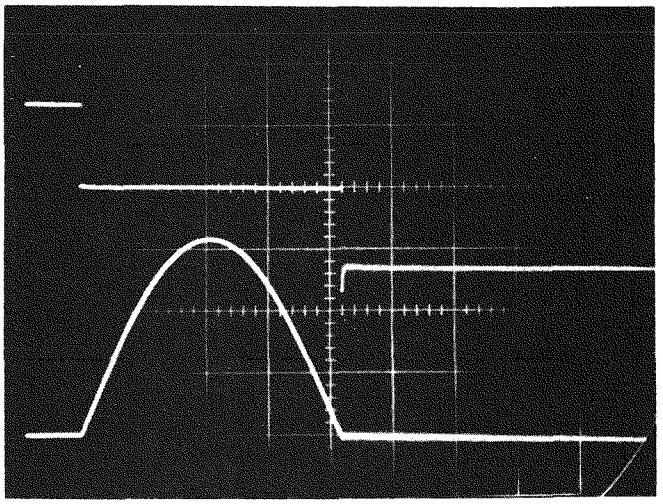

- 0 V 5kV/div.

- 0 I 500A/div.

2μs/div.

Fig. 6.12 Module voltage and current for one cycle operation.

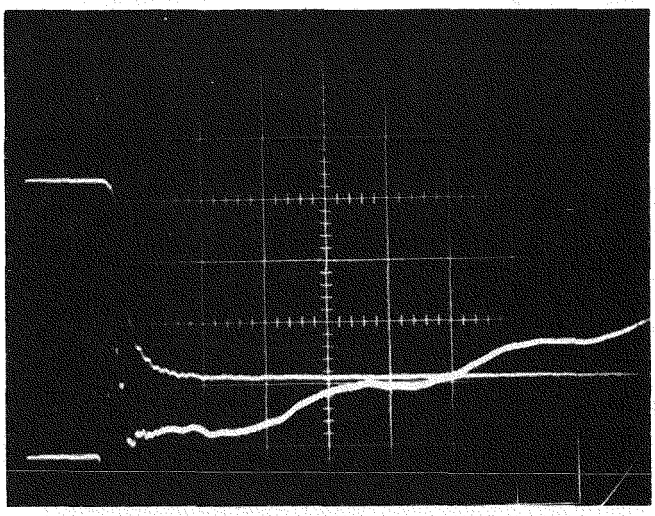

Fig. 6.13 Module voltage and current during turn-on.

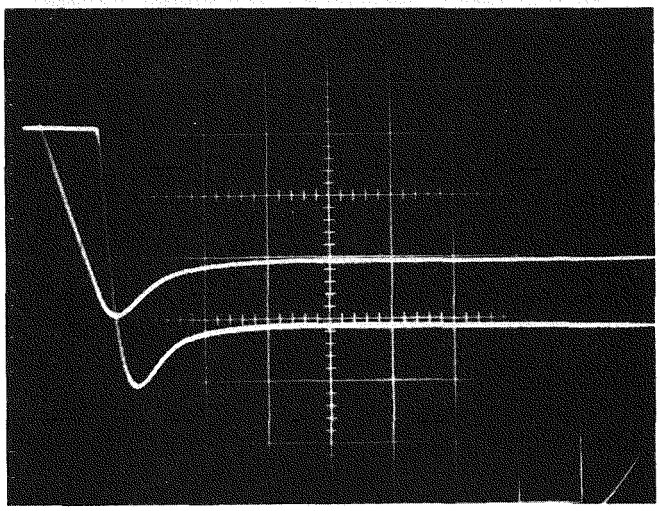

Fig. 6.14 Module voltage and current during turn-off.

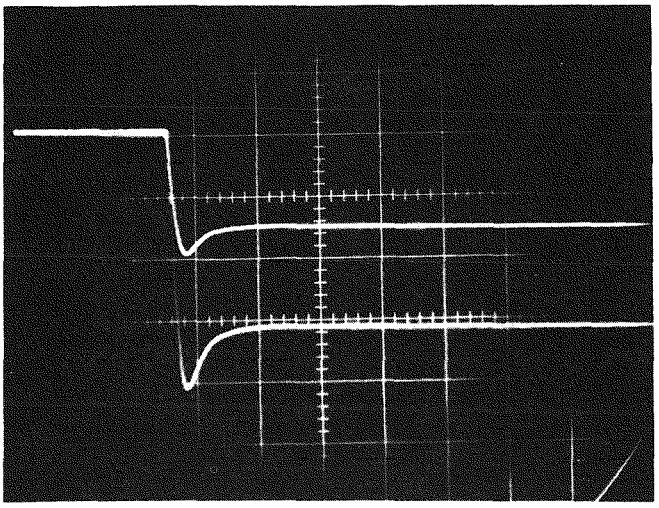

Fig. 6.15 Module voltage division during turn-off.

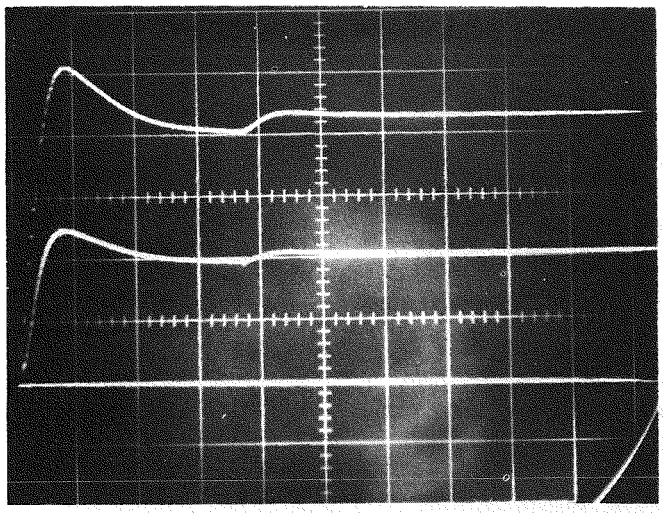

V 2kV/div.

$V_{1/2}$ 2kV/div.

50µs/div.

- 0

Fig. 6.16 Module voltage during line switching (thyristors not triggered, increased voltage).

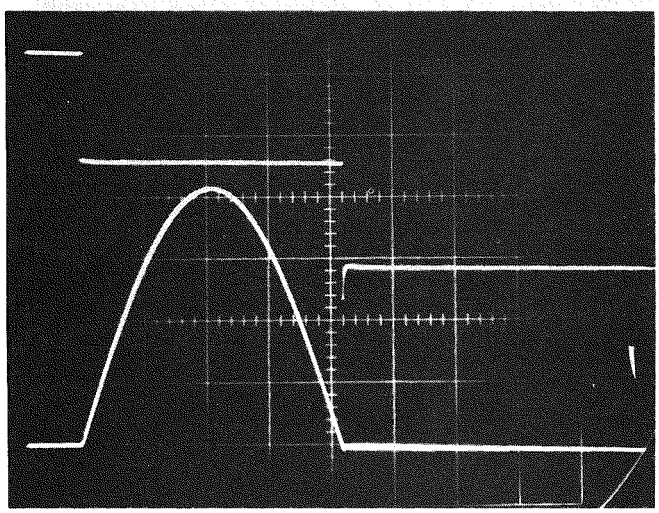

- 0

V 5kV/div.

- 0

I 500A/div.

2µs/div.

Fig. 6.17 Module voltage and current for one cycle operation (increased voltage).

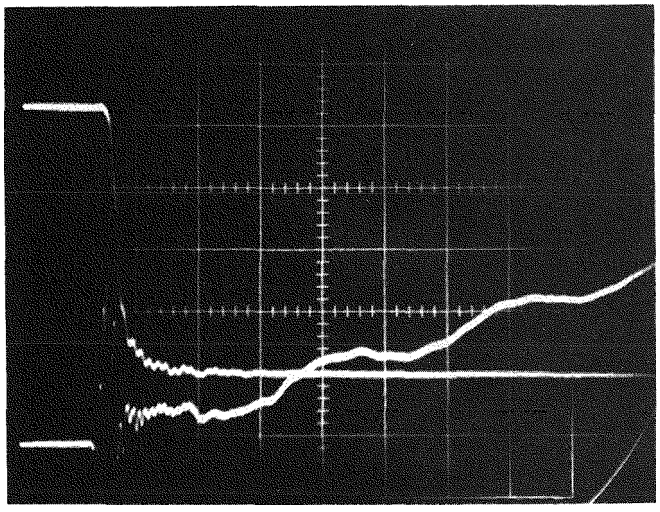

Fig. 6.18 Module voltage and current during turn-on (increased voltage).

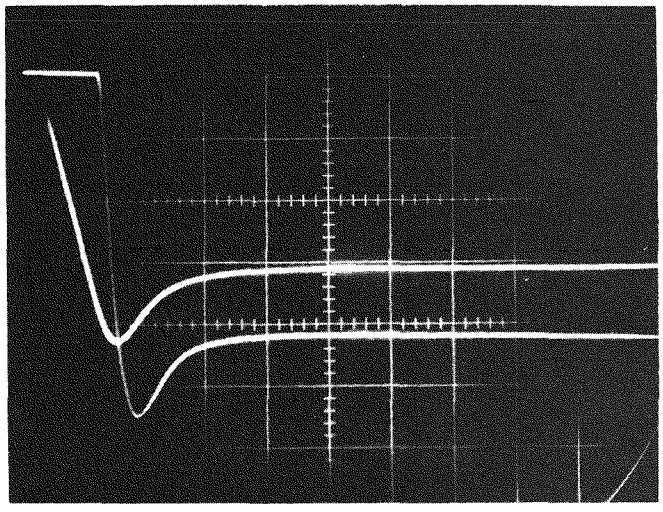

Fig. 6.19 Module voltage and current during turn-off (increased voltage).

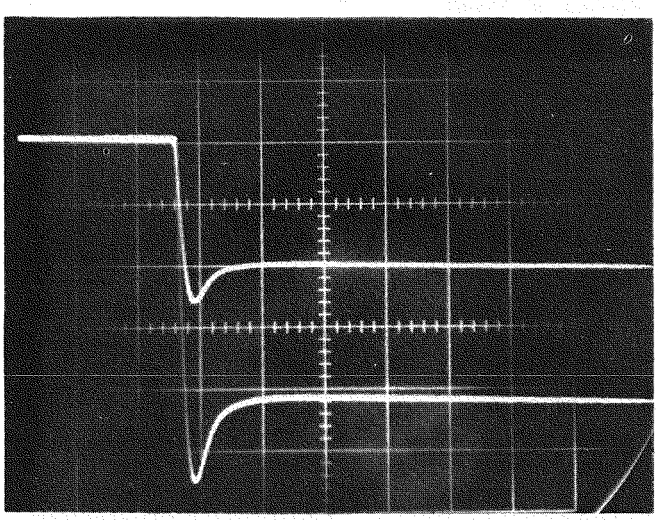

Fig. 6.20 Module voltage division during turn-off (increased voltage).

Section 7

CONCLUSIONS AND RECOMMENDATIONS

The goals of this contract were to develop a high power light-triggered thyristor and to demonstrate its suitability for high voltage VAR generator applications by constructing and testing a module which incorporated a series stack of eight devices. These goals were met.

The work reported here has demonstrated the feasibility of commercial application of light-triggered thyristors to high voltage VAR generator systems in electric power utilities. It is anticipated that the use of electrically insulating fiber optics cables to transmit triggering signals to thyristors which are far above ground potential will result in reduced installed system cost and improved reliability.

The technology improvements which were a result of this contract are judged to be sufficient to demonstrate the advantages which accrue to a light-triggered thyristor system. In the next phase of this program, a demonstration switch will be built and installed at an electric utility site. There it will be evaluated, under actual operating conditions, for efficiency and reliability.

During the course of this program, it became apparent that opportunities for further improvements in light-triggered thyristors exist. Although the present state of the technology is sufficient for demonstration and evaluation, significant improvements resulting in still lower cost and improved reliability can be expected. Among those areas which warrant further investigation and development are:

- Increased thyristor blocking voltage capability resulting in fewer power devices per module. Achievement of higher voltage is expected to result from the availability of very uniform (NTD) silicon starting material.
- The use of improved light sources and fiber optics cable which will furnish higher efficiency and reliability at lower cost. Electro-optics technology continues to advance rapidly.

- Incorporation of transient voltage and overvoltage protection into the thyristor design, eliminating the need for at least some of the protective circuitry now being used.
- Improvements in package design to achieve lower cost and increased reliability. The present design, although suitable for developmental work, is subject to mechanical failures which have not yet been satisfactorily resolved.
- Extension of the light-triggering concept to other areas in which factors such as operating frequency and rate of current rise become important. These extensions will require thyristor design changes which will result from additional development effort.
- Improved VAR generator designs and logic structures for reduced cost and higher efficiency.